Defense Technical Information Center

AD NO. _____
TECOM PROJECT NO. 2-CO-430-APR-156
REPORT NO. ATC-7793

RESEARCH REPORT

OF THE

RADIATION TRANSPORT IN AIR-OVER-GROUND GEOMETRY (SUMMARY: 1992-1993)

CRAIG R. HEIMBACH
MARK A. OLIVER
MICHAEL B. STANKA

RADIATION SIMULATION AND ANALYSIS DIRECTORATE

U.S. ARMY ABERDEEN TEST CENTER
ABERDEEN PROVING GROUND, MD 21005-5059

DECEMBER 1995

19960227 007

Prepared for:
DEFENSE NUCLEAR AGENCY
ALEXANDRIA, VA 22310-3394

U.S. ARMY TEST AND EVALUATION COMMAND
ABERDEEN PROVING GROUND, MD 21005-5055

DISTRIBUTION UNLIMITED.

DTIC QUALITY INSPECTED 1

DISPOSITION INSTRUCTIONS

Destroy this document when no longer needed. Do not return to the originator.

DISCLAIMER NOTICE

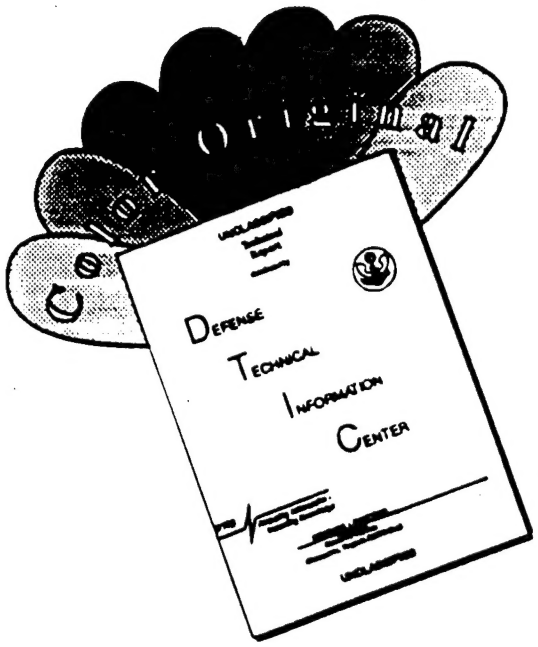

THIS DOCUMENT IS BEST QUALITY AVAILABLE. THE COPY FURNISHED TO DTIC CONTAINED A SIGNIFICANT NUMBER OF COLOR PAGES WHICH DO NOT REPRODUCE LEGIBLY ON BLACK AND WHITE MICROFICHE.

REPORT DOCUMENTATION PAGE

Form Approved
OMB No. 0704-0188

Public reporting burden for this collection of information is estimated to average 1 hour per response, including the time for reviewing instructions, searching existing data sources, gathering and maintaining the data needed, and completing and reviewing the collection of information. Send comments regarding this burden estimate or any other aspect of this collection of information, including suggestions for reducing this burden, to Washington Headquarters Services, Directorate for Information Operations and Reports, 1215 Jefferson Davis Highway, Suite 1204, Arlington, VA 22202-4302, and to the Office of Management and Budget, Paperwork Reduction Project (0704-0188), Washington, DC 20503.

1. AGENCY USE ONLY *(Leave blank)*	2. REPORT DATE	3. REPORT TYPE AND DATES COVERED
	December 1995	Research

4. TITLE AND SUBTITLE

RESEARCH REPORT OF THE RADIATION TRANSPORT IN AIR-OVER-GROUND GEOMETRY (SUMMARY: 1992-1993)

5. FUNDING NUMBERS

6. AUTHOR(S)

Heimbach, Craig R.; Oliver, Mark A.; Stanka, Michael B.

7. PERFORMING ORGANIZATION NAME(S) AND ADDRESS(ES)

Commander
U.S. Army Aberdeen Test Center
ATTN: STEAC-RS
Aberdeen Proving Ground, MD 21005-5059

8. PERFORMING ORGANIZATION REPORT NUMBER

ATC-7793

9. SPONSORING/MONITORING AGENCY NAME(S) AND ADDRESS(ES)

Defense Nuclear Agency
ATTN: RARP
6801 Telegraph Road
Alexandria, VA 22310-3398

10. SPONSORING/MONITORING AGENCY REPORT NUMBER

Same as Item 8

11. SUPPLEMENTARY NOTES

None

12a. DISTRIBUTION/AVAILABILITY STATEMENT

Distribution unlimited.

12b. DISTRIBUTION CODE

13. ABSTRACT *(Maximum 200 words)*

Radiation Transport from a fast-burst reactor has been measured from 60 to 2000 meters. Emphasis was placed on the measurement of thermal neutrons, but both fast neutrons and gamma rays were monitored. Effects investigated were sensitivity to angle of emission from the reactor, height over ground, and proximity to trees.

14. SUBJECT TERMS

15. NUMBER OF PAGES

16. PRICE CODE

17. SECURITY CLASSIFICATION OF REPORT	18. SECURITY CLASSIFICATION OF THIS PAGE	19. SECURITY CLASSIFICATION OF ABSTRACT	20. LIMITATION OF ABSTRACT
Unclassified	Unclassified	Unclassified	SAR

1. INTRODUCTION

A primary source of data for the long-term health effects of radiation is the medical history of survivors of Hiroshima and Nagasaki. This is especially the case for neutrons. In order to correlate the medical record with exposure, the exposure must be known and separable into neutron and gamma dose.

The radiation exposures at Hiroshima and Nagasaki are determined both by calculation and measurement. Only with agreement can the doses be correlated with the medical record with confidence. Unfortunately, agreement has been hard to come by. The data record consists largely of activation products which have long since decayed, and residual gamma energy stored in a few materials, subject to aging and weathering. The calculations depend on knowing the weapons' output, and being able to transport radiation across long distances.

Inconsistencies among data and calculation have plagued this analysis and have made the interpretation of results difficult. The analysis of exposure existing in 1986 was overthrown by the re-analysis done by Dosimetry System 1986 (DS86). Subsequently, calculations performed by Loewe[1,2] seemed to provide a good fit between calculation and measurement.

In addition to studying the effects of radiation on humans, there are some more directly military concerns in being able to match calculation and measurement. These involve the ability to predict and evaluate the effects of nuclear weapons in a battlefield, and to assess the effects on soldiers of radiation exposures which have occurred in weapons' tests.

In an effort to better define the radiation environments at Hiroshima and Nagasaki, Straume developed a new dosimetry technique for determining thermal neutron exposure. This involved counting chlorine atoms resulting from the thermal neutron reaction $^{35}Cl(n,g)^{36}Cl$. Since the product has a 3.1×10^{5} year half-life, samples from Japan can still be counted. In 1992, Straume[3] has applied his technique to determine thermal neutron fluence at both the weapon sites. The match with Nagasaki proved good, but the results at Hiroshima showed discrepancies from calculation of over a factor of ten, discrepancies which grow worse with distance.

Thermal neutrons themselves do not contribute much dose, but they are a good diagnostic of fast neutron fluence and secondary gamma-ray production. The existence of large discrepancies again calls into question the value of the Japanese medical records.

To investigate these discrepancies experimentally, a set of outdoor exposures was required. With a good simulation, calculation could be compared with the chlorine activation technique and with other measures of thermal neutron fluence.

The Aberdeen Pulse Radiation Facility (APRF) has a unique instrument for performing nuclear weapon radiation simulations. It has a compact neutron source which may be operated outdoors in the air. There is no surrounding shield, so the radiation may be measured at large distances limited only by the sensitivity of detectors and natural background. It turned out that data could be taken out to 2000 meters from the reactor. This was a fortunate coincidence, since 2000 meters was the limit of measured health effects at both Hiroshima and Nagasaki.

The APRF was tasked to use its facility to validate the computer codes and cross sections used in the Hiroshima/Nagasaki analysis. Particular emphasis was given to thermal neutrons, since that was the main question in the latest data.

APRF staff made measurements of the thermal neutron fluence with both gold activation foils and BF_3 proportional counters. In each case, both bare and cadmium-covered measurements were made. These were supplemented with measurements of fast neutron fluence through sulfur activation and proton-recoil spectroscopy. A neutron Remmeter was used as an integral monitor.

Gamma-ray measurements were made with thermoluminescent detectors (TLDs) and with Geiger counters.

Not all detectors could be used over all ranges, but efforts were made to have regions of overlap between detectors. Most of the detectors were pushed to their limits by attempting to make measurements beyond their useable range. At this point, background and counting statistics make the results unreliable. These limitations will be noted as the individual results are discussed below.

In addition to measurements made by APRF staff, other institutions participated. These included Los Alamos National Laboratory (LANL), which used its LANL-developed neutron spectrometer at 1100 and 1600 meters. The Environmental Measurements Laboratory of the Department of Energy used several detectors, including Bonner spheres, to make measurements from 170 to 2000 meters. The Defence Research Laboratory, Ottawa, supplemented the APRF proton-recoil measurements with its own similar system, and added its own BF_3 and BGO measurements. In addition, Straume used the same chlorine activation technique applied at Hiroshima/Nagasaki in the APRF environment.

This report does not include the results of laboratories other than the APRF, but it does describe the overall context of all experiments.

2. EXPERIMENTAL CONFIGURATION

The APRF reactor has a compact highly enriched uranium-molybdenum core supported on a moveable transporter. It is normally housed in a thin weather shield, but may be moved outside for operation. The weather shield, or silo, has three aluminum thicknesses for a total of 3.6-mm aluminum, plus 3.8 cm of fiberglass insulation. Appendix A, Figure A-2 shows the reactor on the outdoor test pad. All measurements reported here, except where noted, were with the reactor in its maximum-up, maximum-out position, 12.8 meters high at ground zero on the test pad.

The reactor can be operated up to about 8 kW continuously. This limit in power limited the useable distance for several detectors. In addition, all data for any one configuration were taken in one day, in order to avoid environmental changes.

Appendix A, Figure A-1 diagrams the overall layout of the area. The reactor is located in a 150-meter radius clear area. The clear area is centered on the reactor silo, not on the outdoor test position. Beyond 150 meters, the region is mostly forested. There is a 45-meter wide path cut into the woods, allowing line-of-sight (LOS) exposure out to 450 meters from the reactor.

Within the cleared area, measurements were made along the path out to 450 meters. Measurements were also made at a 90° angle from this direction, and at 180 and 270°. This was done to investigate non-isotropic emission from the reactor and scattering of radiation from the reactor support structures. An additional measurement was made directly behind the reactor, through the transporter and the silo. This was considered a worst-case scenario for scattering and attenuation.

Locations beyond 450 meters were selected to try to provide treeless areas. An additional constraint was to make the measurements over ground. These locations have nominal distances from ground zero of 715, 1080, 1600, and 2000 meters. Appendix A gives details of the exact coordinates, and includes a description of each test location.

At the distances measured, it might be expected that environmental factors would affect the radiation. For this reason, weather data were recorded during each test, and ground moisture recorded before and after each test. Weather data actually come from the Aberdeen Proving Ground (APG) weather station located about 9 km from the APRF.

For passive irradiation, most dosimeters were placed on an aluminum stand, as shown in Appendix A. Horizontal branches were positioned so that dosimeters were placed at 10, 100, and 300 cm above the ground. The aluminum stands were fit to pipes sunk into the ground. The locations were surveyed and reused, so that they were well known (within 1 cm) and repeatable.

Active dosimetry was located from 50 to 100 cm above the ground, except where noted.

In addition to measuring near the ground, a few measurements were made with the detectors supported by a crane. This was done at 715 meters because LOS could be regained by raising the detectors above the trees at this distance. The crane supported the detectors at 30 meters above the ground.

A set of measurements was made with gold foils inside an acrylic block to determine the thermalization of the spectrum. The idea was that, since many of the chlorine samples from Japan were obtained from inside various materials, the ability to calculate neutron slowing-down in the APRF geometry should be verified.

A set of reactor runs was done to investigate the buildup of fission-product gamma rays in the course of a reactor run. For this set of measurements, the reactor was operated in the center of the silo, 6.7 meters above the floor (at the 6-meter limit). The relative amounts of neutrons and gamma rays were measured as a function of time during a reactor run.

The angular distribution of radiation around the reactor was measured with sulfur, gold, and TLDs. This was done with the reactor at the silo center, 6.7 meters above the floor. The expectation was not that the reactor emission depended on angle, but that various materials located around the silo would serve as scattering centers.

3. RESULTS

The data presented in this section are a summary of results. Details of each detector system, calibration, and complete results are given in the appendixes.

Tables 1 and 2 give an overall summary of the reactor runs performed in support of this test. The tests are separated into two types: passive (sulfur, gold, TLD) and active (BF_3, GM, Remmeter, and proton-recoil). A few runs had detectors of both types. A "Y" in Table 1 indicates that a detector of that type was present during the run.

For the active runs, there was usually a group in addition to APRF staff taking data. These were the Department of Energy (DOE) led by Ferenc Hajnal of the Environmental Measurements Laboratory (EML), or the Defense Research Laboratory, Ottawa (DREO), led by Thomas Cousins.

The percentage error quoted in most of the tables is the statistical uncertainty divided by the measured value. The error in percent is the percentage error times 100.

a. Thermal Neutrons.

(1) The thermal neutron fluence was measured with two independent techniques: gold activation and BF_3 proportional counters. The gold activation was less sensitive than the BF_3 system, and data with gold are limited to 715 meters from ground zero. BF_3 data were taken from 170 to 2000 meters from the reactor.

(2) The advantage of using gold foils was that several could be exposed simultaneously. These were used to investigate angular dependence and variation with height. The BF_3 detectors had the high sensitivity which allowed distant measurements.

(3) Both detectors were run bare and with cadmium covers. The thermal neutron fluence, reported here as 2200-m/s fluence, is obtained by subtracting the cadmium-covered results from the bare results. Consistency between the two detectors was reinforced by calibrating both detectors in the National Institute of Standards and Technology (NIST) thermal beam, although at different times.

(4) The cadmium ratio, the ratio of bare to cadmium-covered results, is an indication of the thermalization of the neutrons. A high ratio indicates more complete thermalization. This is true for both types of detectors, although the gold and BF_3 ratios should not be directly compared. Gold has a resonance above the cadmium cutoff which causes a substantial fraction of the overall activation in both bare and covered foils. This causes the gold cadmium ratios to be lower than the BF_3 ratios.

(5) A composite of all thermal neutron results is given in Table 3 and shown in Figure 1. No correction is made here for air or ground moisture effects. The agreement between the detectors is quite good. The only significant discrepancy is at 715 meters, which is at the limit of the useful range of the gold foils.

(6) The data in Figure 1 are generally smooth. The discrepancy at 135 meters is explainable by environmental effects. The 90 and 180° locations were just in front of the trees, and the enhanced thermal fluence is probably due to fast neutrons being thermalized by the trees. The 450-meter location shows a similar effect. The 400-meter thermal fluence may be slightly suppressed due to lower ground moisture. This location was covered with crushed rock.

(7) The 181-meter data point is through the silo. It does not show a substantial thermal neutron deficit.

(8) There is a small effect of fluence with height. This is shown in Appendix A.

b. Fast Neutrons.

(1) Three detectors were used to monitor fast neutron fluence. These were sulfur activation foils, a neutron Remmeter, and a proton-recoil spectroscopy system (ROSPEC).

(2) Each detector measures a different part of the neutron spectrum. The sulfur foils have a neutron threshold of 3 MeV. The proton-recoil system measures spectra from 50 keV to 4.5 MeV. There is some overlap, between 3.0 and 4.5 MeV, which can be compared with sulfur. The Remmeter responds to all neutrons, but with a particular response function. The neutron spectra obtained with proton-recoil may be integrated over the Remmeter response to check for consistency. Unfortunately, about 10 percent of the Remmeter response is due to neutrons not measured by the proton-recoil system.

(3) The sulfur monitors, like the gold foils, were used to map the field. Averaged results are given in Table 4 and shown in Figure 2. No effect of height above ground or angle around the reactor was observed. Although sulfur was exposed out to 700 meters, only the foils within 450 meters had sufficient counts to derive consistent data. The fluence was not a function of angle from the reactor, except in the through-the-silo direction, where attenuation caused a significant reduction.

(4) Proton-recoil spectra are given in Appendix A. Figure A-33 shows spectra as a function of distance from the reactor.

(5) The number of neutrons measured from 3 to 4.5 MeV by the proton-recoil spectrometer may be multiplied by 1.69 to estimate the total fluence >3 MeV. This is compared to the fluence measured by sulfur in Figure 2. The sulfur fluence is adjusted from californium-252-equivalent neutrons to the fluence at the APRF by reducing it by 3 percent. The proton-recoil system generally agrees with the sulfur to within 10 percent out to 400 meters. At 450 meters, there is a 30-percent discrepancy, with the proton-recoil system reporting fluences low as compared to the sulfur. The reason for this discrepancy is not known.

(6) Proton-recoil measurements were made out to 700 meters. Remmeter measurements were made from 170 to 2000 meters from the reactor. The proton-recoil spectra were integrated over a dose response function[4], increased by 12 percent to account for the portion of the spectrum not measured, and plotted against the Remmeter data in Figure 3. Agreement is to within 10 percent, except for 715 meters, where the proton-recoil system records 33 percent more dose than the Remmeter. This is beyond statistical uncertainty. This discrepancy might possibly be due to variations in the neutron spectrum affecting the Remmeter response, or variations in tree density affecting the neutron dose.

(7) The proton-recoil spectra were measured at two heights at 715 meters from the reactor. In addition to the normal height of 110 cm above the ground, the detector was raised by a crane to 30 meters above the ground. This raised the detector such that it regained LOS to the reactor above the trees. The dose measured above the trees was 13 percent higher than the dose measured on the ground.

c. Gamma Rays.

(1) Two gamma detectors were used, TLDs and Geiger counters. As with the other sets of detectors, one (TLD) was less sensitive but allowed a mapping of the radiation field within 450 meters. The other detector (GM) allowed the radiation to be measured out to 2000 meters.

(2) The TLD results in Appendix A are reported in Rad(TLD) as well as Rad(tissue). This is because Rad(TLD) is not sensitive to the gamma-ray spectrum. Results need to be converted to Rad(tissue) for comparison purposes. Agreement between the TLD and GM detector systems is shown in Figure 4, and is surprisingly good. Only the LiF and Al_2O_3 were included in the TLD results, since the CaF_2 showed a bias versus the other materials.

(3) TLDs showed little variation with height above ground. Otherwise, they showed similar behavior as the thermal neutrons as a function of position, with significantly more gamma rays in areas with high thermal neutron fluence. This is probably due to secondary gamma-ray production in areas of high thermal fluence.

(4) The gamma-ray results at 1600 and 2000 meters suffer from background effects. At 1600 meters, the net count rate equaled background, and it was less than 10 percent of background at 2000 meters. This is discussed further in Appendix A. The gamma-ray dose as reported here should not be relied on at these distances.

(5) The neutron-to-gamma dose ratio is plotted in Figure 5. This shows a decreasing ratio as a function of distance. The uncertainties in these results grow quickly because they are composed of uncertainty in both neutron and gamma dose. At 2000 meters, a factor-of-two error is not unrealistic.

d. Acrylic Phantom.

(1) Thermal neutrons are generated from fast neutrons not only through interactions in the air and ground. Typically, there are substantial effects due to the local environment. In the weapons' environments, there were buildings and the material of the dosimeter itself. For example, thermal neutron fluence was measured as a function of depth in walls.

(2) APRF provided a controlled environment to test the ability to calculate thermal neutrons generated from fast neutrons. This consisted of an acrylic block, in which gold and cadmium-covered gold foils were placed. This gives a measurement of thermal neutron fluence as a function of depth into the block. These results are discussed further in Appendix A.

e. Other Diagnostics.

(1) Two sets of supplementary experiments were performed in an attempt to help understand the APRF environment.

(2) The first experiment addressed the fact that the neutron/gamma dose ratio is not a constant as a function of time. As the reactor operates, there is a buildup of fission products. This adds to the prompt gamma rays and decreases the neutron/gamma ratio.

(3) This was investigated by measuring the neutron and gamma output from the reactor as a function of time. A Far-West model GM-1 Geiger counter was used to monitor the gamma-ray fluence. A 5-inch diameter Bonner sphere was used to monitor the neutron fluence. It turned out that, for the operations considered here, there was little effect on the data. This was because the runs were sufficiently long that the N/G ratio approached a stable value. Details are presented in Appendix A.

(4) A second experiment consisted of measuring the output of the reactor as a function of angle. This was done with the reactor in the center of the silo. Gold and sulfur foils and TLDs were placed from 11 to 17 meters around the reactor to look for asymmetry due to scattering centers. Of special concern was the presence of the APRF flash X-ray, which has a large quantity of oil. No effect was found.

f. Summary.

(1) In order to investigate the transport of radiation through air, the APRF reactor was used as a clean source, and measurements were made from 60 to 2000 meters from the reactor. Emphasis was placed on thermal neutron measurements, but fast neutrons and gamma rays were also monitored.

(2) The APRF has a substantial variation in topography which might affect the neutron transport. To avoid this, the attempt was made to stay in treeless areas. Weather conditions were monitored, as well as ground moisture, to provide the calculator with the best possible description of the environment.

(3) It is hoped that this data compilation provides sufficient diagnostics to prove the calculational techniques.

TABLE 1. LISTING OF REACTOR RUNS PERFORMED WITH PASSIVE DOSIMETRY

SS92-66	03/24/92	50 kwhr		
	Sulfur	Gold	TLD	Chlorine
135m/0	Y	Y	Y	Y
135/90	Y	Y	Y	Y
135/180	Y	Y	Y	Y
170m	Y	Y	Y	Y
300m	Y	Y	Y	Y
400m	Y	Y	Y	Y
450m	Y	Y	Y	Y
715m	Y	Y	Y	Y
SS92-186	**06/17/92**	**12 kwhr**		
	Sulfur	Gold	TLD	Chlorine
70m/90	Y	Y	Y	
70m/180	Y	Y	Y	
70m/270	Y	Y	Y	
135m/0	Y	Y	Y	
135/90	Y	Y	Y	
135/180	Y	Y	Y	
170m	Y	Y		
silo	Y	Y	Y	
SS92-210	**07/07/92**	**50 kwhr**		
	Sulfur	Gold	TLD	Chlorine
135m/0	Y	Y		Y
135/90				
135/180				
170m	Y	Y		Y
300m	Y	Y		Y
400m	Y	Y		Y
450m	Y			Y
715m				

SS93-81: Inside silo
SS93-73, SS93-74, SS93-75: Acrylic phantom.

TABLE 2. LISTING OF REACTOR RUNS FOR ACTIVE DETECTORS

5/27/92 to 5/29/92 with DOE

	APRF					DOE
	BF3	REM	GM	Gold	Sulfur	Bon.Sph.
135m				SS92-157	SS92-157	
170m	SS92-155	SS92-155	SS92-155	SS92-154	SS92-154	
170m				SS92-157	SS92-157	
300m				SS92-157	SS92-157	
400m	SS92-156	SS92-156		SS92-154	SS92-154	
400m				SS92-157	SS92-157	
450m				SS92-157	SS92-157	
715m	SS92-158	SS92-158	SS92-158			SS92-158
1080m	SS92-154	SS92-154	SS92-154			SS92-157
1600m	SS92-154	SS92-154	SS92-154			SS92-154
2000m	SS92-157	SS92-157	SS92-157			SS92-157

8/25/92 to 9/2/92 with DREO

	APRF		DREO		
	ROSPEC	BF3	ROSPEC	BGO	BF3
70m/180			SS92-239		SS92-239
135m/0	SS92-230	SS92-230	SS92-230		SS92-230
135m/180	SS92-239	SS92-239			
170m	SS92-228	SS92-228	SS92-228		SS92-228
	SS92-229	SS92-229	SS92-229		SS92-229
300m	SS92-236				SS92-236
	SS92-237	SS92-237			SS92-237
400m	SS92-231	SS92-231	SS92-231		SS92-231
	SS92-232	SS92-232	SS92-232		SS92-232
		SS92-233			
400m*			SS92-242		
450m	SS92-234	SS92-234			
		SS92-235	SS92-235		
715m	SS92-240	SS92-240	SS92-240		SS92-240
		SS92-241			
715m(up)	SS92-241		SS92-241		
silo	SS92-238	SS92-238	SS92-238		SS92-238
1600m				SS92-240	

* Reactor inside silo

6/14/93 to 6/17/93 with DOE

	APRF				DOE
	BF3	REM	ROSPEC	GM	Bon.Sph.
300 m	SS93-71	SS93-71		SS93-71	SS93-71
	SS93-72	SS93-72		SS93-72	SS93-72
	SS93-73		SS93-73		
1600m	SS93-77	SS93-77		SS93-77	SS93-77
2000m	SS93-74	SS93-74		SS93-74	SS93-74
	SS93-75	SS93-75		SS93-75	SS93-75
	SS93-76	SS93-76		SS93-76	SS93-76
				SS93-73	

Gamma Buildup: SS93-78, SS93-79, SS93-80, P93-90, P93-91.
SS91-123: LASL at 1080/1600 meters. SS95-33, SS95-34: extra GM runs.

TABLE 3. THERMAL NEUTRON SUMMARY

Distance (m)	Angle (deg)	Gold ($n/cm^2/kwhr$)	Pctg. Error	BF3 ($n/cm^2/kwhr$)	Pctg. Error	Ratio (BF_3/Gold)
63	90	9.39e+07	0.007			
63	180	8.96e+07	0.007			
66	270	8.59e+07	0.007			
135	0	2.37e+07	0.003	2.65e+07	0.000	1.12
135	90	3.38e+07	0.004			
135	180	3.53e+07	0.005	3.84e+07	0.001	1.09
170		1.46e+07	0.003	1.66e+07	0.000	1.13
181		1.31e+07	0.009	1.37e+07	0.000	1.04
300		3.72e+06	0.004	4.04e+06	0.001	1.08
400		1.02e+06	0.004	1.07e+06	0.000	1.05
450		8.21e+05	0.004	9.45e+05	0.000	1.15
715		6.60e+04	0.015	5.43e+04	0.000	0.82
1080				4.72e+03	0.003	
1588				1.24e+02	0.009	
1986				1.04e+01	0.019	

TABLE 4. FAST NEUTRON DIAGNOSTICS

Distance (m)	Angle (deg)	Φ(>3 MeV) (n/cm²/kwhr)			Ratio (Rospec/Sulfur)	Rad(Tissue) (mRad(Ti)/kwhr)			Ratio (Rospec/Remmeter)
		Sulfur	Error	Rospec		Remmeter	Error	Rospec	
63	90	3.26e+07	0.007						
63	180	3.24e+07	0.007						
66	270	2.97e+07	0.007						
135	0	4.96e+06	0.004	4.73e+06	0.95			1.32e+02	
135	90	5.05e+06	0.009						
135	180	5.00e+06	0.012	5.67e+06	1.13			1.52e+02	
170		2.69e+06	0.005	2.34e+06	0.87	6.53e+01	0.032	7.19e+01	1.10
181		1.19e+06	0.058	1.28e+06	1.07			4.39e+01	
300		3.88e+05	0.020	3.65e+05	0.94	1.03e+01	0.010	1.14e+01	1.10
400		1.07e+05	0.051	9.92e+04	0.93	3.32e+00	0.101	3.54e+00	1.06
450		6.86e+04	0.071	5.76e+04	0.84			2.05e+00	
715				3.11e+03		1.32e-01	0.018	1.76e-01	1.33
1080						1.02e-02	0.019		
1588						3.79e-04	0.047		
1986						2.53e-05	0.157		

TABLE 5. GAMMA-RAY DOSE SUMMARY

Distance (m)	Angle (deg)	TLD (mR/kwhr)	Pctg. Error	GM (mR/kwhr)	Pctg. Error	Ratio (GM/TLD)
63	90	155.0	0.039			
63	180	147.8	0.055			
66	270	139.3	0.028			
135	0	30.4	0.014			
135	90	34.2	0.014			
135	180	38.0	0.023			
170		18.3	0.014			
181		13.0	0.071			
300		4.06	0.013	3.92	0.001	0.96
400		1.35	0.019	1.42	0.001	1.05
450		1.10	0.009			
715		0.103	0.047	9.44e-02	0.014	0.92
1080				1.73e-02	0.009	
1588				7.87e-04	0.101	
1986				6.84e-05	0.417	

TLD: No CaF_2. No special cover.

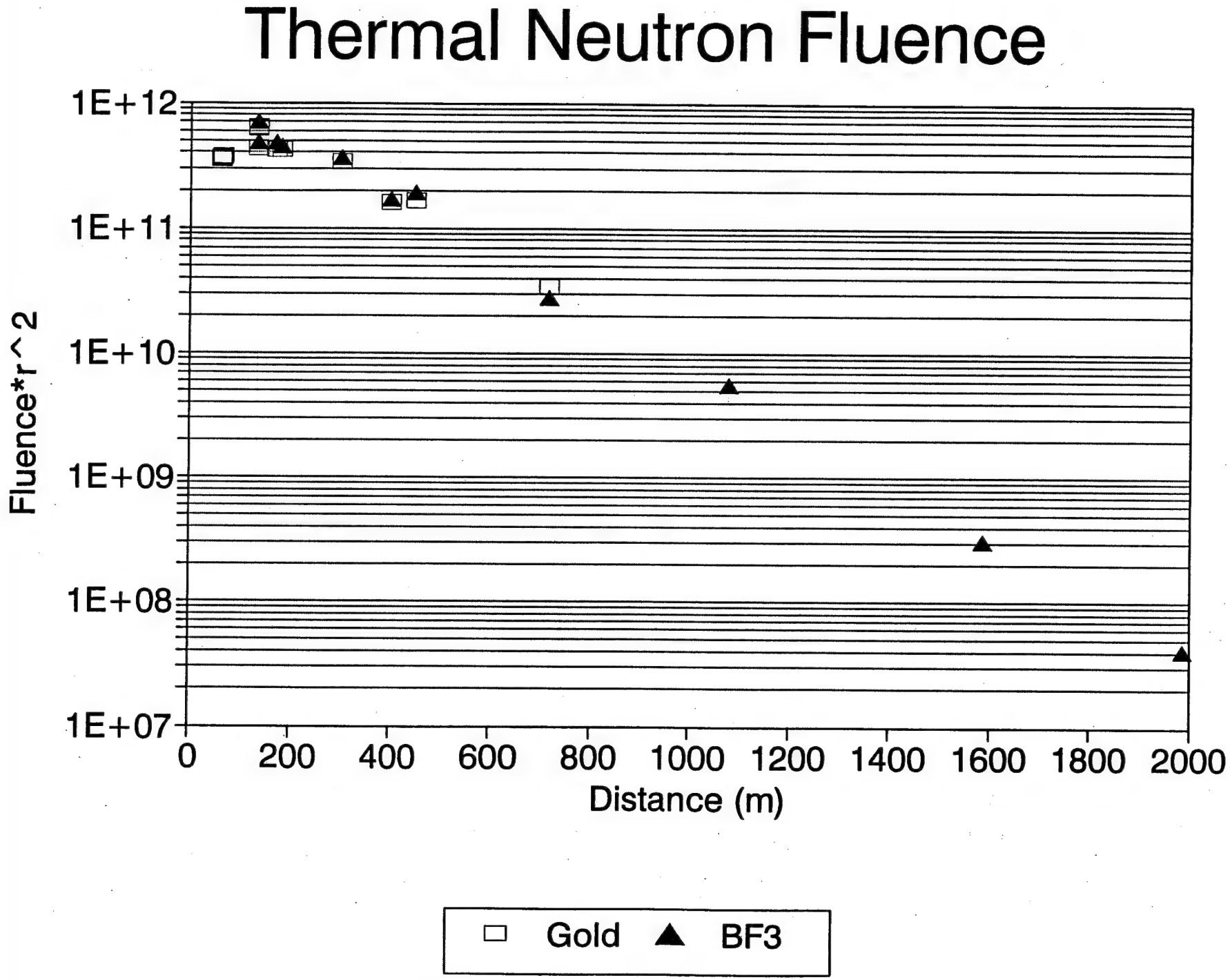

Figure 1. Thermal neutron fluence.

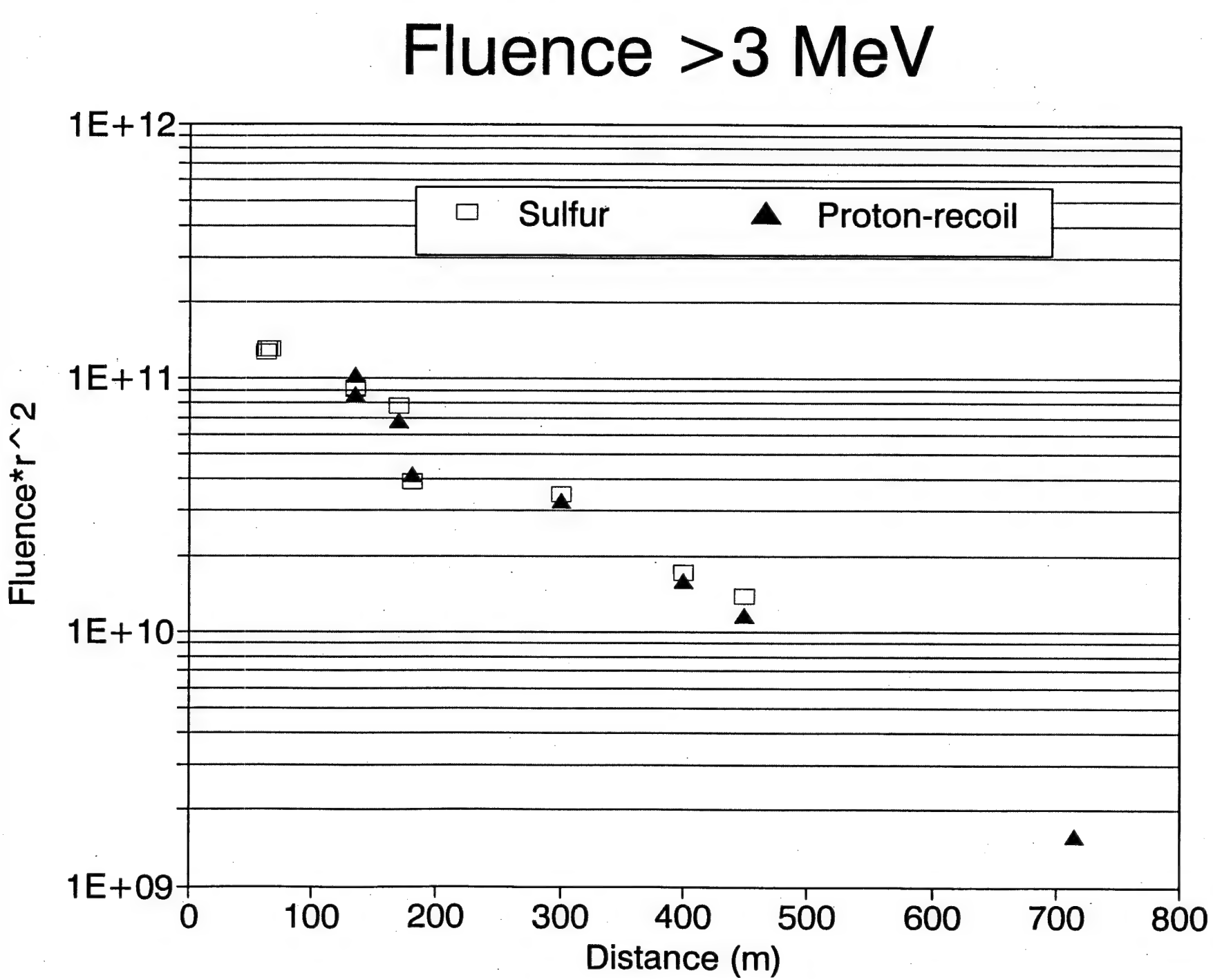

Figure 2. Fluence >3 MeV.

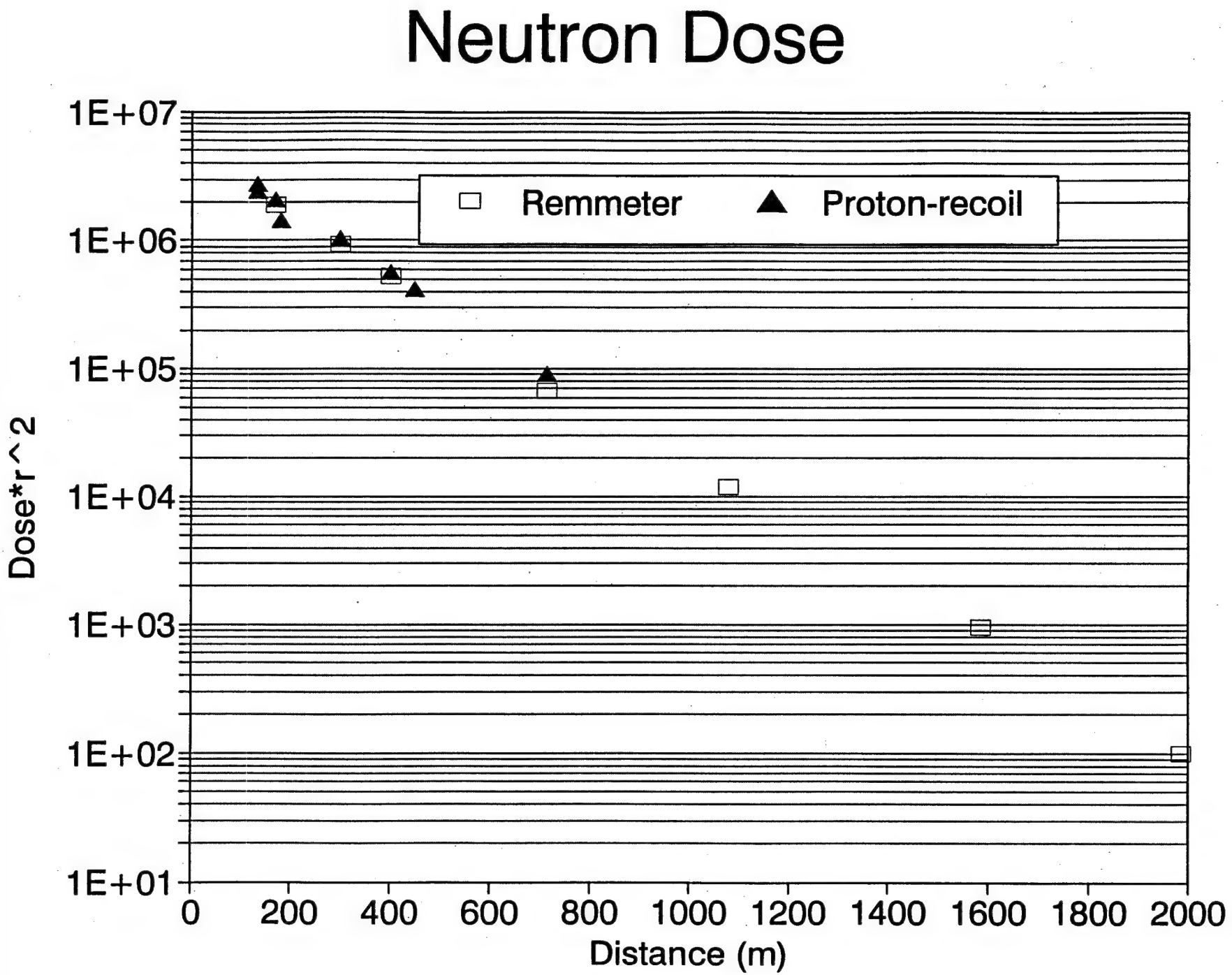

Figure 3. Neutron dose.

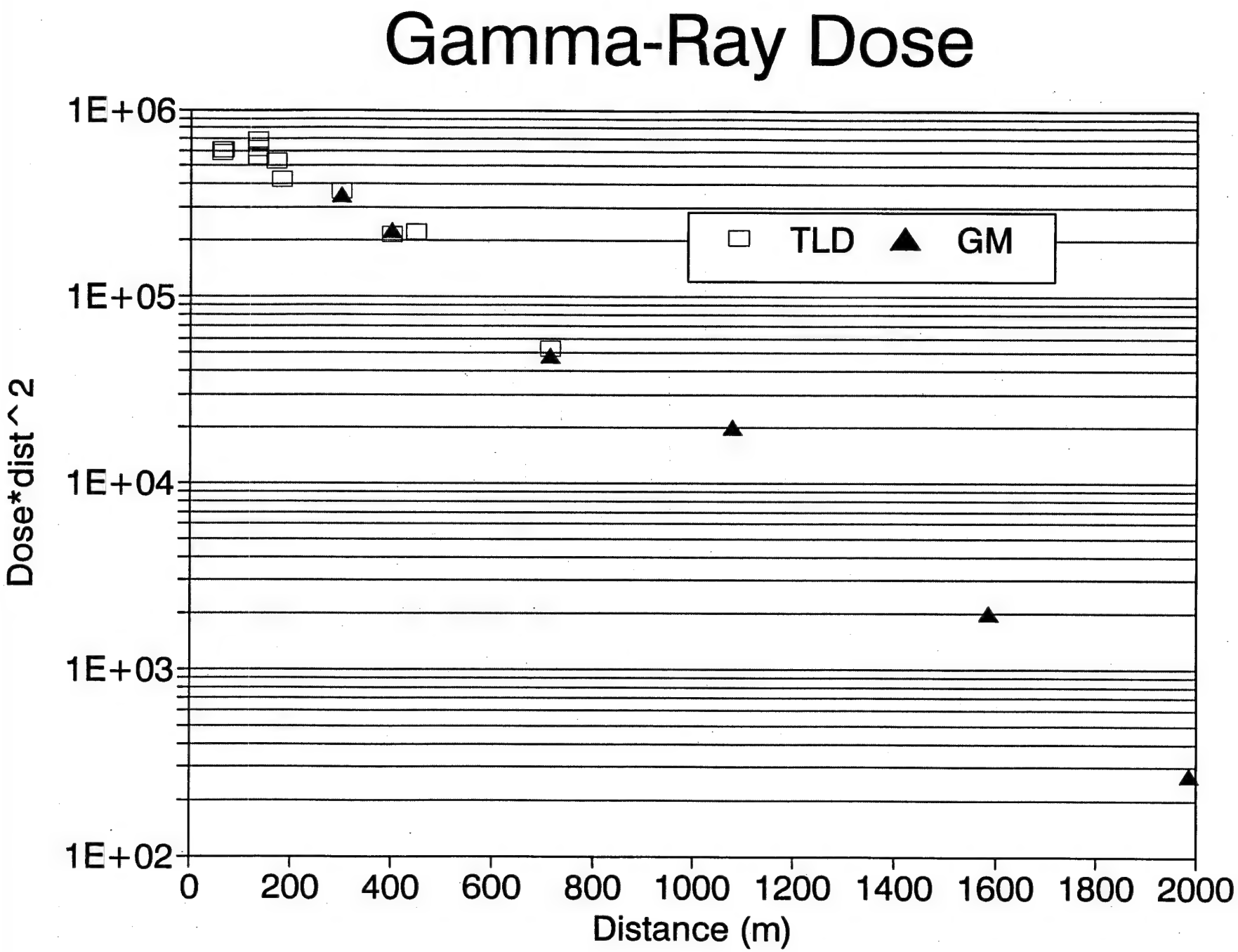

Figure 4. Gamma-ray dose.

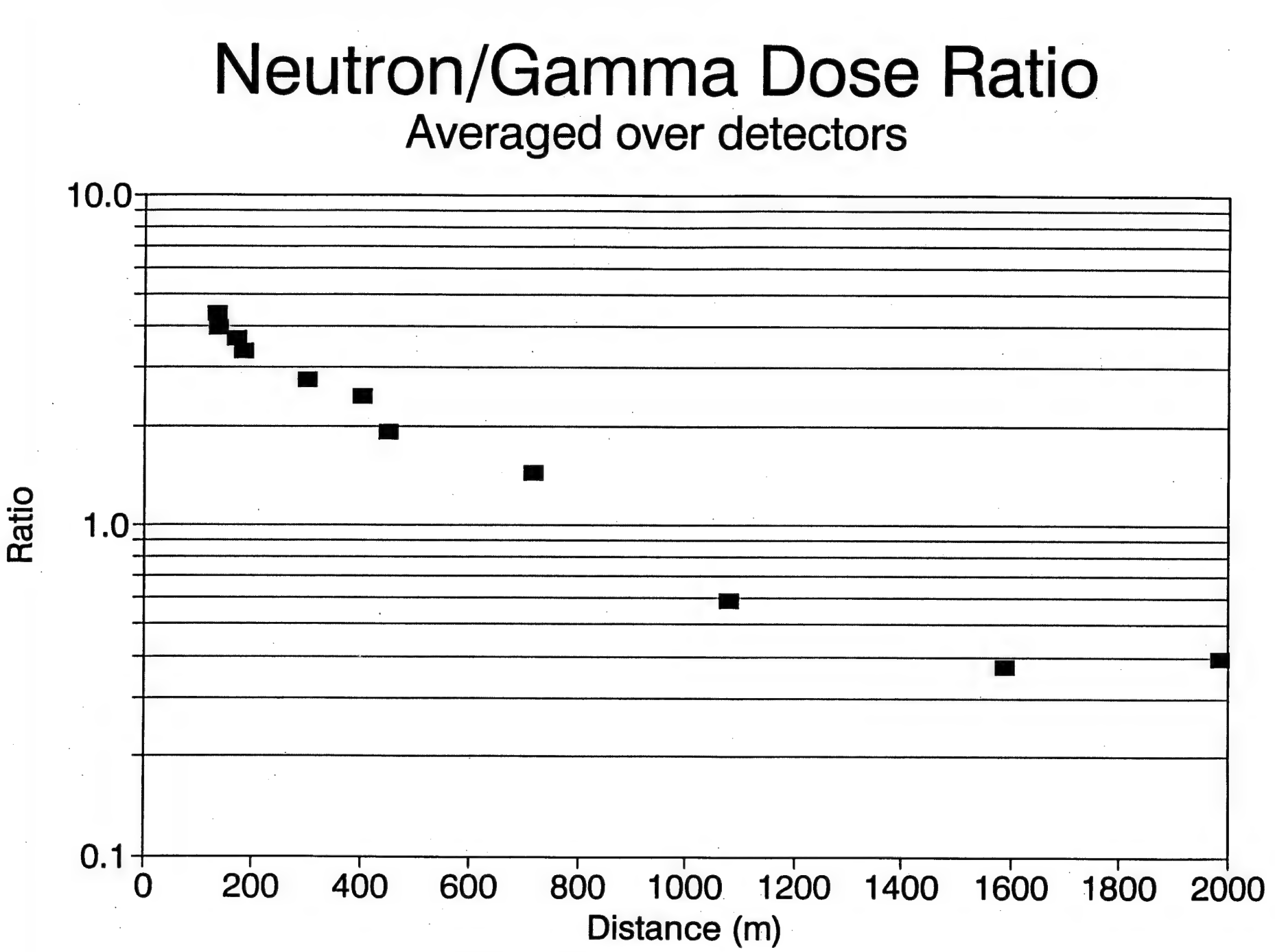

Figure 5. Neutron/gamma-dose ratio.

4. REFERENCES

1. W.E. Loewe, W.A. Turin, C.W. Pollock, A.C. Springer and B.L. Richardson, "Validated Deep-Penetration, Air-Over-Ground, Neutron/Gamma-Ray Transport", Nucl. Sci. Eng., **85**, 87-115 (1983).

2. A.H. Kazi, C.R. Heimbach, R.C. Harrison, H.A. Robitaille, "Comparison of Measured and Calculated Radiation Transport in Air-Over-Ground Geometry to 1.6 km from a Fission Source", Nucl. Sci. Eng., **85**, 371-386 (1983).

3. T. Straume, et. al. Health Physics, **63**, 421-6 (1992).

4. G.D. Kerr, "Photon and Neutron Fluence-to-Kerma Conversion Factors for ICRP-1975 Reference Man Using Improved Elemental Compositions for Bone and Marrow of the Skeleton", ORML-TM-8318 (1982).

APPENDIX A. TEST DATA

1. GEOMETRY OF TEST SITES

The purpose of this appendix is to present the details of the test locations, especially as they might affect the radiation levels. Thermal neutrons were expected to be sensitive to details of the local environment.

The test locations were marked so that they could be reused in successive measurements. Inside 450 meters, the locations were fixed by pipes sunk into the ground. These pipes served as supports for the aluminum stands which held the passive dosimeters. Outside 450 meters, the locations were fixed by stakes, and by noting the location relative to permanent fixtures of the landscape.

All of the positions used are listed in Table A-1. The reference position is the point on the ground directly below the reactor. All other positions are given relative to this location. The angles are given as counterclockwise from above, relative to a line connecting ground zero to the 400-meter position.

The test locations are plotted in Figure A-1 in a map of the area. In selecting measurement locations, an attempt was made to stay away from trees, and to avoid local variations (especially trees and roads), because these would complicate computer modeling.

Some of the locations, especially at 63 meters, turned out to be not quite exact. This was because they were used before they could be surveyed.

The non-zero-degree measurement positions at 63 and 135 meters were used to demonstrate the uniformity of radiation emitted by the reactor.

Figure A-2 shows a test stand in place at 135 meters/180°. The reactor is visible in the background in its test position. Passive dosimetry was attached to a stand. The upright pieces were aluminum angle (2-inch by 2-inch, 1/4-inch thick), 10 feet long. The cross members were aluminum channel (three sides), 1/8-inch thick, 1/2-inch square in cross-section, 2 feet long. Care was taken to keep cadmium-covered detectors at least 3 inches from other detectors.

Figure A-3 shows a standard loading of passive dosimetry. On the left edge is a cadmium-covered large gold foil. On the wire mesh is a cadmium-covered/bare small gold foil set. The cadmium-covered foil is closest to the left. Next is a sulfur foil, a TLD packet, and a large bare gold foil.

Figure A-4 is an areal view of the APRF clear area. The reactor is in its test position. The pickup truck on the right is in the 63-meter/90° location. Zero degrees is from the reactor, through the middle of the path, towards the bottom of the photograph. The clear area, 150 meters in radius, is centered on the silo, not on the reactor outdoor test position.

TABLE A-1. TEST LOCATIONS

Distance (m)	Angle	Relative Position		
		North (m)	East (m)	Height (m)
0.00		0.00	0.00	0.00
62.60	92	-37.98	-49.76	-4.34
63.36	180	-51.28	37.23	-5.75
66.24	271	39.80	52.95	-4.12
135.00	0	109.63	-78.77	-2.76
135.00	90	-78.77	-109.63	-5.78
135.00	180	-109.63	78.77	-7.80
170.00	0	138.06	-99.20	-1.35
181.12	323	181.07	4.06	-3.51
300.00	0	243.63	-175.05	-1.46
400.00	0	324.84	-233.40	-3.18
450.00	0	365.45	-262.58	-3.88
715.00	0	580.65	-417.22	-3.54
1093.61	355	940.94	-557.31	9.22
1588.44	266	825.99	1356.80	-6.60
1986.34	249	509.76	1919.81	-7.00
Reactor		0.00	0.00	12.80

At 90°, the 135-meter location was 9.75 meters from the tree line; at 180°, 18.5 meters.

The 135-meter/0° location was between the road and the gravel path. The through-the-silo location was beyond the parking lot, in front of the woods (22 meters from the parking lot near edge, 20.7 meters from the trees). The 170-meter test position was inside the clear area, to the right of the gravel road.

Figure A-5 shows the same view as Figure A-4, but from the opposite side. At 400 meters, the gravel road across the path is visible. The trailer near 1080 meters is visible as a white dot, beyond the end of the path, and slightly to the right.

Figure A-6 shows a ground view of the 135- and 170-meter test locations. Both are at 0°. The stakes were close to, but not exactly at, the test locations. The survey measurements were to the test locations.

Figure A-7 shows a view of the 400- and 450-meter test locations. The 400-meter location is in the center of a 15-meter wide gravel path. The distance between the trees is 44 meters at the 400-meter test position. The 450-meter location was 10 meters inside the fence, about 16 meters from the trees.

Figures A-8 and A-9 show the 100-foot high crane in place at 715 meters. Figures A-10 and A-11 show experiments being set up at 715 meters. Figure A-12 shows the trailer in place at 1080 meters. The reactor silo is visible in the background. The dirt road going across the picture between the trailer and the silo was the location of the 715-meter position. Figure A-13 is a view outward from the silo towards the 1080-meter location. The dirt road to the lower right of the photograph led to the 715-meter position. Figures A-14 and A-15 show details of the 1040-meter test location.

The reason the 1080-meter position is surveyed at 1093 meters is that the survey position was at the far edge of the hill, and not in the actual test location. Similarly, measurements at the 715-meter location were actually at about 710 meters, since the marker was at the edge of the road towards the reactor.

Figure A-16 is an areal view of the 1600-meter position. The reactor silo is visible in the background. The test location was marked with a circle. Figure A-17 shows more details of this test site, showing a test being set up.

Figures A-18 and A-19 show the 2000-meter test location. The site was in the triangular grassy area above and across the road from the building at the bottom center of the photograph.

Figures A-20 through A-23 are maps of the distant test locations.

DESCRIPTOR	NORTH (METERS)	EAST (METERS)	ELEV (FEET)
"X" Cut	4364779.4758	396554.6370	44.9565
135 N Pos	4364889.1095	396475.8634	35.5000
170 N Pos	4364917.5332	396455.4406	40.1242
300 N Pos	4365023.1072	396379.5845	39.7633
400 N Pos	4365104.3179	396321.2337	34.1270
450 N Pos	4365144.9232	396292.0583	31.8139
715 N Pos	4365360.1260	396137.4214	32.9300
Aluminum Stake	4365530.1825	396193.5013	32.9500
Pt. 1	4364960.5456	396558.6953	33.0400
Pt. 2	4364819.2788	396607.5902	31.0300
Pt. 3	4364728.1987	396591.8637	25.6900
Pt. 4	4364741.4959	396504.8802	30.3100
Pt. 5	4364669.8407	396633.4108	19.9600
Pt. 6	4364700.7612	396449.0027	25.5900
Hub & Tack Set-Top of Mound	4365720.4178	395987.5233	74.8300
Hub & Tack Set @ 1500N	4365405.4459	397911.4328	22.9130
Hub & Tack Set @ 2000N	4365289.2302	398474.4508	21.6040

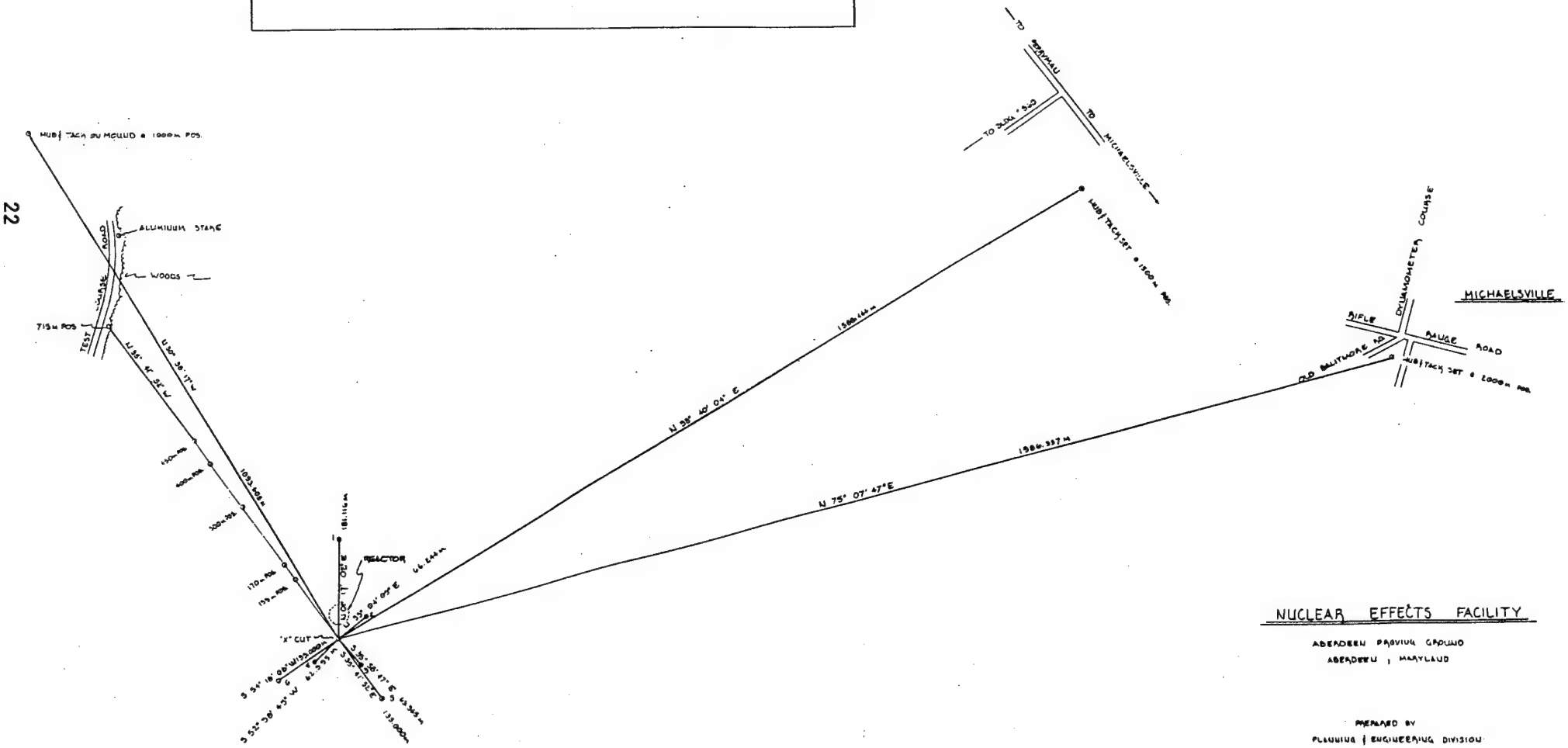

NUCLEAR EFFECTS FACILITY

ABERDEEN PROVING GROUND
ABERDEEN, MARYLAND

PREPARED BY
PLANNING & ENGINEERING DIVISION
COMBAT SYSTEMS TEST ACTIVITY

DRAWN BY: A.D. MATHIAS
CHECKED BY: D.A. GILBERT
DATE: 24 FEB 98
SCALE: 1" = 100m

Figure A-1. Nuclear effects facility map.

Figure A-2. Aluminum test stand at 135 meters, 180°.

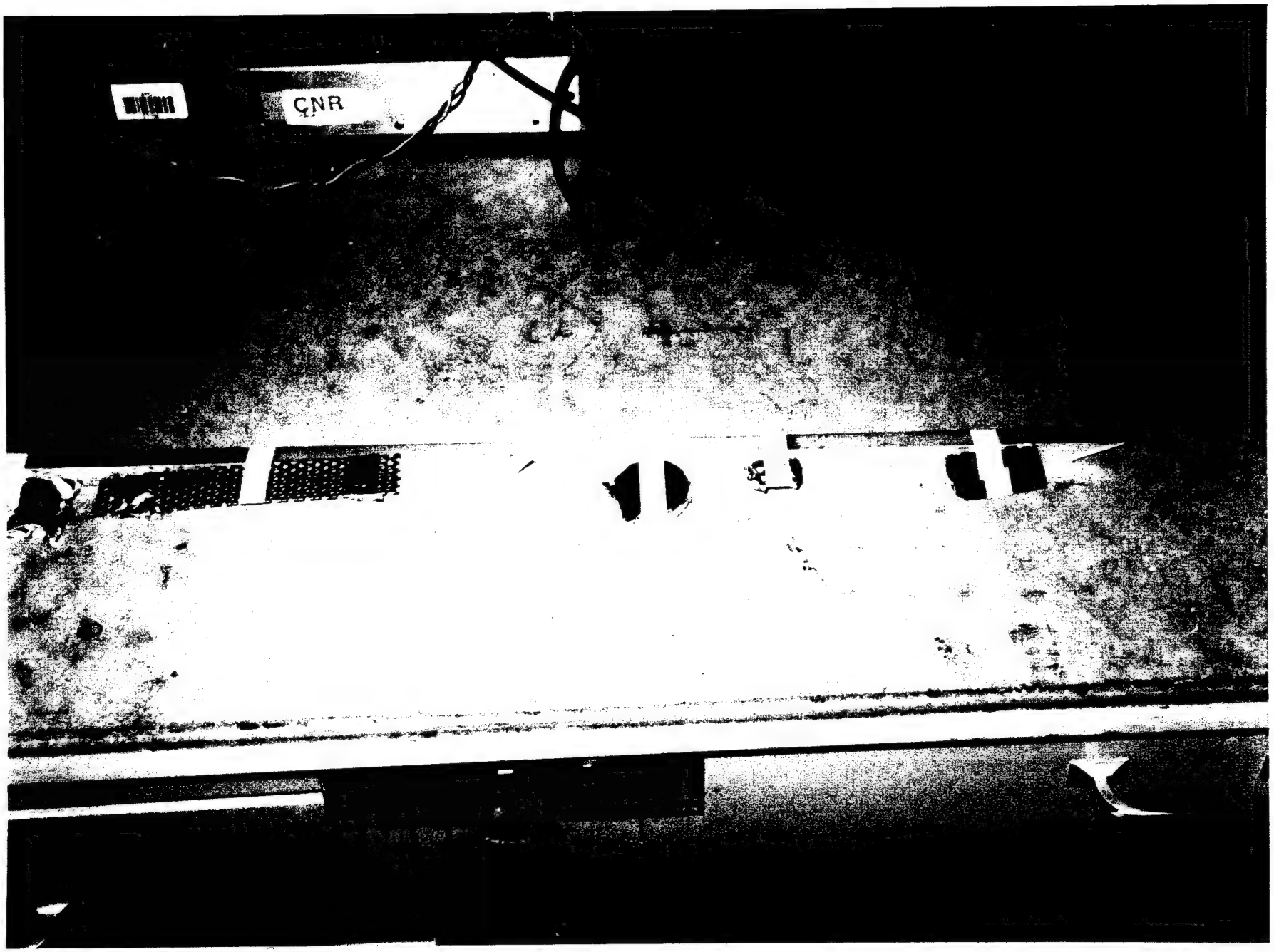

Figure A-3. Aluminum cross piece.

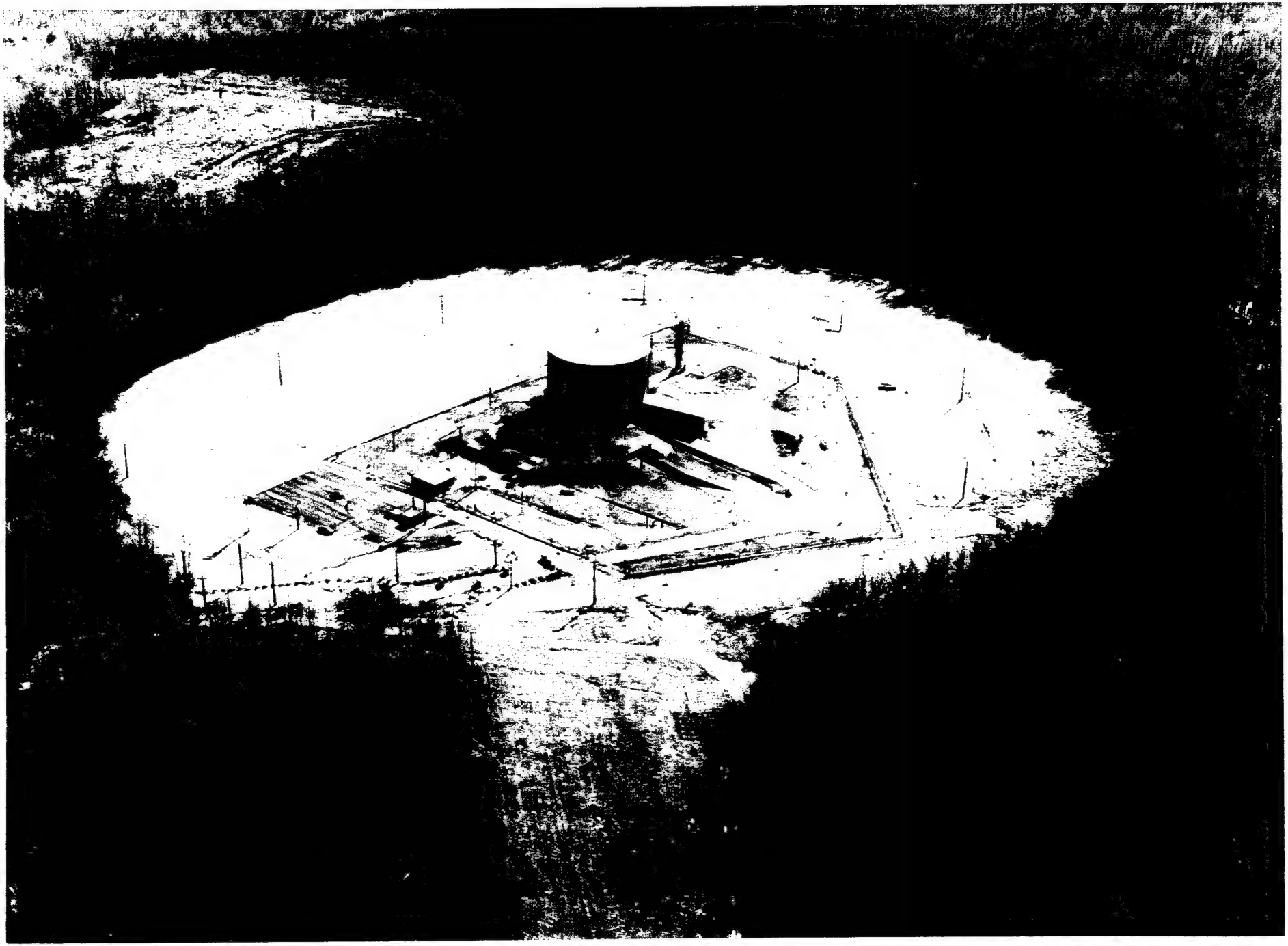

Figure A-4. Areal view of APRF clear area, looking from 0°.

Figure A-5. Areal view of APRF clear area, looking from near 180°.

Figure A-6. 135- and 170-meter test positions.

Figure A-7. 400- and 450-meter test positions.

Figure A-8. 30-meter crane at 715-meter test position (distant view).

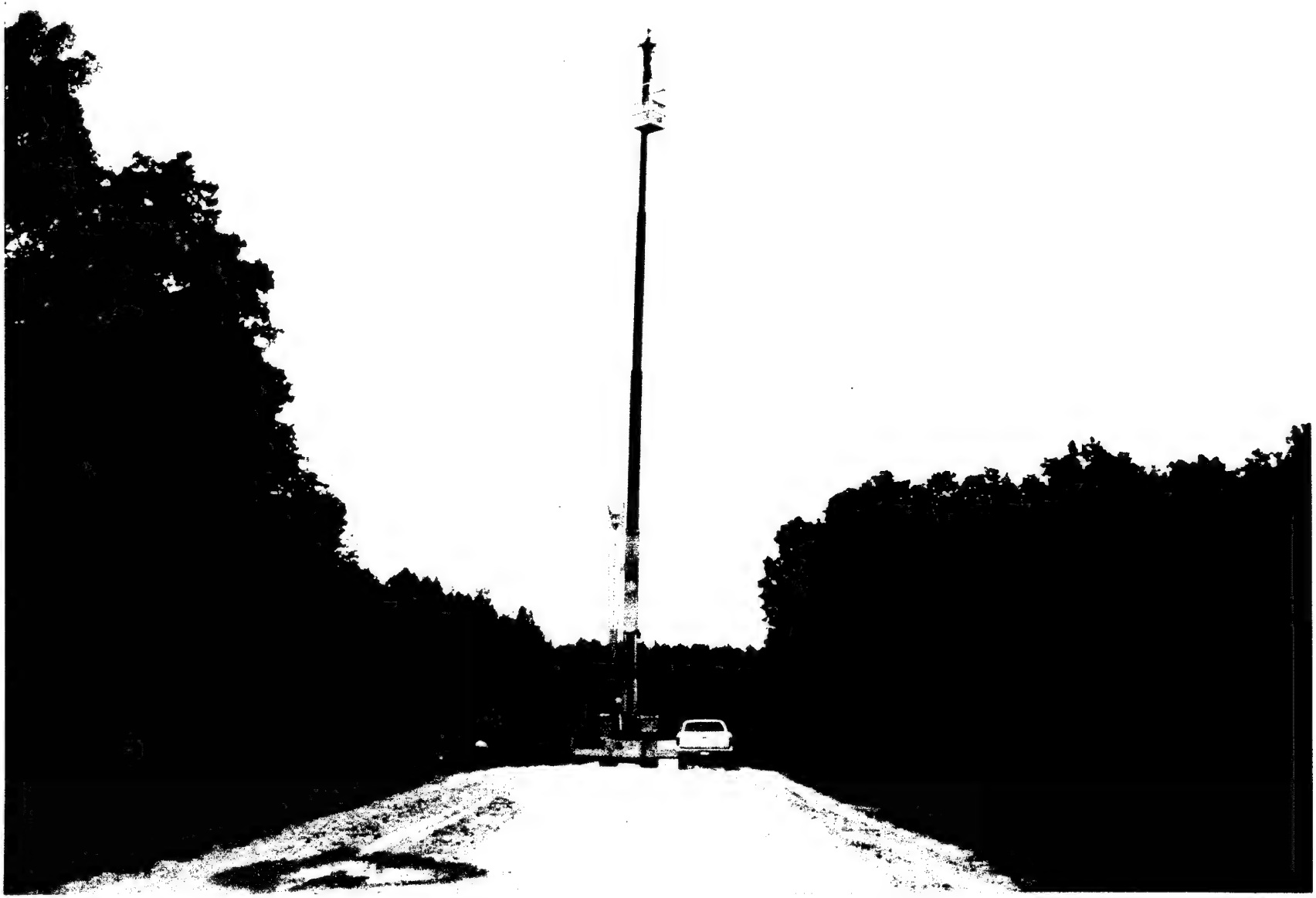

Figure A-9. 30-meter-high crane at 715-meter test position (close view).

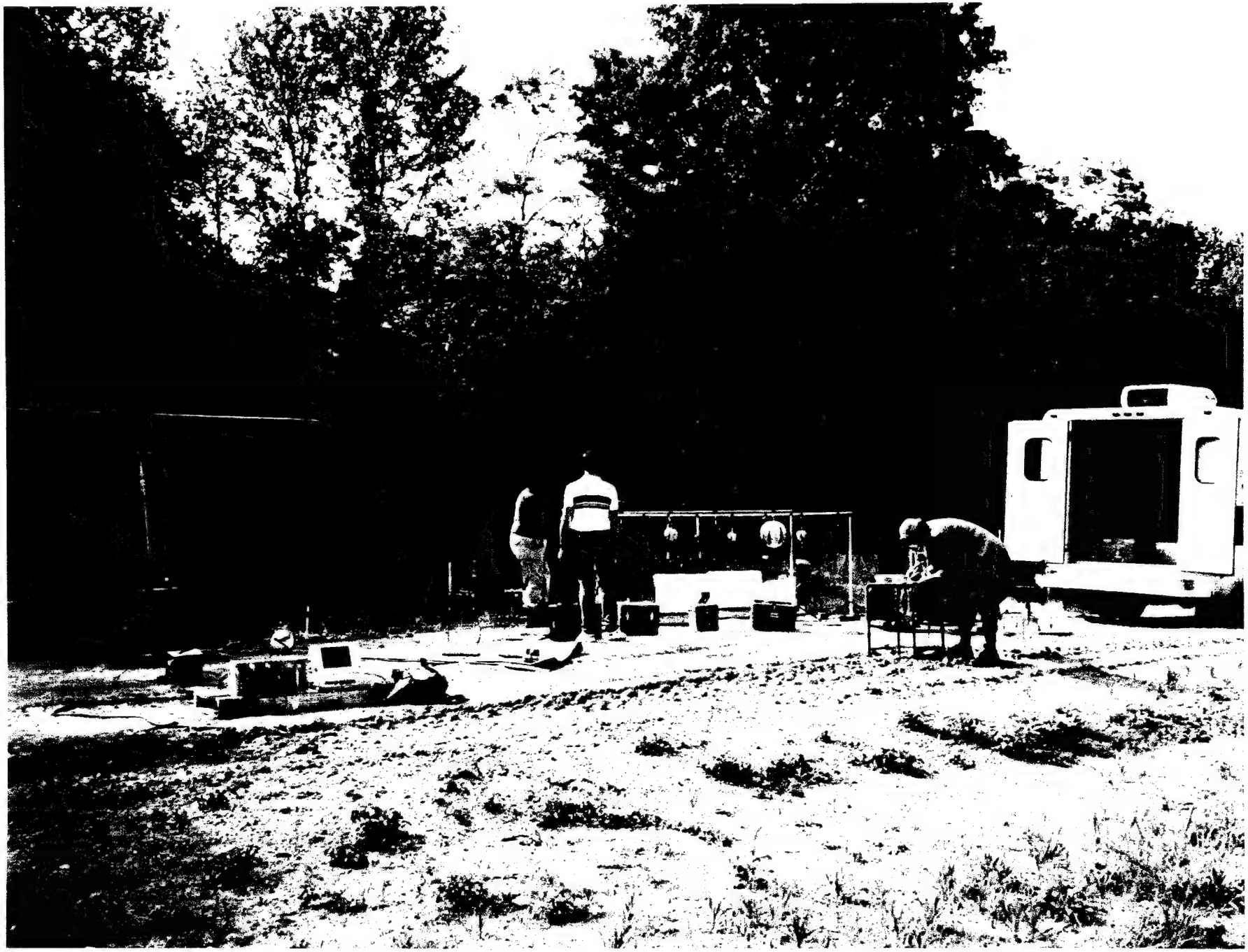

Figure A-10. 715-meter test position.

Figure A-11. 715-meter test position (distant view).

Figure A-12.

Figure A-13. 1080-meter test position, looking from silo direction.

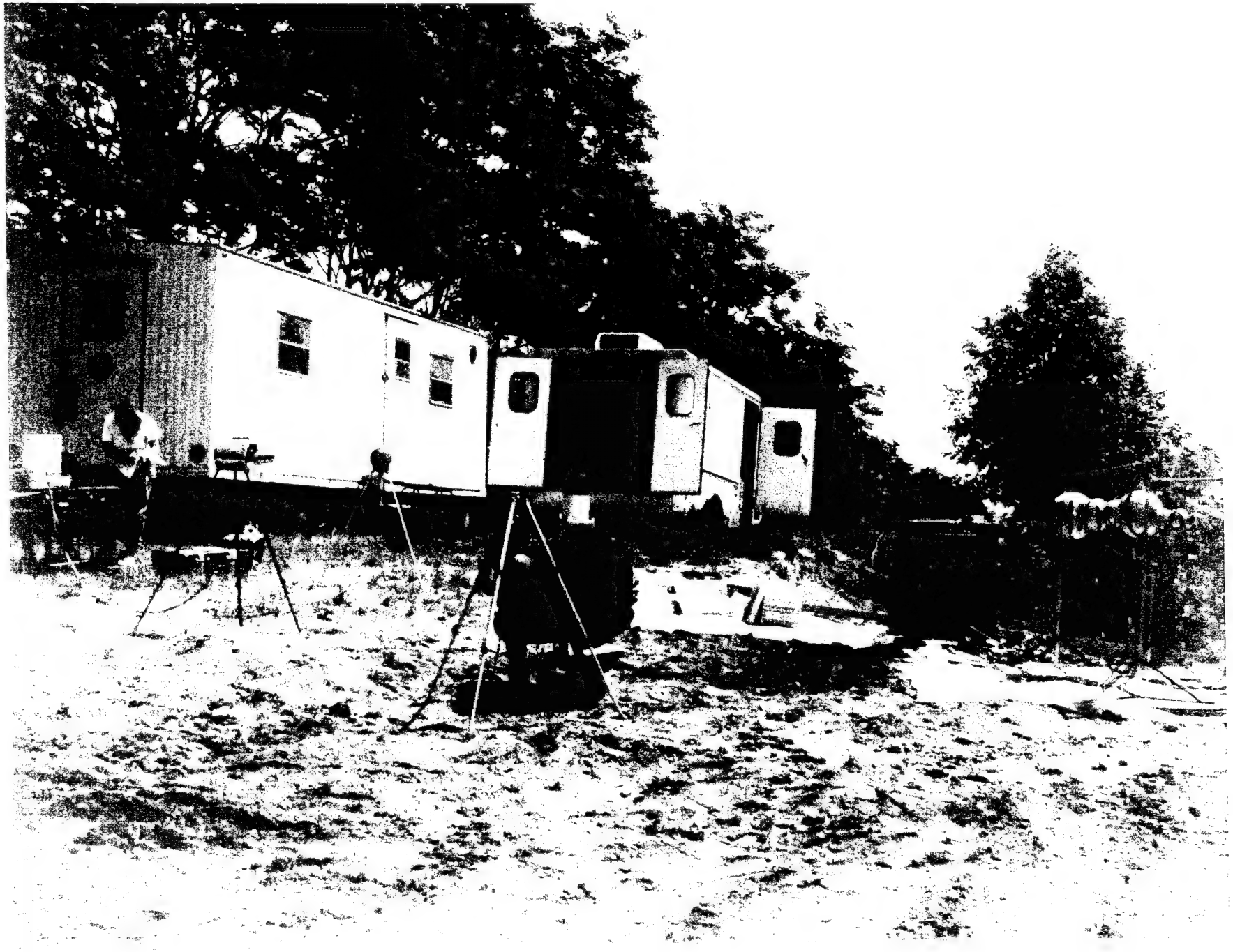

Figure A-14. DOE setup at 1080 meters.

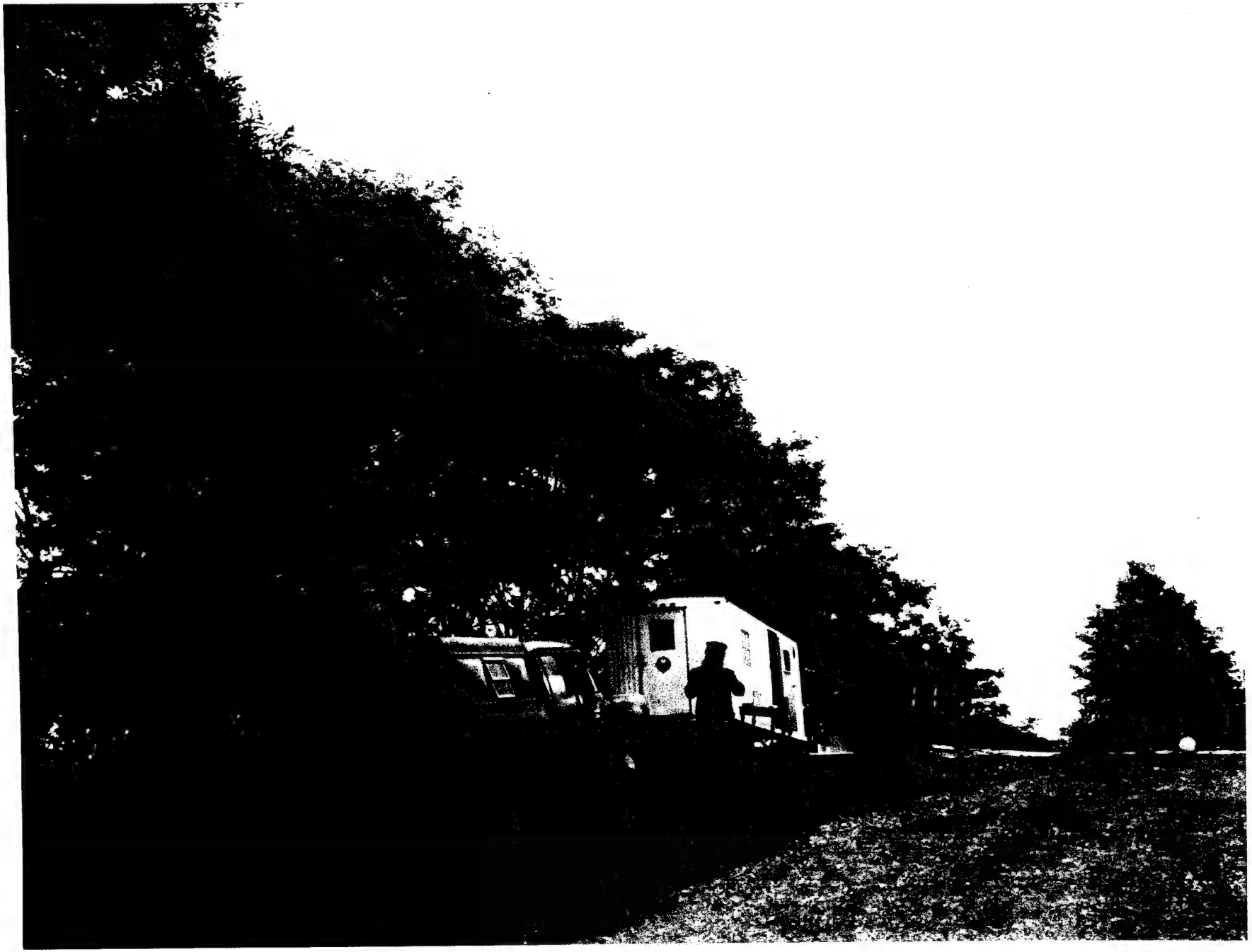

Figure A-15. APRF setup under construction at 1080 meters.

Figure A-16. Overview of 1600-meter test position.

Figure A-17. 1080-meter test position, looking towards silo.

Figure A-18. Overview of 2000-meter test area.

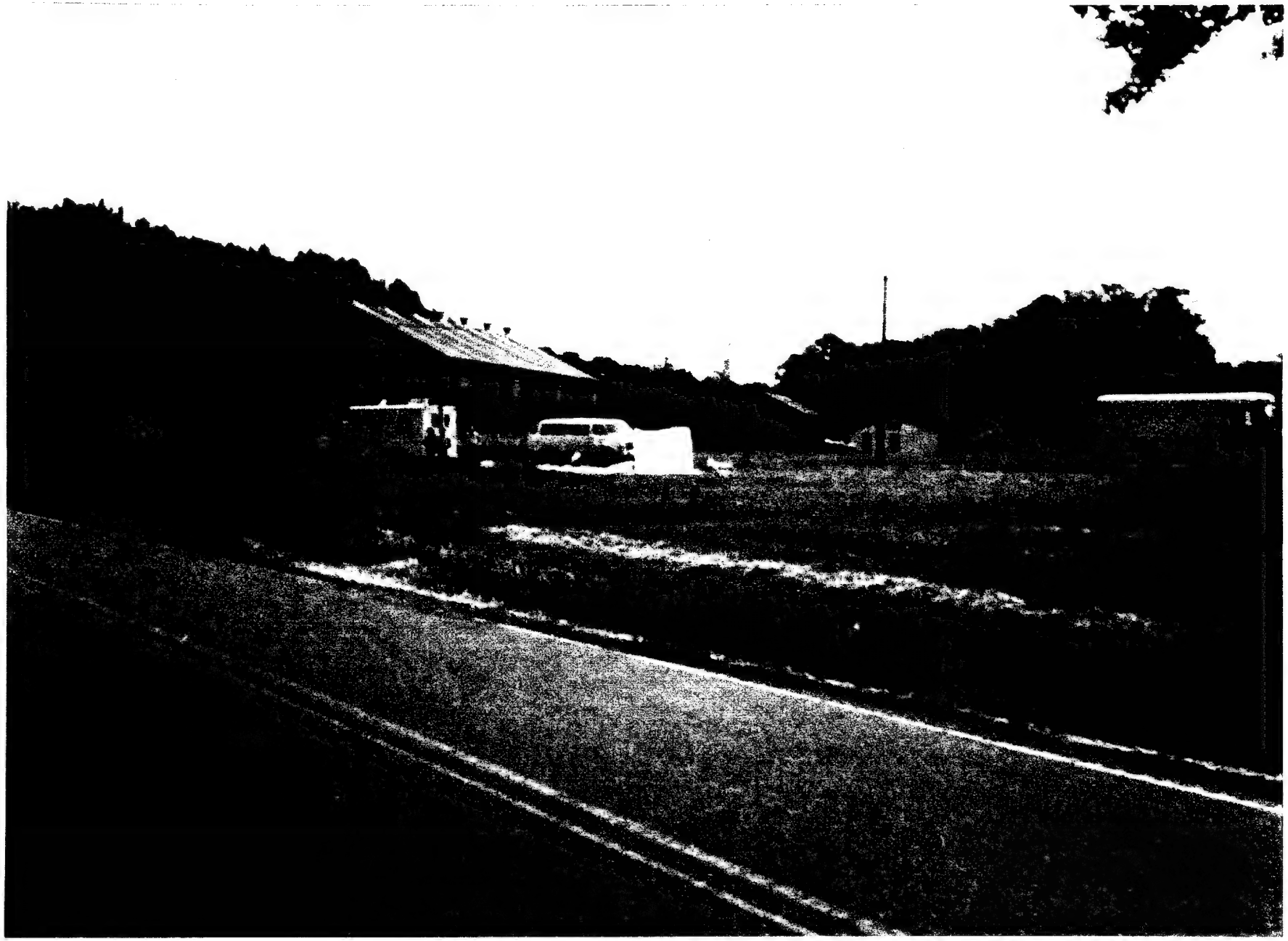

Figure A-19. Ground view of 2000-meter test area.

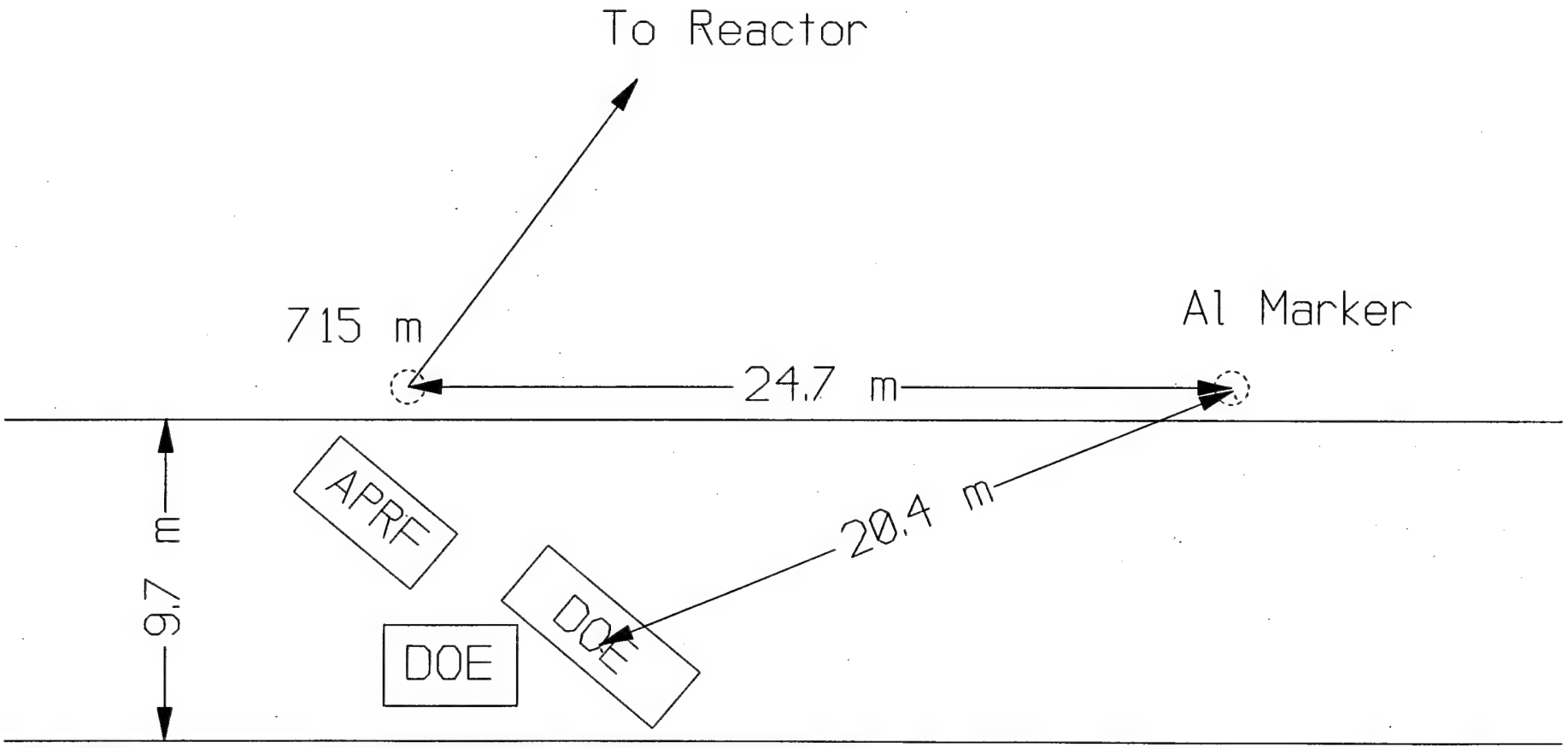

Figure A-20.

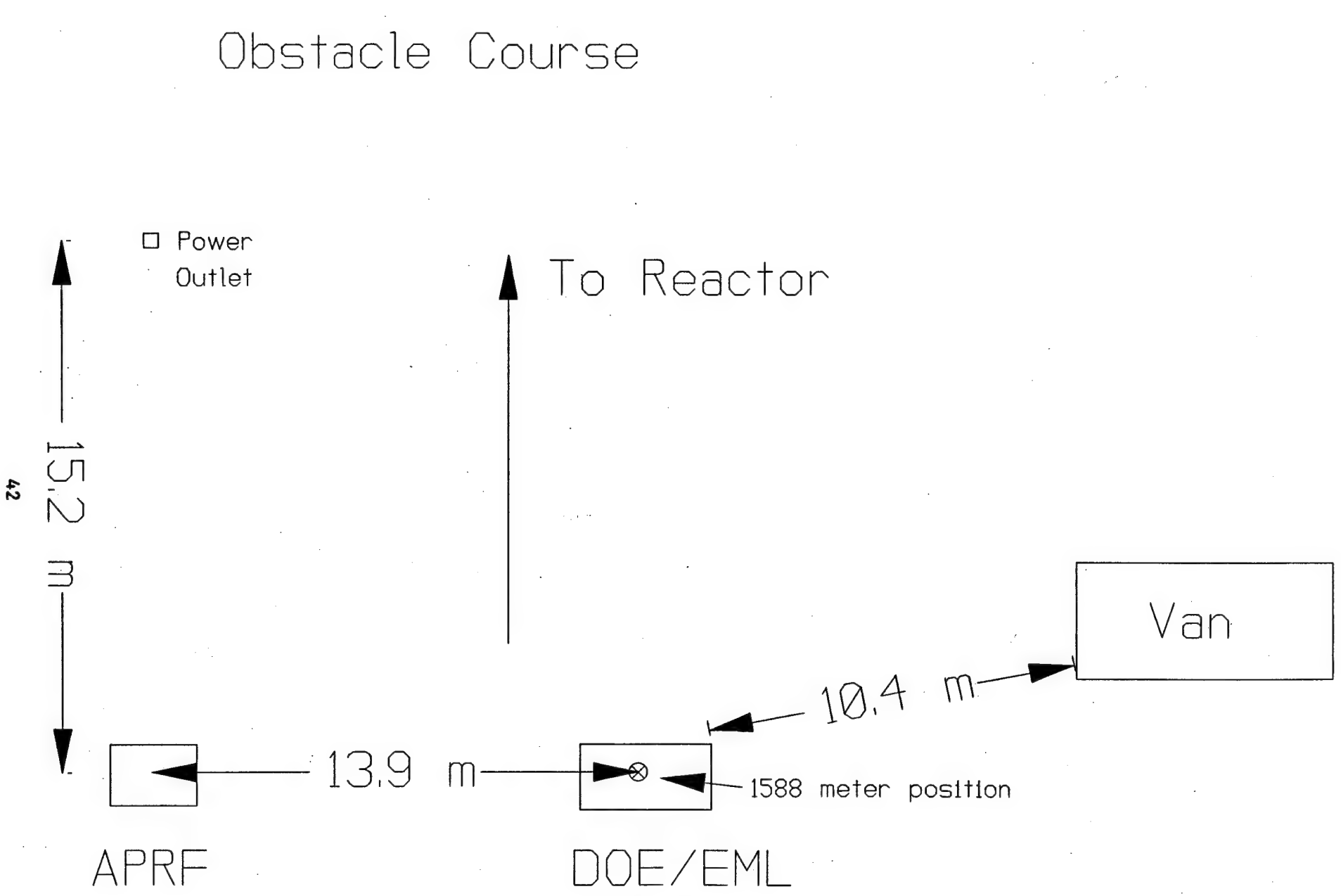
Obstacle Course
Power Outlet
To Reactor
15.2 m
Van
10.4 m
13.9 m
1588 meter position
APRF
DOE/EML

Figure A-21.

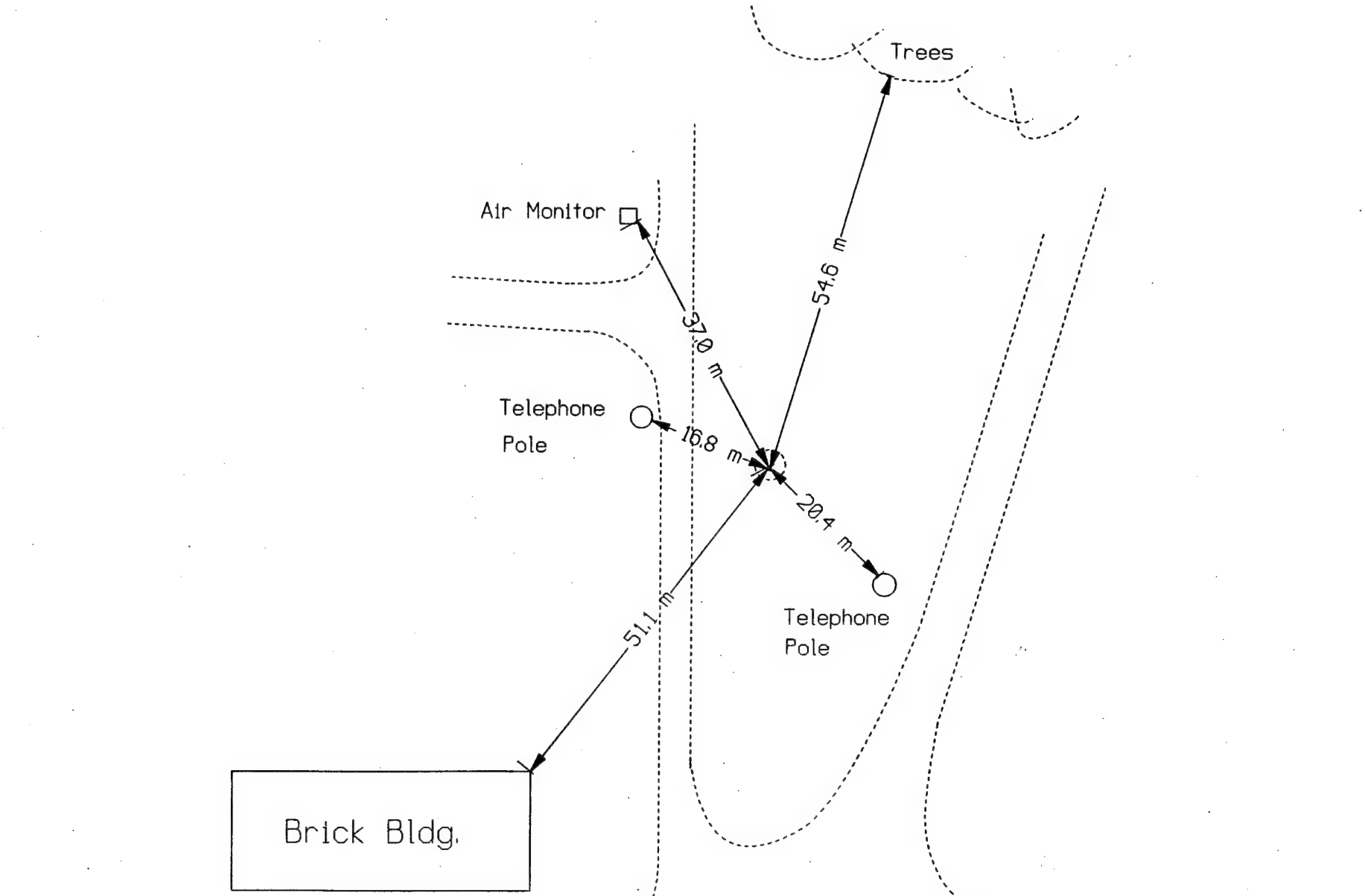
Trees
Air Monitor
54.6 m
37.0 m
Telephone
Pole
16.8 m
20.4 m
Telephone
Pole
51.1 m
Brick Bldg.

Figure A-22.

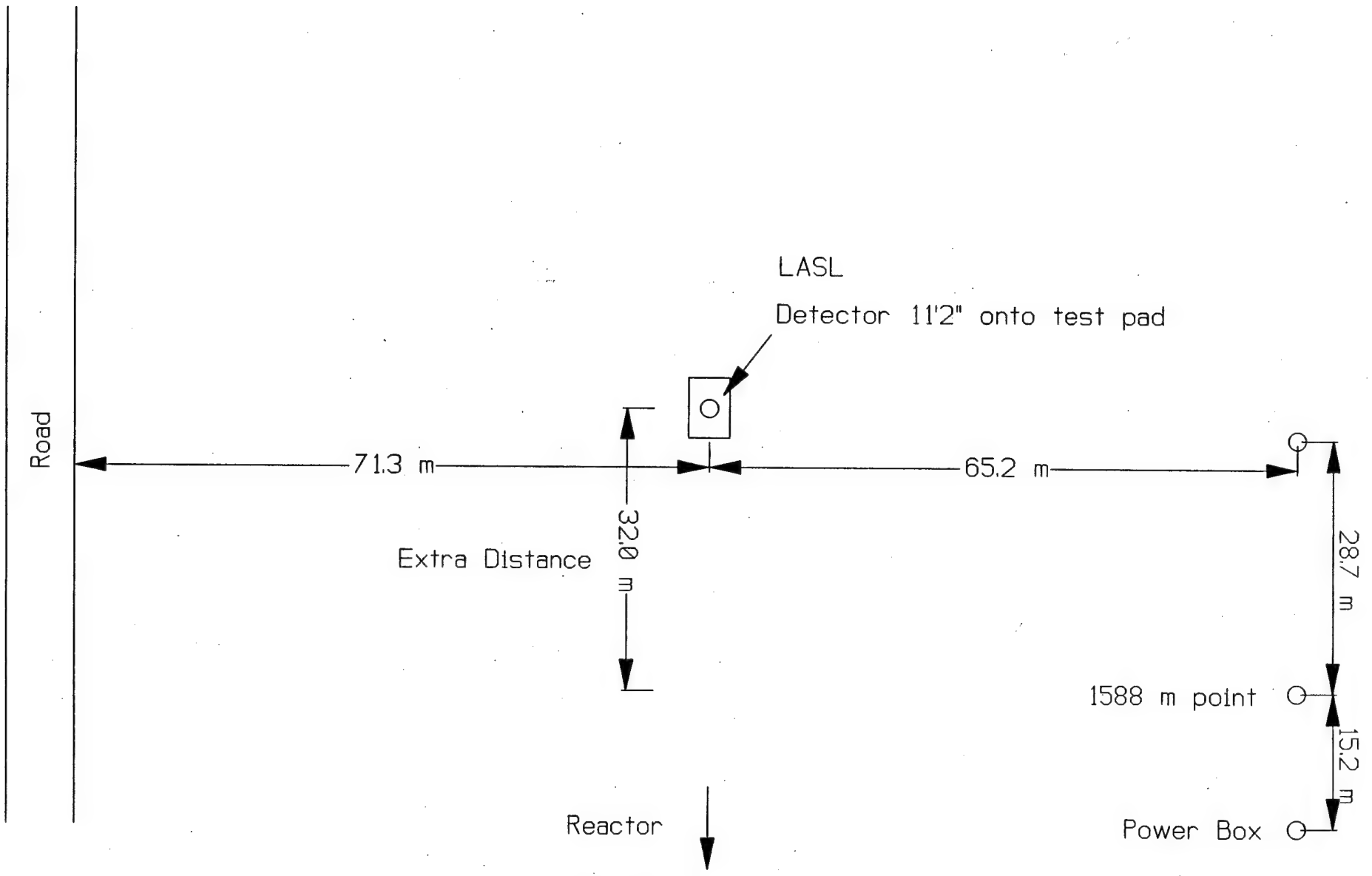
LASL
Detector 11'2" onto test pad
Road
71.3 m
65.2 m
32.0 m
Extra Distance
28.7 m
1588 m point
15.2 m
Reactor
Power Box

Figure A-23.

2. DATA SUMMARY/GOLD DATA FOR DNA OUTDOOR EXPOSURES

Gold foils were used to monitor the thermal neutron fluence around the APRF. The gold reaction of interest is $^{197}Au(N,G)^{198}Au$. This has a 2.69-day half-life, allowing counting to be done for about a week after irradiation.

Bare and cadmium-covered gold foils are used in pairs to monitor thermal neutrons. Gold has a high thermal-neutron cross section, making it a good monitor. It also has a resonance at 5 eV, which can contribute to the activation. To separate the portion due to thermal neutrons, gold foils are run in pairs, one bare and one with a cadmium cover, and the difference is used to determine the thermal neutron fluence.

The ratio of bare to cadmium-covered gold foil activation is known as the cadmium ratio. A high ratio indicates a high degree of thermalization of the neutron spectrum.

Two sizes of foils were used. The small gold foils were circular, 1.11-cm (7/16-in.) diameter by 0.0127-cm (0.005-in.) thick, approximately 0.25 grams each. The large gold foils were rectangular, 1-inch by 1.75-inch, 0.005-inch thick, approximately 2.5 grams each. The cadmium covers were 0.051- and 0.0245-cm (0.020- and 0.010-in.) thick for the small and large foils, respectively.

All irradiations were performed with the foils having the flat side vertical, facing the reactor.

Typically, there were three sets of small gold foils and one large gold foil irradiated at each distance. The small foils were placed at heights of 10, 100, and 300 cm above the ground. The large foils were at 100 cm above the ground.

The gold foils were counted on two high-purity germanium (HPGE) counters and on a Tennelec beta counter. The germanium counters were calibrated with NIST-traceable calibration sources. The beta counter was calibrated relative to the HPGE detectors. Subsequent to the experiment, both counters were calibrated to 5 percent by irradiating gold foils at the NIST thermal beam. The gamma-source and thermal beam calibrations matched to 10 percent. The thermal beam calibration values were used for the results reported here. Using the sources, the reported fluences would be 10 percent lower.

All the gold activation results are listed in Tables A-2 through A-6. The errors given are percentage, and reflect counting statistics only. The net fluences given result from subtracting the cadmium-covered results from the bare results. The units are 2200 m/s equivalent $n/cm^2/kWhr$.

In Table A-2, the gold foils exposed at 715 meters had two heights. The "up" foils were supported by a crane and were 30 meters (100 ft) above the ground. The "down" foils were on a stand, positioned 100 cm above the ground.

All the gold foil data are plotted in Figure A-24. The spread in the data is due to counting statistics, counting reproducibility (uncertainty in mass, positioning on detector, counter drift, etc.), and, possibly, environmental effects. The data given are not corrected for variations in air density, humidity, or ground moisture.

The spread in data at 715 meters is due to the gold foil count rate approaching background. The variation in fluence with angle, apparent at 135 meters, is probably due to the relative location of trees at the different locations, or possibly to variations in ground moisture at these locations. The higher points are at 90 and 180°, which are closer to the trees than the 0° point.

The cadmium ratios are listed in Tables A-2 to A-6, along with the fluence data. The individual bare and cadmium-covered fluences are not listed separately, but may be derived from the data in the tables. For example:

$$\phi_{bare} = \frac{\phi}{1-1/CR}$$

This equation may be used to find the fluence indicated by the bare detector. The fluence for the cadmium-covered detector may be found by subtracting the net fluence from the fluence of the bare detector, or by dividing the bare fluence by the cadmium ratio.

The cadmium ratio is plotted as a function of distance in Figure A-25. This ratio ranges from about 2.2 to 3.5. There is a dependence of this ratio on the location. This ratio tends to be higher at places where more thermalization may be expected to take place. For example, at 135 meters at angles of 90 and 180°, which are located near trees, this ratio is higher than at 0°, which is away from trees. Also, the 400-meter position shows a lower ratio, probably due to the crushed rock covering this area. All of the low ratios at 700 meters are from gold foil pairs raised in the air with a crane during the run.

Figure A-26 shows the variation in thermal neutron fluence with height above ground. Plotted are the ratios of fluence at 10 and 300 cm versus 100 cm. There seems to be a small gradient with height above ground. The 10-cm data show consistently higher fluences than the 100-cm data, by about 5 percent, especially at distances out to 300 meters. Similarly, the 300-cm data are consistently lower than the 100-cm data, again by about 5 percent. Beyond 300 meters, there is no trend, possibly due to poorer statistics.

There is no clear difference in fluence between the 30-meter high and the 1-meter high gold foils at the 715-meter distance. This is almost certainly due to poor statistics.

TABLE A-2. THERMAL NEUTRON FLUENCE AS MEASURED BY GOLD FOILS, SORTED BY FOIL SIZE AND HEIGHT ABOVE GROUND, SS92-66

SS92-66

a. Fluence ($n/cm^2/kwhr$). Error is percentage error.

	large gold		small gold					
Location	100 cm	error	10 cm	error	100 cm	error	300 cm	error
135/0			2.63e+07	0.01	2.62e+07	0.01	2.26e+07	0.02
135/90	3.22e+07	0.01	3.45e+07	0.01	3.26e+07	0.01	3.20e+07	0.01
135/180			3.69e+07	0.01	3.41e+07	0.01	3.14e+07	0.01
170	1.50e+07	0.01	1.81e+07	0.01	1.55e+07	0.01	1.54e+07	0.02
300	3.82e+06	0.01	4.15e+06	0.01	3.86e+06	0.02	3.41e+06	0.02
400	9.80e+05	0.01	1.05e+06	0.03	1.11e+06	0.03	1.08e+06	0.03
450	8.03e+05	0.02	8.71e+05	0.04	8.98e+05	0.03	1.12e+06	0.03
700/up	3.96e+04	0.07			1.20e+05	0.30	5.35e+04	0.19
700/down	6.59e+04	0.02	8.72e+04	0.12				

b. Cadmium Ratio. Error is percentage error.

	large gold		small gold					
Location	100 cm	error	10 cm	error	100 cm	error	300 cm	error
135/0			2.76	0.01	2.82	0.01	2.48	0.01
135/90	3.06	0.01	3.31	0.01	3.16	0.01	3.08	0.01
135/180			3.58	0.01	3.32	0.01	3.13	0.01
170	2.55	0.01	3.10	0.01	2.72	0.01	2.64	0.01
300	3.14	0.01	3.45	0.02	3.25	0.02	2.85	0.02
400	2.44	0.01	2.56	0.03	2.68	0.03	2.66	0.03
450	3.02	0.01	3.28	0.04	3.37	0.04	3.58	0.04
700/up	1.73	0.03			3.32	0.77	1.76	0.10
700/down	2.66	0.03	2.54	0.11				

700/up = 30 meters above ground. 700/down = 1 meter above ground.

TABLE A-3. THERMAL NEUTRON FLUENCE AS MEASURED BY GOLD FOILS, SORTED BY FOIL SIZE AND HEIGHT ABOVE GROUND, SS92-154

SS92-154

a. Fluence ($n/cm^2/kwhr$). Error is percentage error.

	large gold		small gold					
Location	100 cm	error	10 cm	error	100 cm	error	300 cm	error
170	1.37e+07	0.02						
400	1.04e+06	0.02						

b. Cadmium ratio. Error is percentage error.

	large gold		small gold					
Location	100 cm	error	10 cm	error	100 cm	error	300 cm	error
170	2.38	0.03						
400	2.50	0.03						

TABLE A-4. THERMAL NEUTRON FLUENCE AS MEASURED BY GOLD FOILS, SORTED BY FOIL SIZE AND HEIGHT ABOVE GROUND, SS92-157

SS92-157

a. Fluence ($n/cm^2/kwhr$). Error is percentage error.

	large gold		small gold					
Location	100 cm	error	10 cm	error	100 cm	error	300 cm	error
135	2.26e+07	0.01	2.57e+07	0.02	2.52e+07	0.02	2.19e+07	0.02
170	1.42e+07	0.01	1.62e+07	0.02	1.48e+07	0.02	1.34e+07	0.02
300	3.57e+06	0.01	4.16e+06	0.02	3.92e+06	0.02	4.14e+06	0.02
400	9.75e+05	0.01	1.15e+06	0.03	1.19e+06	0.03	1.18e+06	0.03
450	7.60e+05	0.01	8.99e+05	0.03	9.08e+05	0.03	8.32e+05	0.03

b. Cadmium ratio. Error is percentage error.

	large gold		small gold					
Location	100 cm	error	10 cm	error	100 cm	error	300 cm	error
135	2.39	0.02	2.89	0.01	2.86	0.01	2.45	0.01
170	2.36	0.02	2.60	0.02	2.54	0.01	2.39	0.01
300	2.87	0.02	3.14	0.02	3.15	0.02	3.37	0.02
400	2.39	0.02	2.67	0.03	2.69	0.03	2.47	0.03
450	2.76	0.03	3.25	0.04	3.12	0.03	3.01	0.03

TABLE A-5. THERMAL NEUTRON FLUENCE AS MEASURED BY GOLD FOILS, SORTED BY FOIL SIZE AND HEIGHT ABOVE GROUND, SS92-186

SS92-186

a. Fluence ($n/cm^2/kwhr$). Error is percentage error.

	large gold		small gold					
Locatio	100 cm	error	10 cm	error	100 cm	error	300 cm	error
63/90			9.81e+07	0.01	8.98e+07	0.01		
64/180			9.07e+07	0.01	8.85e+07	0.01		
66/270			8.44e+07	0.01	8.74e+07	0.01		
135/0			2.47e+07	0.01	2.26e+07	0.01		
135/90			3.44e+07	0.01	3.59e+07	0.01		
135/180			3.62e+07	0.01	3.64e+07	0.01		
181/sil			1.36e+07	0.01	1.26e+07	0.01		
170/0			1.41e+07	0.03	1.39e+07	0.01		

b. Cadmium ratio. Error is percentage error.

	large gold		small gold					
Locatio	100 cm	error	10 cm	error	100 cm	error	300 cm	error
63/90			2.67	0.01	2.56	0.01		
64/180			2.60	0.01	2.55	0.01		
66/270			2.56	0.01	2.57	0.01		
135/0			2.51	0.01	2.31	0.01		
135/90			3.02	0.01	3.21	0.01		
135/180			3.20	0.01	3.26	0.01		
181/sil			2.66	0.01	2.42	0.01		
170/0			2.35	0.02	2.36	0.01		

TABLE A-6. THERMAL NEUTRON FLUENCE AS MEASURED BY GOLD FOILS, SORTED BY FOIL SIZE AND HEIGHT ABOVE GROUND, SS92-210

SS92-210

a. Fluence ($n/cm^2/kwhr$). Error is percentage error.

	large gold		small gold					
Location	100 cm	error	10 cm	error	100 cm	error	300 cm	error
135/0	2.30e+07	0.01	2.70e+07	0.01	2.36e+07	0.01	2.18e+07	0.01
170	1.36e+07	0.01	1.51e+07	0.01	1.49e+07	0.01	1.44e+07	0.01
300	3.58e+06	0.01	3.84e+06	0.01	3.74e+06	0.01	3.43e+06	0.01
400	1.01e+06	0.01	1.15e+06	0.02	9.96e+05	0.02	1.07e+06	0.02
450	8.26e+05	0.01	8.25e+05	0.03	8.77e+05	0.03	7.44e+05	0.03

b. Cadmium ratio. Error is percentage error.

	large gold		small gold					
Location	100 cm	error	10 cm	error	100 cm	error	300 cm	error
135/0	2.48	0.01	2.89	0.01	2.51	0.01	2.38	0.01
170	2.33	0.01	2.54	0.01	2.57	0.01	2.47	0.01
300	2.86	0.01	3.02	0.01	2.96	0.01	2.76	0.01
400	2.41	0.00	2.66	0.02	2.41	0.02	2.50	0.02
450	2.97	0.00	2.84	0.03	3.08	0.03	2.38	0.03

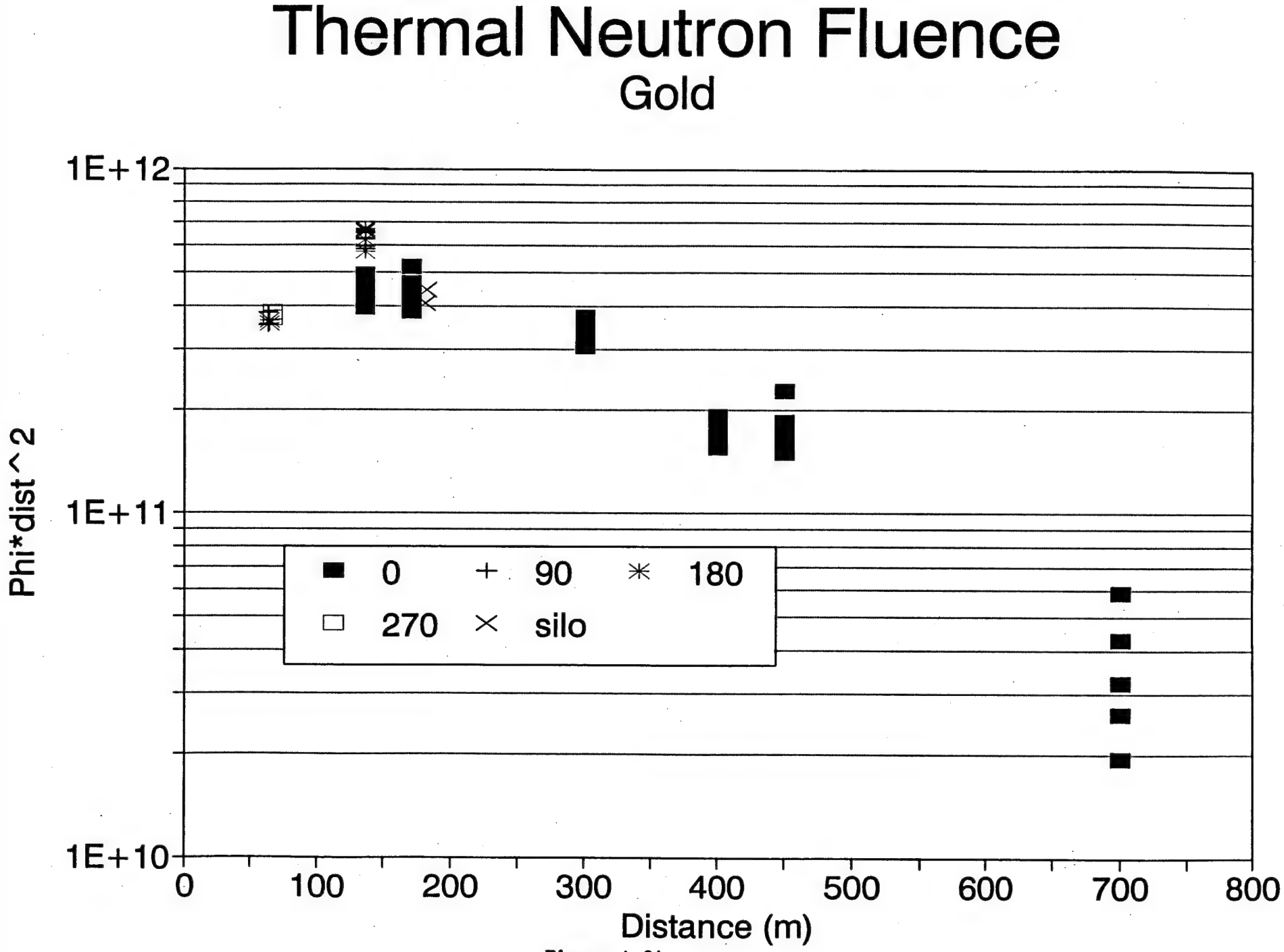
Thermal Neutron Fluence
Gold
1E+12
1E+11
1E+10
Phi*dist^2
0
90
180
270
silo
0
100
200
300
400
500
600
700
800
Distance (m)

Figure A-24.

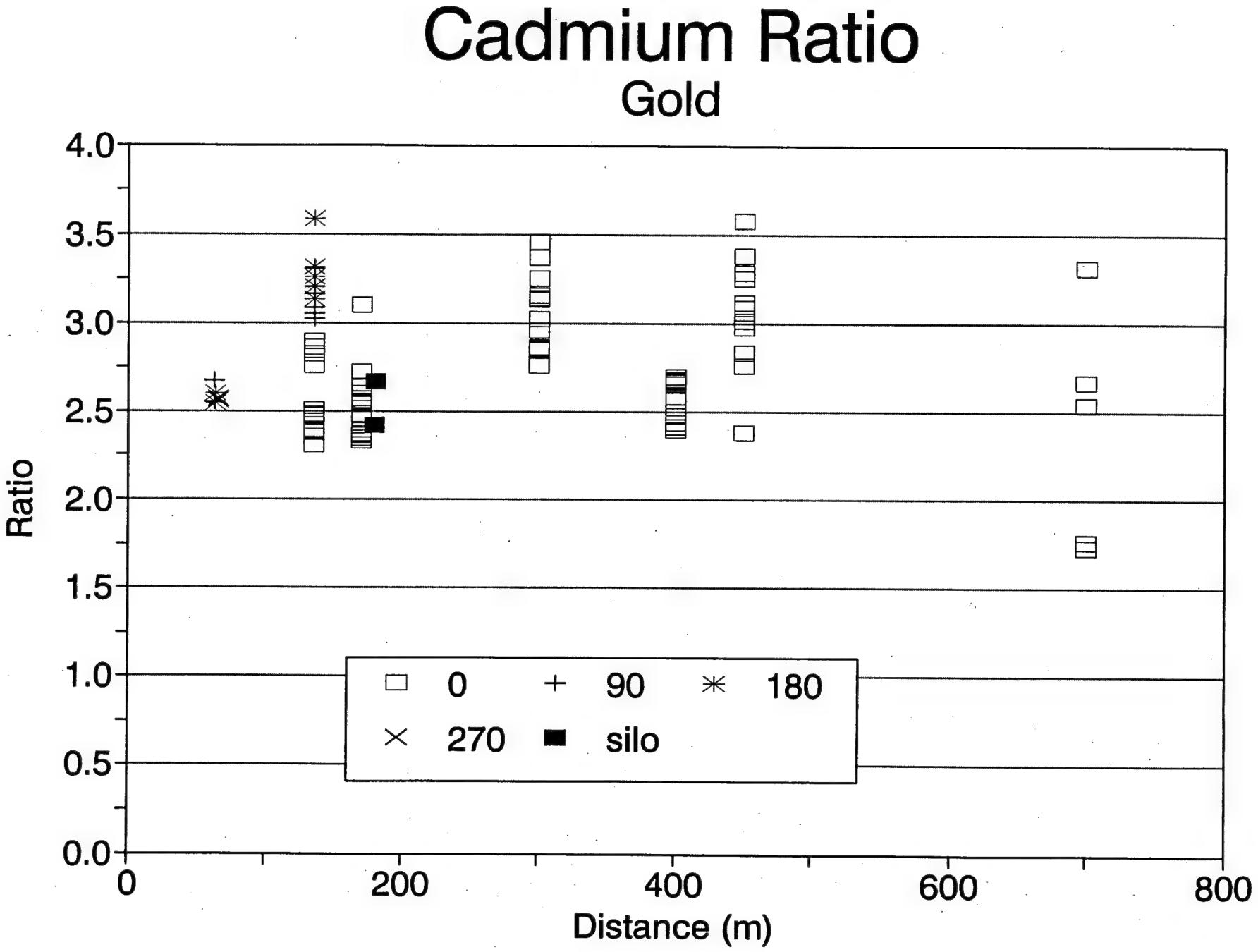
Cadmium Ratio
Gold
Ratio
4.0
3.5
3.0
2.5
2.0
1.5
1.0
0.5
0.0
0
200
400
600
800
Distance (m)
0
90
180
270
silo

Figure A-25.

Thermal Neutron Height Effect

Gold

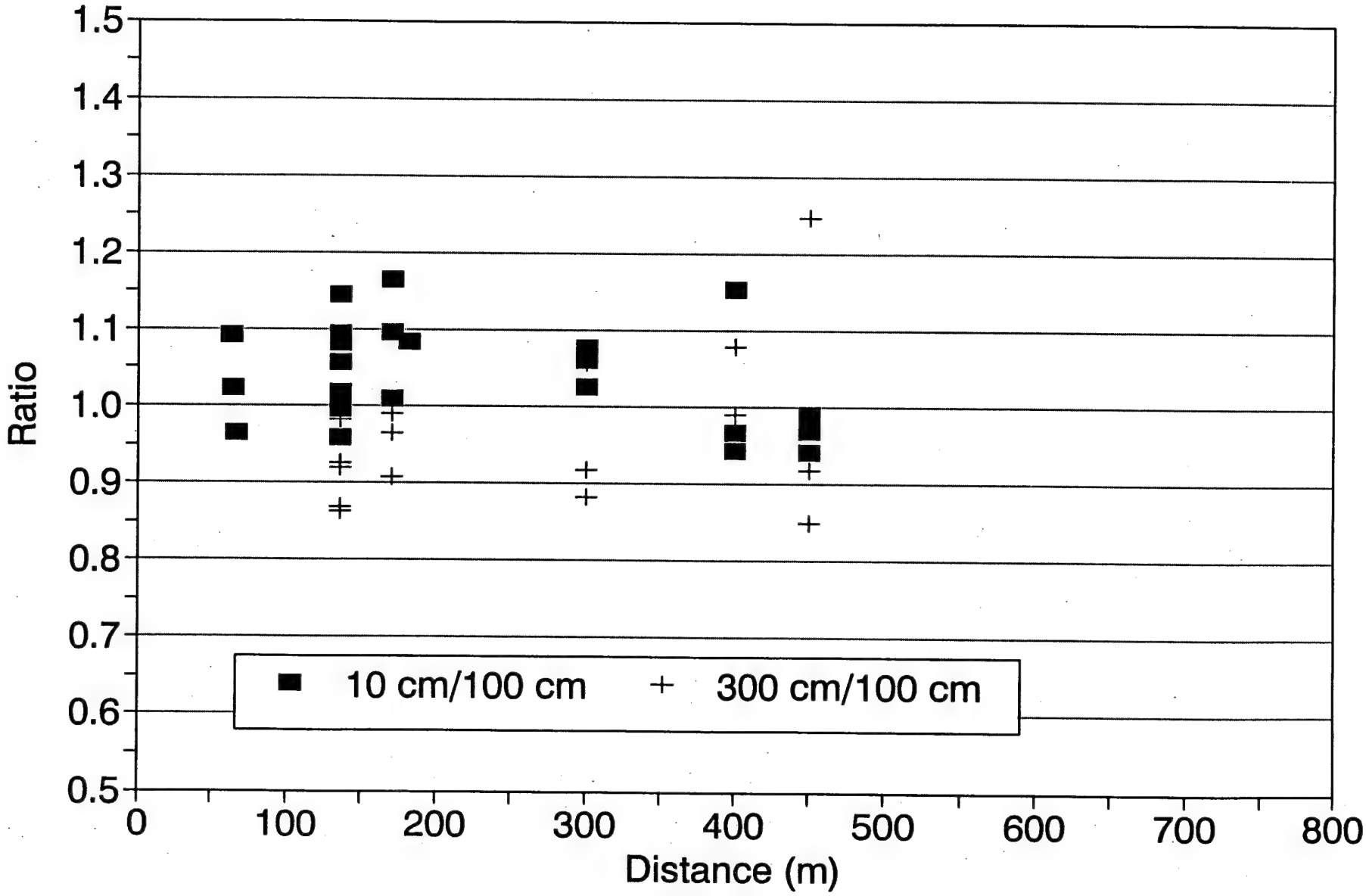

Figure A-26.

3. DATA SUMMARY/BF_3 DATA FOR DNA OUTDOOR EXPOSURES

Bare and cadmium-covered gas-filled BF_3 detectors were used to monitor thermal neutrons for outdoor measurements. They were always run as a pair. The bare minus the cadmium-covered measurements was proportional to the thermal neutron fluence.

The cadmium thickness used was 0.040 inch. The tubes are cylindrical, with outside dimensions of 2.5-cm diameter by 25-cm high. They were filled with 94 cc of BF_3 gas enriched to 96-percent boron-10 to a pressure of 40 cm (Hg). The detectors were run with the centers 70 cm above the ground.

The measurement used active electronics, so only one location could be measured at any time. The signal from each detector was fed into a multichannel analyzer for subsequent analysis. All counts above a valley separating neutrons from gamma rays were used to determine the number of events in each detector.

All detectors were calibrated directly in the NIST thermal neutron beam. The calibration factor used is for side-on incidence of the neutrons. In the field, the detectors were normally vertical. No corrections were made for additional attenuation that might be seen in the actual neutron distribution.

All the measurements are given in Table A-7. The BF_3-measured thermal neutron fluence is plotted in Figure A-27. The data closely follow an $e^{-\mu r}/r^2$ behavior despite variations in ground moisture and proximity to trees. The data at 715 meters seem slightly depressed relative to the others. This might be due to the trees near the test area between the detector location and the reactor.

The cadmium ratio, the ratio of bare to cadmium-covered fluences, is plotted in Figure A-28. The data tend to cluster around a value of 12, but with local variations. For example, the 135-meter point near the trees (135 m/180°) is significantly higher than the 135-meter/0° point, which has no trees and less ground moisture. Similarly, 300 and 450 meters have higher moisture than 170 and 400 meters, and higher cadmium ratios. These local variations explain what appears to be a slight decrease of cadmium ratio with distance. The large variations in cadmium ratio at farther distances is due to low count rates.

Table A-8 gives the results of measurements with one of the tubes vertical and one horizontal. All tubes were bare for this set. The horizontal tube was either end-on or broadside to the reactor. Orientation had little effect on count rate.

The fluences for the bare and cadmium-covered detectors are not given separately, but may be derived from the given data. For example:

$$\phi_{bare} = \frac{\phi}{1-1/CR}$$

This equation may be used to find the fluence measured by the bare detector, where CR is the cadmium ratio. The fluence for the cadmium-covered detector may be found by subtracting the net fluence from the fluence of the bare detector, or by dividing the bare fluence by the cadmium ratio.

TABLE A-7. THERMAL NEUTRON FLUENCE AS MEASURED BY BF_3; ERRORS ARE PERCENTAGE

Date	Run	Dist. (m)		Φ_{th} ($n/cm^2/kwhr$)	Error	Cad. Ratio	Error
27May92	SS92-154	1600		1.34e+02	0.041	12.2	1.50
27May92	SS92-154	1600		1.31e+02	0.027	13.1	0.97
27May92	SS92-154	1600		1.35e+02	0.025	14.3	1.08
27May92	SS92-154	1080		4.64e+03	0.005	12.0	0.19
27May92	SS92-154	1080		4.74e+03	0.003	12.0	0.17
27May92	SS92-155	170		1.66e+07	0.007	12.3	0.27
28May92	SS92-156	400		1.13e+06	0.019	12.1	0.73
28May92	SS92-157	2000		1.25e+01	0.083	13.1	2.18
28May92	SS92-157	2000		1.24e+01	0.060	10.2	1.20
28May92	SS92-157	2000		1.19e+01	0.039	11.3	0.89
29May92	SS92-158	715		5.92e+04	0.008	11.5	0.20
29May92	SS92-158	715		5.99e+04	0.005	11.0	0.17
29May92	SS92-158	715		5.99e+04	0.006	10.7	0.21
24Aug92	SS92-228	170		1.66e+07	0.000	12.1	0.01
24Aug92	SS92-229	170		1.62e+07	0.001	11.8	0.02
25Aug92	SS92-230	135	0	2.65e+07	0.000	12.1	0.01
25Aug92	SS92-231	400		1.07e+06	0.000	11.3	0.01
26Aug92	SS92-234	450		9.45e+05	0.000	15.7	0.02
27Aug92	SS92-237	300		4.05e+06	0.002	14.6	0.12
28Aug92	SS92-238	180	silo	1.37e+07	0.000	12.5	0.01
31Aug92	SS92-239	135	180	3.84e+07	0.001	15.8	0.03
01Sep92	SS92-240	715		4.60e+04	0.001	10.2	0.02
02Sep92	SS92-241	715		6.50e+04	0.000	11.8	0.02
14Jun93	SS93-71	300		3.84e+06	0.004	14.3	0.03
14Jun93	SS93-72	300		4.10e+06	0.002	14.3	0.02
15Jun93	SS93-73	2000		2.25e+01	0.151	4.5	0.02
15Jun93	SS93-74	2000		8.81e+00	0.081	7.3	0.03
15Jun93	SS93-74	2000		8.44e+00	0.076	11.3	0.02
15Jun93	SS93-74	2000		1.11e+01	0.063	10.6	0.02
15Jun93	SS93-74	2000		1.06e+01	0.073	8.2	0.02
16Jun93	SS93-75	2000		9.77e+00	0.104	7.8	0.03
16Jun93	SS93-75	2000		1.01e+01	0.094	15.4	0.03
16Jun93	SS93-75	2000		9.28e+00	0.077	6.5	0.02
17Jun93	SS93-76	2000		1.03e+01	0.077	9.3	0.03
17Jun93	SS93-76	2000		9.40e+00	0.067	10.0	0.02
17Jun93	SS93-76	2000		8.87e+00	0.104	7.0	0.03
17Jun93	SS93-77	1600		1.24e+02	0.023	8.6	0.03
17Jun93	SS93-77	1600		1.18e+02	0.019	8.5	0.03
17Jun93	SS93-77	1600		1.19e+02	0.018	9.4	0.02
17Jun93	SS93-77	1600		1.23e+02	0.026	10.3	0.02

TABLE A-8. COMPARISON OF HORIZONTAL AND VERTICAL BF_3 TUBES

Date	Run	Dist. (m)	cps/kw		Ratio	
			normal	Rotated	Rot/Nrml	Rotation
25Aug92	SS92-232	400	1128.8	1230.7	1.09	broadside
26Aug92	SS92-233	400	1197.3	1193.5	1.00	end-on
01Sep92	SS92-240	715	19.2	18.9	0.98	broadside

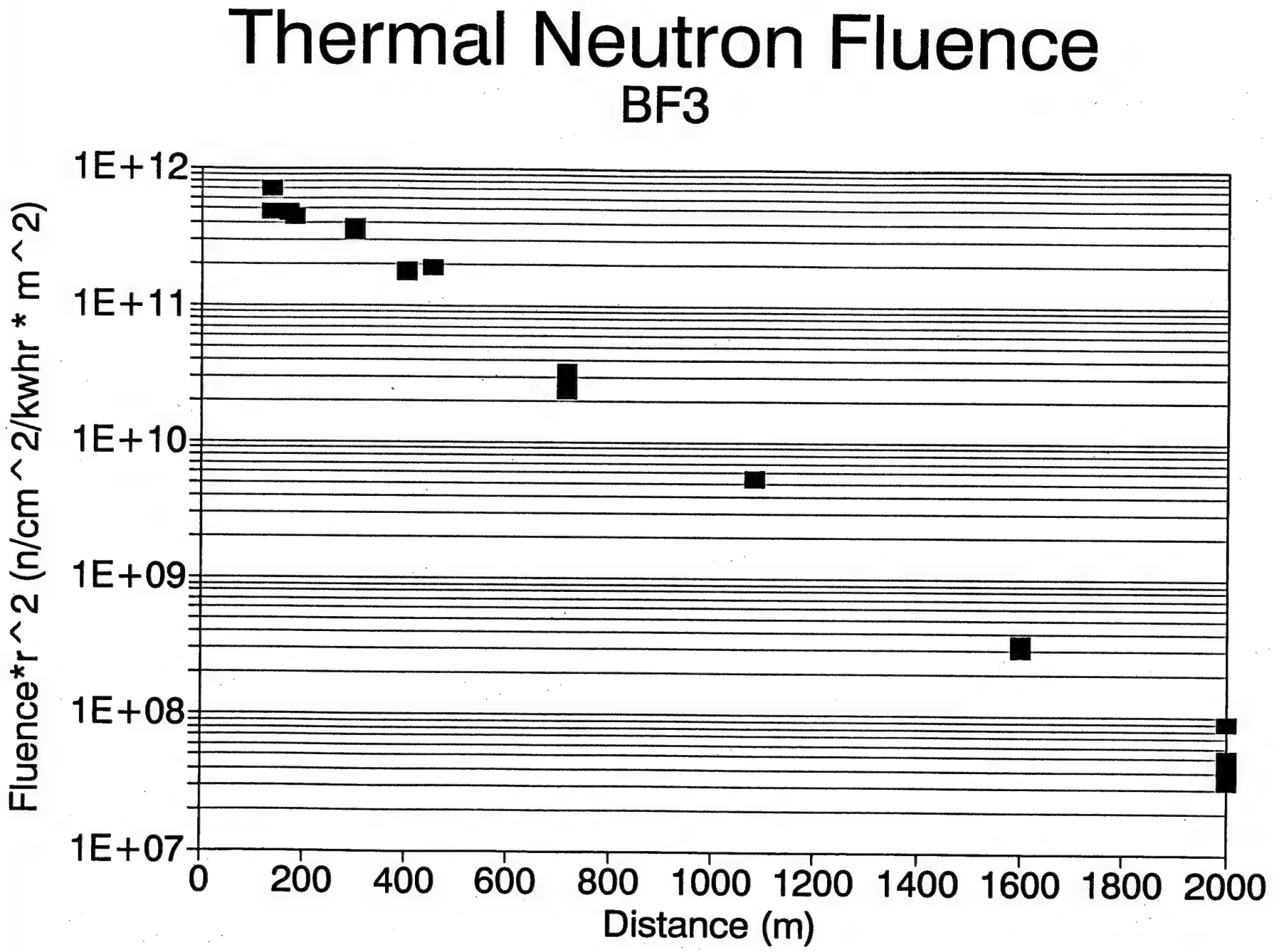
Thermal Neutron Fluence
BF3
Fluence*r^2 (n/cm^2/kwhr * m^2)
1E+12
1E+11
1E+10
1E+09
1E+08
1E+07
0
200
400
600
800
1000
1200
1400
1600
1800
2000
Distance (m)

Figure A-27.

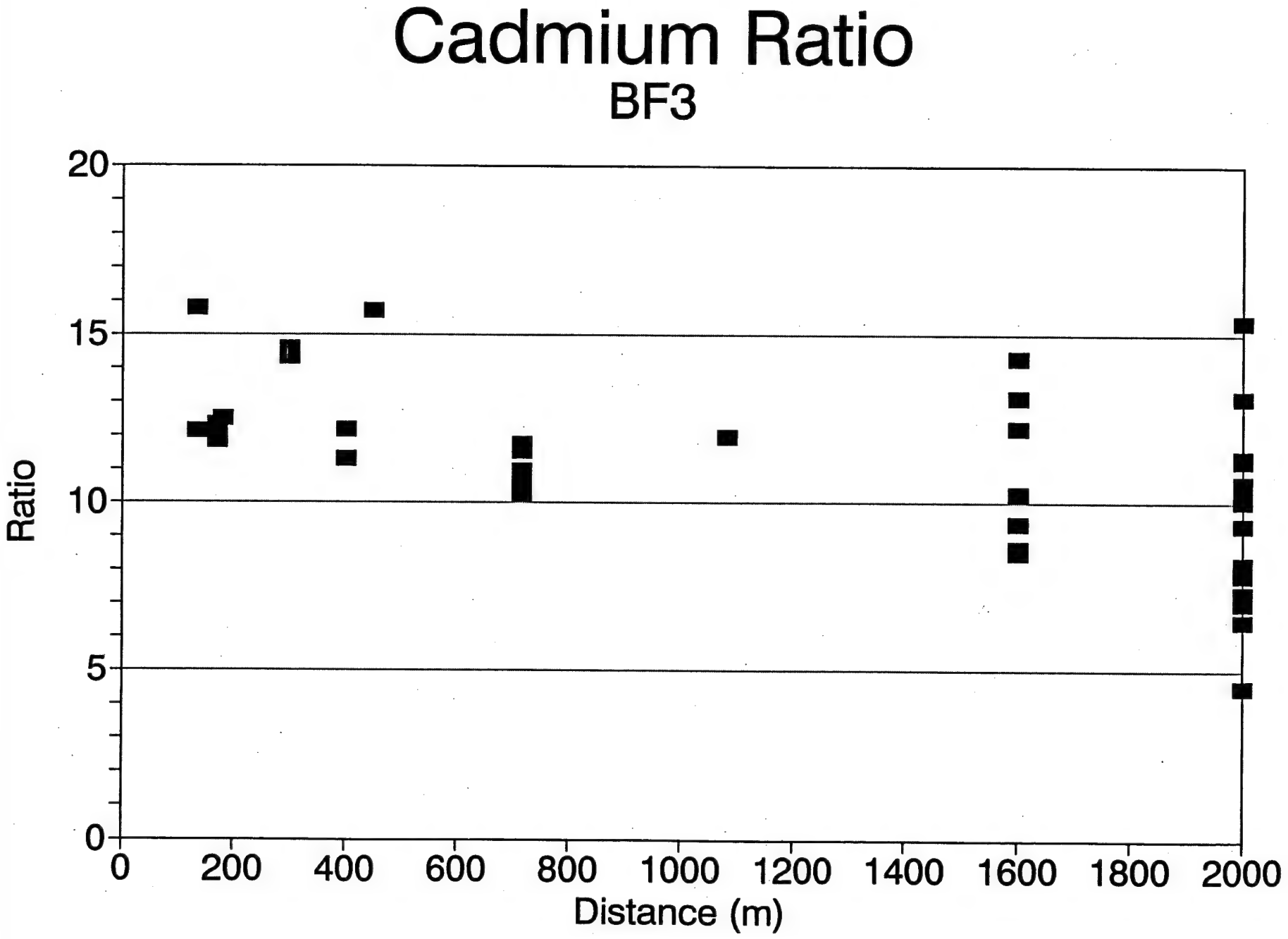

Figure A-28.

(Page 60 Blank)

4. DATA SUMMARY/SULFUR DATA FOR DNA OUTDOOR EXPOSURES

As part of the DNA outdoor experimental program, sulfur was exposed at various locations to monitor the fast neutron fluence. On exposure to neutrons, sulfur becomes radioactive, emitting low-energy beta rays. The reaction is $^{32}S(n,p)^{32}P$. This has a neutron threshold of approximately 3 MeV, so only the fast portion of the neutron spectrum is measured. Sulfur dosimetry is routine at APRF, so it was believed that reliable data could be obtained with a minimum of effort.

Sulfur measurements were attempted from 70 to 700 meters from the reactor. It was soon discovered that 700 meters exceeded the useable range of the APRF system. An attempt was made to extend the range by using 3.8-cm (1.5 in.) diameter sulfurs instead of the 2.5-cm (1-in.) diameter sulfurs normally used at APRF. The large sulfurs gave better counting statistics, but useable data were obtained only out to 450 meters.

The sulfur fluences reported here are Cf-252 equivalent; i.e., if a Cf-252 neutron source were used to activate the sulfurs, the fluences reported here would be the fluence >3 MeV in Cf-252. The 2.5-cm sulfurs were calibrated at a NIST Cf-252 source to 3 percent. The 3.8-cm sulfurs were calibrated by comparison with the 2.5-cm sulfurs.

The errors quoted in the tables are counting uncertainties only. They do not include the calibration uncertainty of 3 percent or a system drift of about 1 percent. For the small sulfurs at the larger distances, the background count rate matched, and sometimes exceeded, the signal count rate. This caused the large deviations in results that may be seen in the figures.

All sulfur results are reported in Tables A-9 through A-13. The sulfurs with four-digit IDs are 2.5 cm in diameter. The sulfurs with one- and two-digit IDs are 3.8 cm in diameter. All data are background corrected and decay-corrected for decay during and after the run.

Figure A-29 shows all the sulfur data. The two data points at 180 meters represent data taken through the transporter and silo and show the resulting attenuation. They are not to be mixed with the free-field results. The increasing spread in the data with distance is due to poorer counting statistics.

Figure A-30 shows the sulfur data sorted by size. As might be expected, the larger sulfurs have better counting statistics. This makes their results more consistent, especially at the larger distances.

A typical reactor run included small sulfurs at three heights, 10, 100, and 300 cm above the ground. Two ratios are plotted in Figure A-31: the ratio of 10- to 100-cm fluence, and the ratio of 300- to 100-cm fluence. All numbers are consistent with there being no vertical gradient.

The background count rate of the sulfur counter was about 0.5 counts/minute for both the 2.5- and 3.8-cm (1- and 1.5-in.) sized sulfur foils. This corresponded to the net count rate at about 350 meters for the 2.5-cm sulfur and 450 meters for the 3.8-cm sulfur, assuming no decay. That is, at these distances, the net count rate equaled background. While counting statistics were propagated into uncertainties, any drift in counter stability between the background calibration and the actual count would be magnified. Sulfur data beyond 400 meters are unreliable for the 2.5-cm sulfurs, and are unreliable for both sizes at 715 meters.

TABLE A-9. SULFUR RESULTS FOR SS92-66

SS92-66	25 Mar 1992	50 kwhr			
Location	Angle	Height	ID	Fluence	Error
135	0	100	4	4.98e+06	0.01
135	90	100	5	5.17e+06	0.01
170	0	100	1	2.57e+06	0.02
300	0	100	3	3.65e+05	0.07
400	0	100	2	8.81e+04	0.22
450	0	100	10	1.13e+05	0.18
715	0	3048	7	1.06e+04	1.63
715	0	3048	6	-7.13e+03	2.35
715	0	100	8	1.78e+03	9.66
135	0	10	1522	4.88e+06	0.03
135	0	100	1521	5.10e+06	0.03
135	0	300	1520	5.52e+06	0.03
135	90	10	1528	4.96e+06	0.03
135	90	100	1523	5.38e+06	0.03
135	90	300	1527	5.20e+06	0.03
135	180	10	1524	4.73e+06	0.03
135	180	100	1525	5.12e+06	0.03
135	180	300	1526	5.36e+06	0.03
170	0	10	1510	2.87e+06	0.04
170	0	100	1509	3.07e+06	0.03
170	0	300	1511	2.75e+06	0.04
300	0	10	1513	6.09e+05	0.11
300	0	100	1515	4.50e+05	0.12
300	0	300	1516	4.01e+05	0.14
400	0	10	1519	2.41e+05	0.20
400	0	100	1512	1.58e+05	0.29
400	0	300	1517	1.51e+05	0.31
450	0	10	1535	9.70e+03	4.41
450	0	100	1529	2.39e+04	1.80
450	0	300	1538	6.48e+04	0.70
715	0	3048	1530	-8.34e+04	0.46
715	0	3048	1532	3.33e+03	12.74
715	0	100	1537	2.35e+04	1.84

TABLE A-10. SULFUR RESULTS FOR SS92-154

SS92-154 27 May 1992 37.53 kwhr					
Location	Angle	Height	ID	Fluence	Error
170	0	100	22	2.74e+06	0.01
400	0	100	21	1.31e+05	0.10

TABLE A-11. SULFUR RESULTS FOR SS92-157

SS92-157 28 May 1992 50 kwhr					
Location	Angle	Height	ID	Fluence	Error
135	0	100	20	5.07e+06	0.01
170	0	100	23	2.74e+06	0.01
300	0	100	24	3.89e+05	0.03
400	0	100	25	9.98e+04	0.10
450	0	100	26	5.44e+04	0.17
450	0	100	27	6.96e+04	0.13
135	0	10	1871	5.09e+06	0.02
135	0	100	1870	5.32e+06	0.02
135	0	300	1869	5.32e+06	0.02
170	0	10	1874	3.04e+06	0.03
170	0	100	1873	2.77e+06	0.03
170	0	300	1872	2.68e+06	0.03
300	0	10	1877	3.57e+05	0.13
300	0	100	1876	3.90e+05	0.12
300	0	300	1875	3.84e+05	0.12
400	0	10	1880	6.98e+04	0.59
400	0	100	1879	6.56e+04	0.63
400	0	300	1878	1.20e+05	0.35
450	0	10	1883	4.97e+05	0.10
450	0	100	1882	8.47e+04	0.50
450	0	300	1881	-2.98e+04	1.31

TABLE A-12. SULFUR RESULTS FOR SS92-186

SS92-186 17 Jun 1992 12.0 kwhr					
Location	Angle	Height	ID	Fluence	Error
63	90	10	1988	3.32e+07	0.01
63	90	100	1987	3.36e+07	0.01
63	180	10	1990	3.29e+07	0.01
63	180	100	1989	3.36e+07	0.01
66	270	10	1992	3.08e+07	0.01
66	270	100	1991	3.02e+07	0.01
135	0	10	1982	5.01e+06	0.03
135	0	100	1981	5.18e+06	0.03
135	90	10	1984	5.28e+06	0.03
135	90	100	1983	5.03e+06	0.03
135	180	10	1986	5.31e+06	0.03
135	180	100	1985	5.20e+06	0.03
170	0	10	1996	2.68e+06	0.05
170	0	100	1995	3.07e+06	0.04
181	silo	10	1994	1.13e+06	0.09
181	silo	100	1993	1.32e+06	0.08

TABLE A-13. SULFUR RESULTS FOR SS92-210

SS92-210 7 JUl 1992 50 kwhr					
Location	Angle	Height	ID	Fluence	Error
135	0	100	31	5.02e+06	0.01
170	0	100	32	2.79e+06	0.01
300	0	100	33	4.18e+05	0.04
400	0	100	34	1.20e+05	0.10
450	0	100	35	8.52e+04	0.13
135	0	10	2022	4.83e+06	0.02
135	0	100	2020	5.16e+06	0.02
135	0	300	2019	5.32e+06	0.02
170	0	10	2025	2.78e+06	0.02
170	0	100	2024	2.67e+06	0.03
170	0	300	2023	2.78e+06	0.02
300	0	10	2028	3.49e+05	0.08
300	0	100	2027	4.29e+05	0.08
300	0	300	2026	4.12e+05	0.09
400	0	10	2031	9.21e+04	0.37
400	0	100	2030	8.33e+04	0.40
400	0	300	2029	6.41e+04	0.51
450	0	10	2034	6.85e+04	0.49
450	0	100	2033	3.66e+04	0.89
450	0	300	2032	3.42e+04	0.95

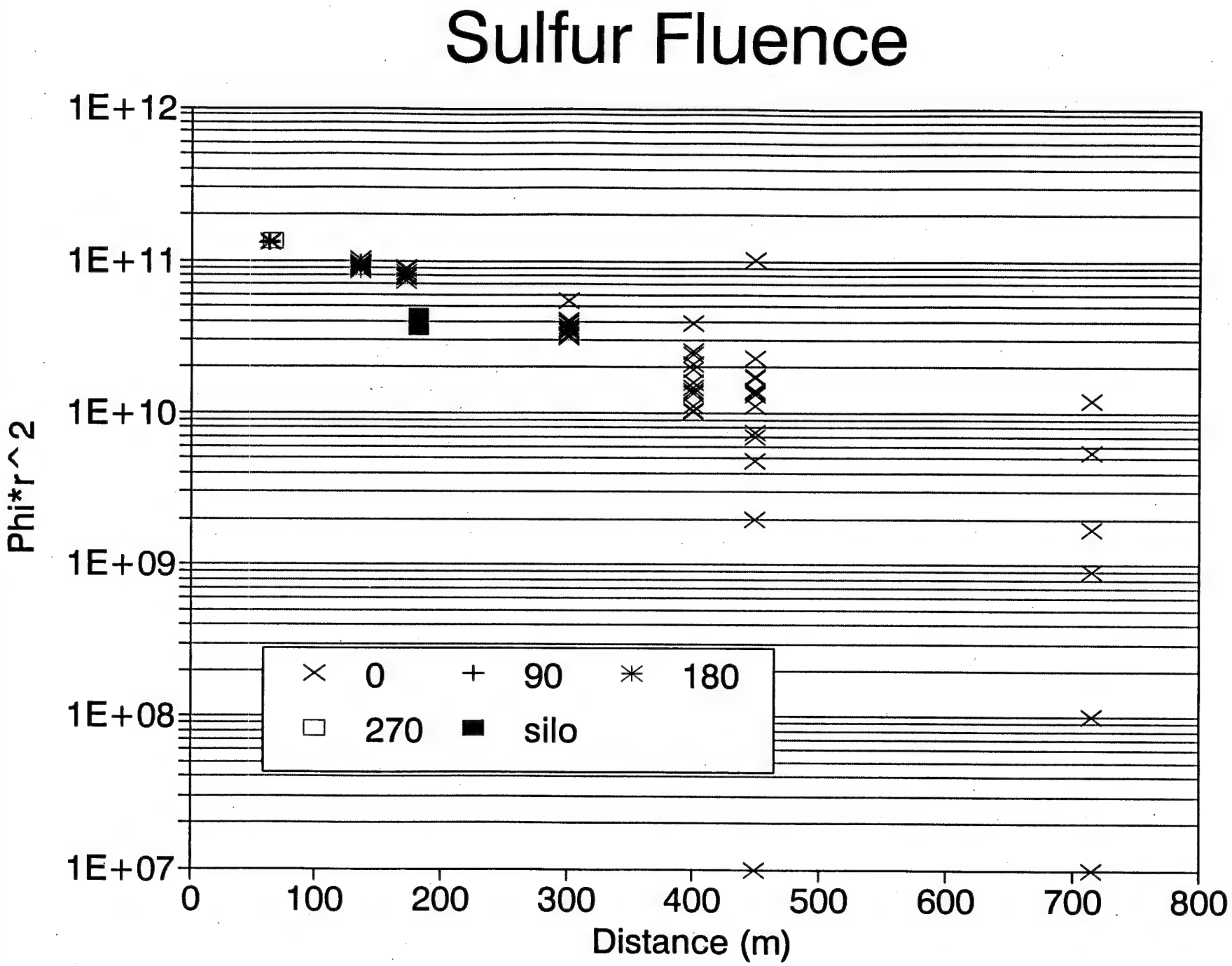
Sulfur Fluence
1E+12
1E+11
1E+10
1E+09
1E+08
1E+07
Phi*r^2
0
90
180
270
silo
0
100
200
300
400
500
600
700
800
Distance (m)

Figure A-29.

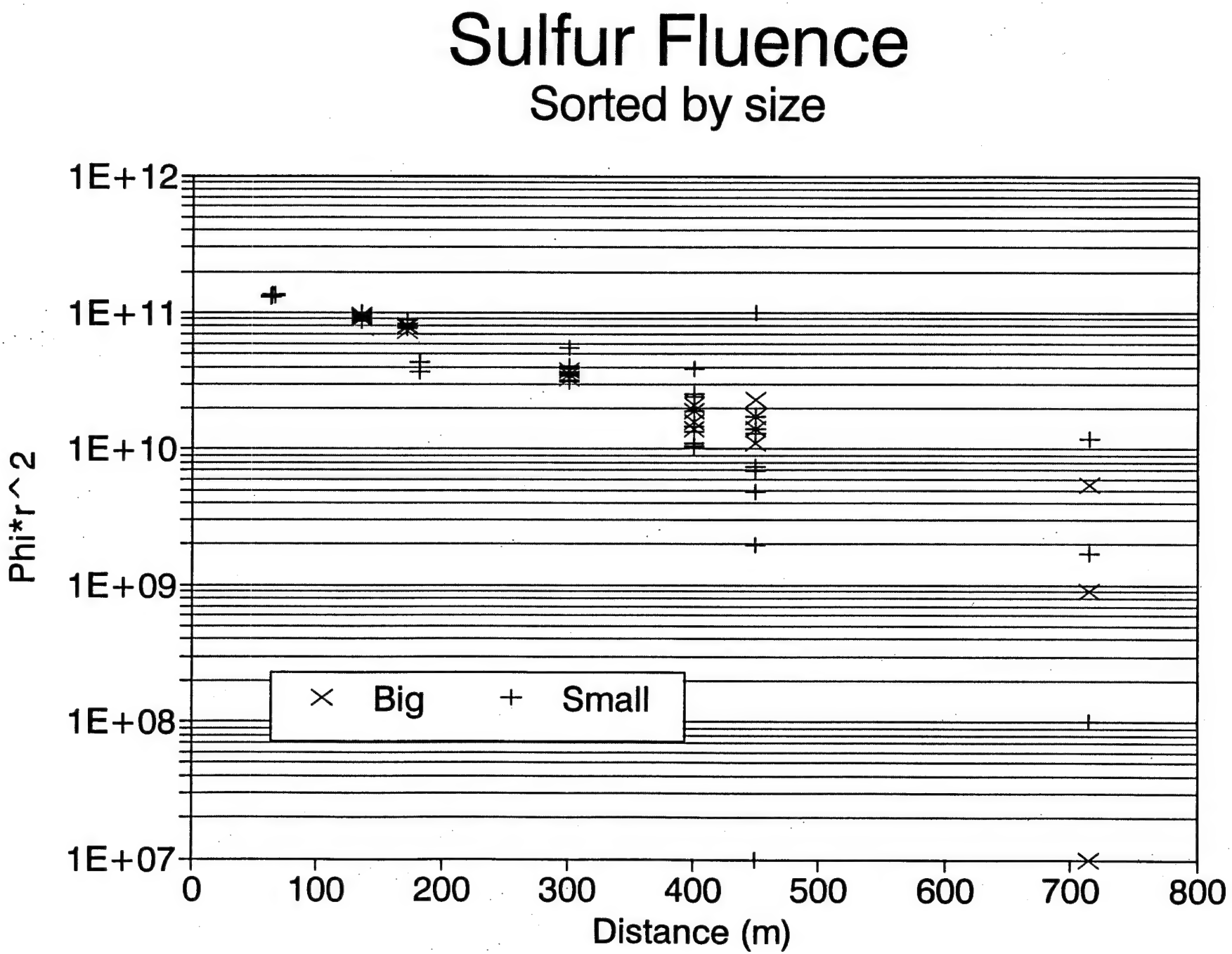
Sulfur Fluence
Sorted by size
1E+12
1E+11
1E+10
1E+09
1E+08
1E+07
Phi*r^2
Big
Small
0
100
200
300
400
500
600
700
800
Distance (m)

Figure A-30.

Sulfur Fluence

Height Effect

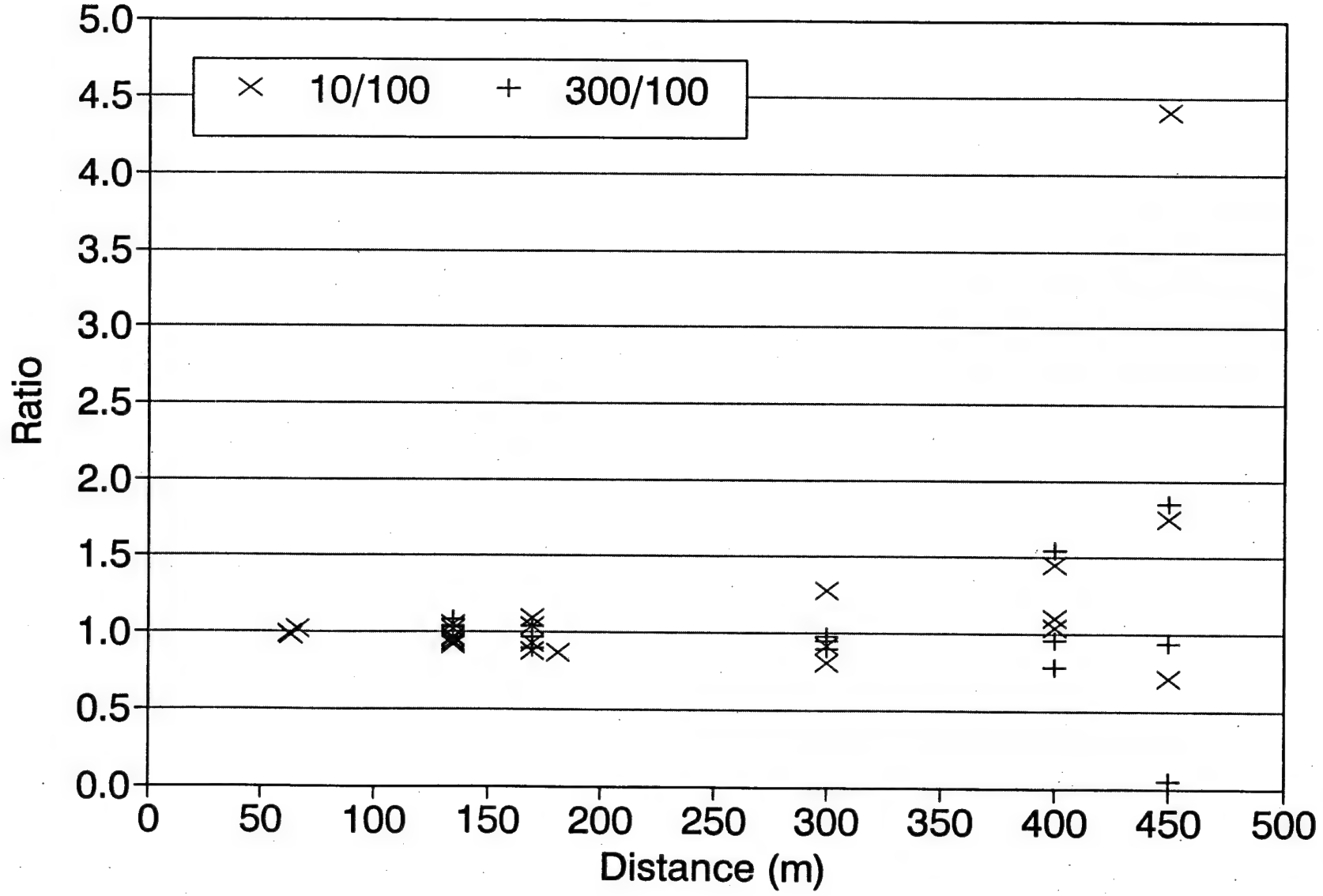

Figure A-31.

5. DATA SUMMARY/NEUTRON REMMETER

An Eberline NRD neutron Remmeter was used to monitor the fast neutron fluence. This consists of a 23-cm (9-in.) diameter polyethylene sphere with a cadmium loading[1]. A BF_3 detector is used to count thermal neutrons at the center. This device has good sensitivity and low background. Unfortunately, since it measures only an integral fluence, it gives no information on the neutron spectrum.

To interpret the Remmeter results, two calibrations were performed at NIST. One was in a bare Cf-252 field and one in a D_2O-shielded Cf-252 field. The procedure was to verify the response function in these two fields, and then derive a calibration constant for use in the APRF environment. Table A-14 shows these results.

TABLE A-14. CALCULATED AND MEASURED REMMETER RESPONSES

Remmeter calibration					
	Calculated			NIST	
Field	mRem	mRad	relative response	c/mRem	calc/meas
D_2O/Cf	1.0	0.095	3.67e-3	2645	1.39e-6
Bare Cf	1.0	0.089	2.75e-3	1866	1.47e-6
APRF	1.0	0.081	3.99e-3		

For Table A-14, the bare and moderated Cf spectra and Remmeter response function were taken from Ref[2]. A calculated 400-meter APRF neutron spectrum was taken from Ref[3]. The calculated portions of Table A-14 were then derived. The ratio of the calculated relative response to the NIST calibration differed by only 6 percent in the two calibration fields. This shows good consistency in a hard and soft neutron spectrum.

The value of 2645 c/mRem as measured in with D_2O was used to derive the APRF response since the D_2O spectrum is a better match to the APRF spectrum than bare californium. The counts/mRem for APRF was found by multiplying this value by the relative response in the APRF field ($3.99\times10^{-3}/3.67\times10^{-3}$) to find 2876 c/mRem for APRF. This is equivalent to 35,501 c/mRad.

For measurements in 1992, the Remmeter was on the ground. In 1993, it was 40 cm off the ground, on a cardboard box.

The raw data are reported in Table A-15. The relative error in the last column in Table A-15 applies to both mRad/kWhr and mRem/kWhr. It includes counting statistics only. The counting errors are substantial due to the low count rate at the larger distances. For example, there was a total of 485 counts at 1600 meters and only 51 counts (7 background) at 2000 meters, including all runs.

TABLE A-15. REMMETER DATA

Run ID	Distance	c/kwhr	mrad/kwhr	mRem/kwhr	Error
SS92-154	1600	8.10e+00	2.29e-04	2.82e-03	0.15
SS92-154	1600	8.64e+00	2.44e-04	3.01e-03	0.30
SS92-154	1080	3.60e+02	1.02e-02	1.25e-01	0.02
SS92-155	170	2.31e+06	6.53e+01	8.03e+02	0.03
SS92-156	400	1.17e+05	3.32e+00	4.09e+01	0.10
SS92-157	2000	9.75e-01	2.76e-05	3.39e-04	0.31
SS92-158	720	4.67e+03	1.32e-01	1.63e+00	0.02
SS93-71	300	3.71e+05	1.05e+01	1.29e+02	0.02
SS93-72	300	3.61e+05	1.02e+01	1.25e+02	0.01
SS93-74	2000	6.00e-01	1.70e-05	2.09e-04	0.49
SS93-75	2000	1.72e+00	4.85e-05	5.97e-04	0.27
SS93-76	2000	8.33e-01	2.36e-05	2.90e-04	0.25
SS93-77	1600	1.59e+01	4.49e-04	5.51e-03	0.05

The mRad/kWhr is plotted in Figure A-32. The results follow an $e^{-\mu r}/r^2$ behavior quite closely.

1. "A Modified Sphere Neutron Detector", D.E. Hankins, LA-3595.

2. "Compendium of Neutron Spectra and Detector Responses for Radiation Protection Purposes", Technical Reports Series No. 318, IAEA, 1990.

3. AEP-14, "Guidelines for the Armored Fighting Vehicle Designer to Improve Nuclear Radiation Protection", December 1993, Edition 3.

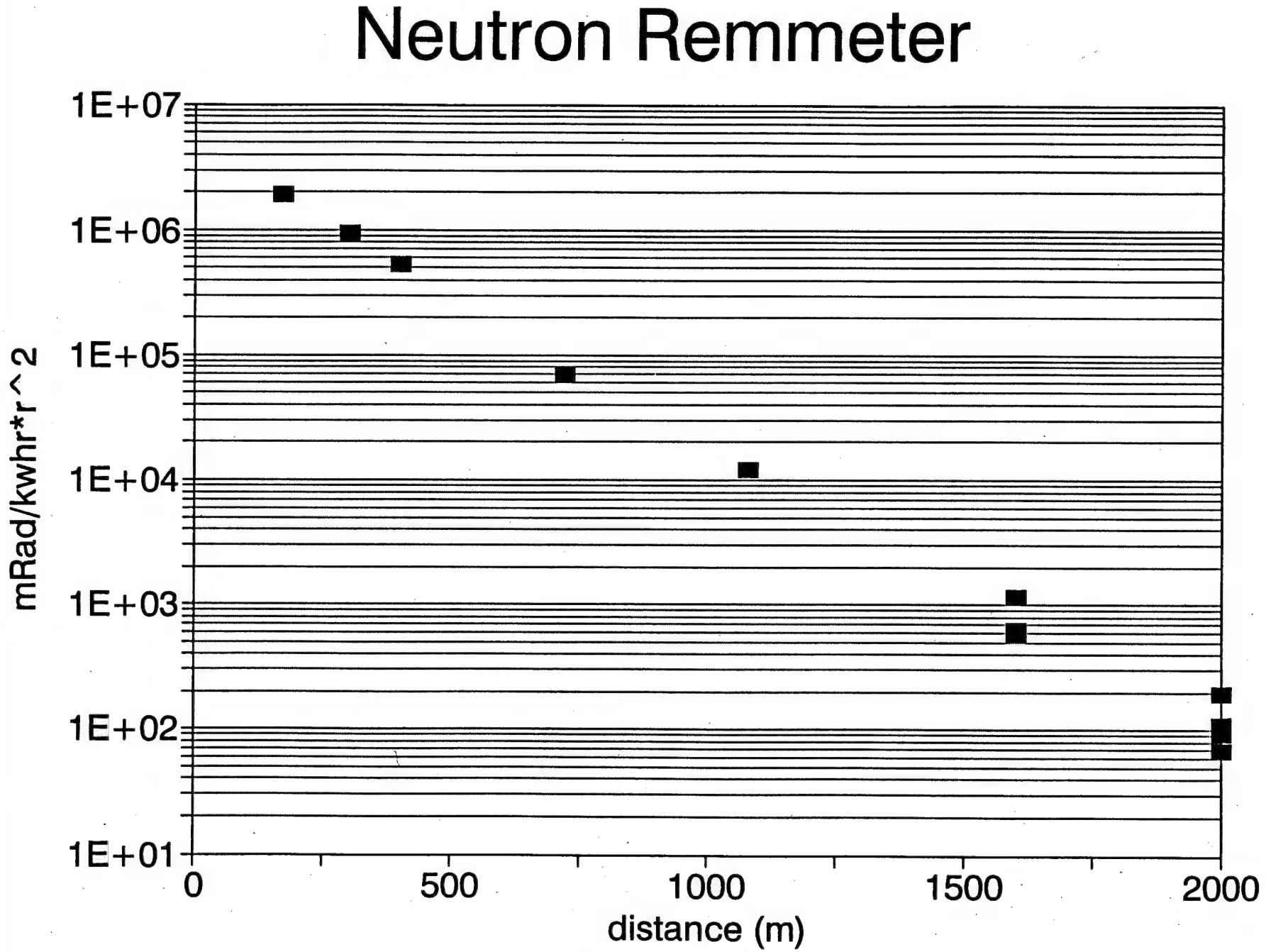

Figure A-32.

(Page 72 Blank)

6. DATA SUMMARY/PROTON-RECOIL DATA FROM DNA OUTDOOR EXPOSURES

APRF has a proton-recoil spectroscopy system, ROSPEC[1], which can measure the neutron spectrum from 50 keV to 4.5 MeV. It consists of four spherical gas-filled tubes which are operated simultaneously, rotating around a common axis.

This system was calibrated at NIST in four neutron spectra: bare californium, and californium moderated with D_2O, water, and iron[2]. Calibration is ensured by periodic measurement of an APRF-owned Cf-252 source.

A complete listing of unfolded neutron spectra is given in Table A-16. Most measurements were made in the 0° direction. One measurement at 135 meters was made at 180°, and one was made in the through-the-silo direction, as noted in the table. All measurements except one were made with the detector on a stand, such that the detectors were 110 cm above the ground. The exception was that SS92-241 was made with the system lifted into the air with a crane, such that it was 30 meters above the ground.

Figure A-33 shows typical spectra as measured at various distances from the reactor. There does not seem to be a substantial spectral shift with distance.

Table A-17 shows integral diagnostics obtained from the neutron spectra. These are neutron kerma and fluence greater than 3 MeV. Each diagnostic is presented in two forms. The first is obtained directly from the spectrum. The second form is adjusted to account for the portion of the spectrum that the spectrometer misses. It misses 12 percent of the kerma and 69 percent of the fluence above 3 MeV.

Both the neutron kerma and $\Phi_{>3MeV}$ follow an $e^{-\mu r}/r^2$ behavior, as shown in Figures A-34 and A-35. The exception is the 180-meter point which is measured through the silo.

Of the two spectra measured at 715 meters, one on the ground and one 30 meters up, the one in the air shows 13 percent more dose and 40 percent more >3 MeV fluence. This is because the trees shield all neutrons, but few scattered neutrons survive above 3 MeV. There is a trend towards a higher mRad/>3 MeV ratio with increasing distance, indicating a softening of the spectrum at larger distances.

1. Manufactured by Bubble Technologies, Inc.

2. "Test of a Neutron Spectometer in NIST Standard Fields", R. B. Schwartz and C. M. Eisenhauer, Rad. Prot. Dos. 55, No. 2, p 94 (1994).

TABLE A-16. PROTON-RECOIL SPECTRA

n/cm²/MeV/kwhr	SS92-228	SS92-229	SS92-230	SS92-231	SS92-232	SS92-234	SS92-236	SS92-237	SS92-238	SS92-239	SS92-240	SS92-241	SS93-73
Dist->	170	170	135	400	400	450	300	300	180	135	715	715	300
kwmin->	34.66	4.1	7.9	225	90	117	39	0.95	15.4	1.5	1575	1680	60
									silo	180		up	
Energy													
0.0573	1.48e+08	1.53e+08	2.64e+08	8.42e+06	8.03e+06	4.59e+06	2.30e+07	3.77e+07	1.12e+08	2.72e+08	4.87e+05	5.53e+05	2.48e+07
0.0690	1.21e+08	1.32e+08	2.21e+08	6.20e+06	6.22e+06	4.17e+06	2.01e+07	1.71e+07	8.75e+07	2.08e+08	4.50e+05	4.18e+05	1.84e+07
0.0833	1.00e+08	9.03e+07	1.43e+08	4.81e+06	5.59e+06	2.21e+06	1.51e+07	1.34e+07	6.17e+07	2.10e+08	2.89e+05	2.51e+05	1.37e+07
0.1002	6.39e+07	6.71e+07	1.36e+08	3.35e+06	3.24e+06	1.52e+06	8.79e+06	7.82e+06	5.10e+07	1.41e+08	2.06e+05	2.26e+05	1.05e+07
0.1210	7.00e+07	8.91e+07	1.27e+08	3.44e+06	4.22e+06	2.30e+06	1.20e+07	4.01e+06	5.28e+07	1.70e+08	2.31e+05	2.76e+05	1.13e+07
0.1457	5.80e+07	5.73e+07	1.03e+08	2.97e+06	2.54e+06	1.82e+06	8.35e+06	1.86e+07	4.49e+07	9.97e+07	2.14e+05	1.89e+05	9.41e+06
0.1756	5.14e+07	5.38e+07	9.36e+07	2.59e+06	2.55e+06	1.42e+06	7.54e+06	6.92e+06	3.43e+07	8.92e+07	1.57e+05	1.58e+05	7.10e+06
0.2120	4.29e+07	4.15e+07	7.42e+07	2.13e+06	2.08e+06	1.15e+06	5.70e+06	6.88e+06	3.17e+07	9.86e+07	1.14e+05	1.09e+05	6.71e+06
0.2729	3.35e+07	3.36e+07	6.13e+07	1.74e+06	1.78e+06	9.19e+05	4.91e+06	3.27e+06	2.16e+07	7.32e+07	9.64e+04	8.79e+04	4.53e+06
0.2996	2.43e+07	2.90e+07	4.95e+07	1.19e+06	1.29e+06	7.33e+05	3.41e+06	4.27e+06	1.50e+07	5.32e+07	7.38e+04	6.79e+04	3.30e+06
0.3371	2.39e+07	2.63e+07	4.45e+07	1.11e+06	9.61e+05	8.74e+05	3.84e+06	3.99e+06	1.64e+07	5.41e+07	6.85e+04	7.39e+04	3.34e+06
0.3745	2.24e+07	2.22e+07	3.89e+07	9.99e+05	1.17e+06	6.20e+05	3.81e+06	2.03e+06	1.59e+07	4.94e+07	5.72e+04	6.43e+04	3.38e+06
0.4120	1.92e+07	1.85e+07	3.14e+07	9.52e+05	9.68e+05	5.21e+05	2.73e+06	1.07e+07	1.26e+07	4.02e+07	5.07e+04	5.93e+04	2.62e+06
0.4601	1.97e+07	2.13e+07	3.46e+07	1.07e+06	1.03e+06	5.44e+05	3.09e+06	3.98e+06	1.15e+07	4.01e+07	6.47e+04	6.02e+04	2.93e+06
0.5083	2.13e+07	2.29e+07	3.89e+07	1.09e+06	1.12e+06	6.49e+05	3.30e+06	5.17e+06	1.41e+07	4.70e+07	6.45e+04	6.65e+04	3.24e+06
0.5671	2.15e+07	2.33e+07	3.74e+07	1.09e+06	1.15e+06	6.35e+05	3.37e+06	4.37e+06	1.38e+07	4.06e+07	6.06e+04	6.95e+04	3.34e+06
0.6313	1.68e+07	1.73e+07	3.06e+07	8.34e+05	9.67e+05	4.95e+05	2.80e+06	1.74e+06	1.02e+07	3.58e+07	4.84e+04	4.59e+04	2.75e+06
0.7927	1.40e+07	1.34e+07	2.57e+07	6.89e+05	6.46e+05	3.74e+05	2.10e+06	1.70e+06	8.28e+06	3.02e+07	3.54e+04	4.11e+04	2.07e+06
0.8970	1.02e+07	8.39e+06	2.03e+07	4.39e+05	3.27e+05	2.55e+05	1.60e+06	5.82e+05	6.34e+06	2.27e+07	2.67e+04	2.76e+04	1.66e+06
1.0221	8.28e+06	1.07e+07	1.57e+07	4.01e+05	4.55e+05	2.49e+05	1.25e+06	1.96e+06	5.10e+06	1.86e+07	1.65e+04	2.20e+04	1.27e+06
1.1577	9.20e+06	9.31e+06	1.60e+07	4.30e+05	5.18e+05	2.62e+05	1.44e+06	1.79e+06	5.34e+06	1.88e+07	2.01e+04	2.20e+04	1.24e+06
1.3246	7.07e+06	6.80e+06	1.27e+07	3.34e+05	3.56e+05	1.93e+05	1.10e+06	1.25e+06	4.13e+06	1.47e+07	1.68e+04	1.86e+04	1.03e+06
1.5783	5.62e+06	5.73e+06	1.03e+07	2.64e+05	2.69e+05	1.45e+05	8.33e+05	5.81e+05	3.22e+06	1.19e+07	1.28e+04	1.44e+04	8.75e+05
1.7711	4.80e+06	4.73e+06	8.85e+06	2.45e+05	2.42e+05	1.49e+05	7.80e+05	6.62e+05	2.63e+06	9.81e+06	1.07e+04	1.31e+04	7.26e+05
1.9880	4.05e+06	4.22e+06	7.98e+06	2.18e+05	2.33e+05	1.43e+05	7.11e+05	8.77e+05	2.32e+06	9.04e+06	9.82e+03	1.21e+04	6.99e+05
2.2290	3.50e+06	3.63e+06	6.77e+06	1.94e+05	2.01e+05	1.17e+05	6.16e+05	5.06e+05	2.01e+06	7.39e+06	7.67e+03	1.20e+04	6.17e+05
2.5182	2.77e+06	2.78e+06	5.10e+06	1.38e+05	1.34e+05	8.55e+04	4.67e+05	4.40e+05	1.66e+06	5.68e+06	4.46e+03	7.35e+03	4.84e+05
2.8315	1.73e+06	1.65e+06	3.51e+06	7.91e+04	8.50e+04	4.63e+04	3.00e+05	3.00e+05	9.27e+05	4.06e+06	2.60e+03	4.07e+03	2.87e+05
3.1689	1.26e+06	1.26e+06	2.46e+06	5.11e+04	4.82e+04	3.05e+04	1.76e+05	2.60e+05	6.77e+05	2.92e+06	1.14e+03	2.35e+03	1.85e+05
3.5545	8.71e+05	8.18e+05	1.53e+06	2.86e+04	3.55e+04	1.50e+04	1.41e+05	9.21e+04	4.11e+05	1.93e+06	1.34e+03	1.39e+03	1.14e+05
4.0124	6.43e+05	6.22e+05	1.49e+06	3.02e+04	3.13e+04	2.03e+04	9.52e+04	9.84e+04	3.97e+05	1.75e+06	9.66e+02	1.16e+03	9.86e+04
4.4944													

TABLE A-17. PROTON-RECOIL DIAGNOSTICS

Run	Distance (m)	kwmin	mRad/kwhr	mRad/kwhr adj*	>3MeV	>3MeV adj**	Ratio (mRad/>3 MeV)
SS92-228	170	34.66	71.25	79.80	1.40e+06	2.38e+06	0.0000508
SS92-229	170	4.10	72.65	81.37	1.36e+06	2.30e+06	0.0000535
SS92-230	135/0°	7.90	131.51	147.29	2.79e+06	4.73e+06	0.0000471
SS92-231	400	225.00	3.47	3.89	5.69e+04	9.64e+04	0.0000611
SS92-232	400	90.00	3.60	4.03	6.02e+04	1.02e+05	0.0000598
SS92-234	450	117.00	2.05	2.30	3.40e+04	5.76e+04	0.0000604
SS92-236	300	39.00	11.19	12.53	2.14e+05	3.63e+05	0.0000522
SS92-237	300	0.95	11.89	13.32	2.26e+05	3.83e+05	0.0000526
SS92-238	181/silo	15.40	43.95	49.22	7.53e+05	1.28e+06	0.0000584
SS92-239	135/180°	1.50	152.00	170.25	3.35e+06	5.67e+06	0.0000454
SS92-240	715/ground	1575.00	0.176	0.197	1.83e+03	3.11e+03	0.0000958
SS92-241	715/up	1680.00	0.198	0.222	2.59e+03	4.40e+03	0.0000764
SS93-73	300	60.00	10.98	12.30	2.06e+05	3.49e+05	0.0000534

* mRad/kwhr × 1.12
** >3 MeV fluence × 1.69

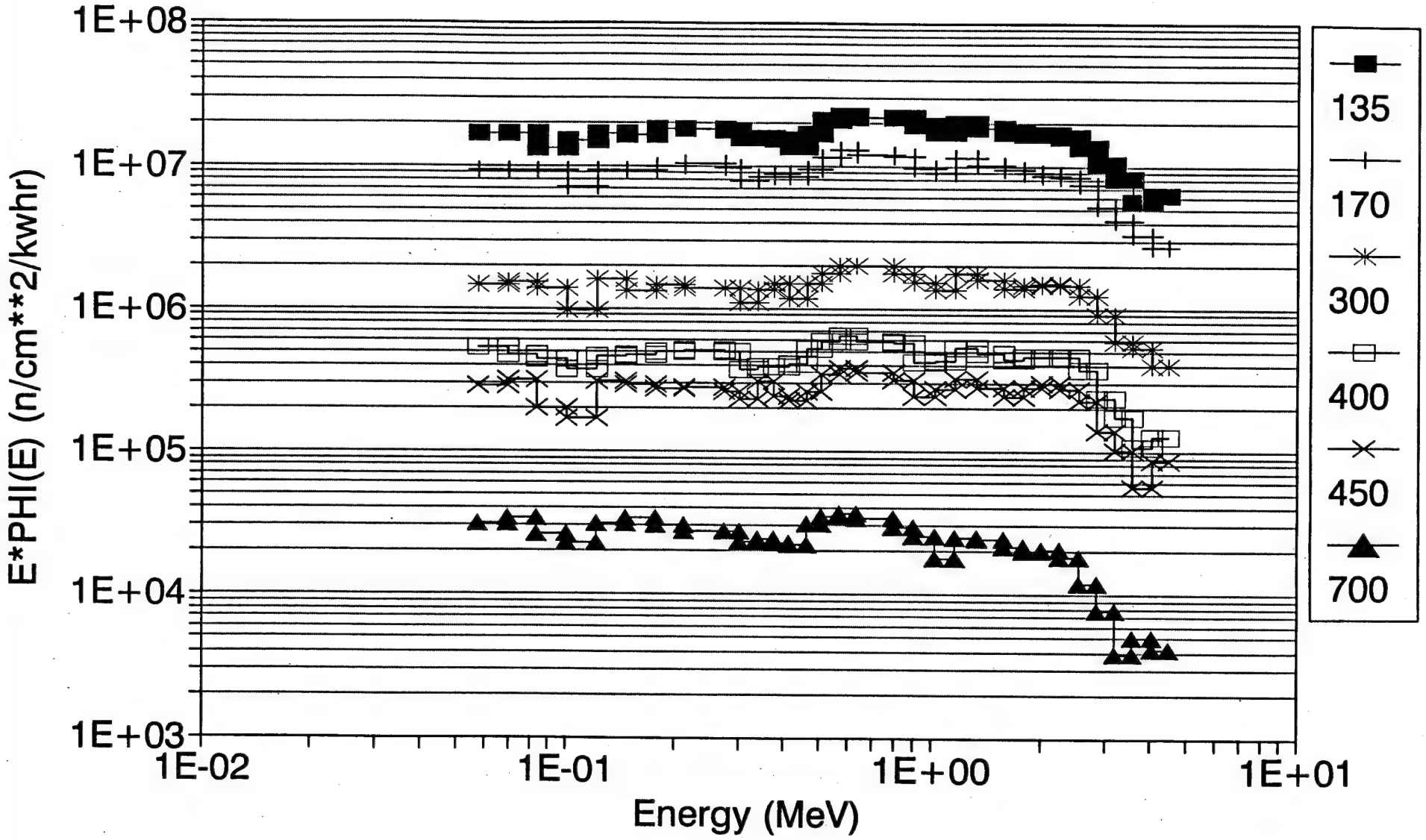
Neutron Spectra
Proton Recoil
E*PHI(E) (n/cm**2/kwhr)
1E+08
1E+07
1E+06
1E+05
1E+04
1E+03
1E-02
1E-01
1E+00
1E+01
Energy (MeV)
135
170
300
400
450
700

Figure A-33.

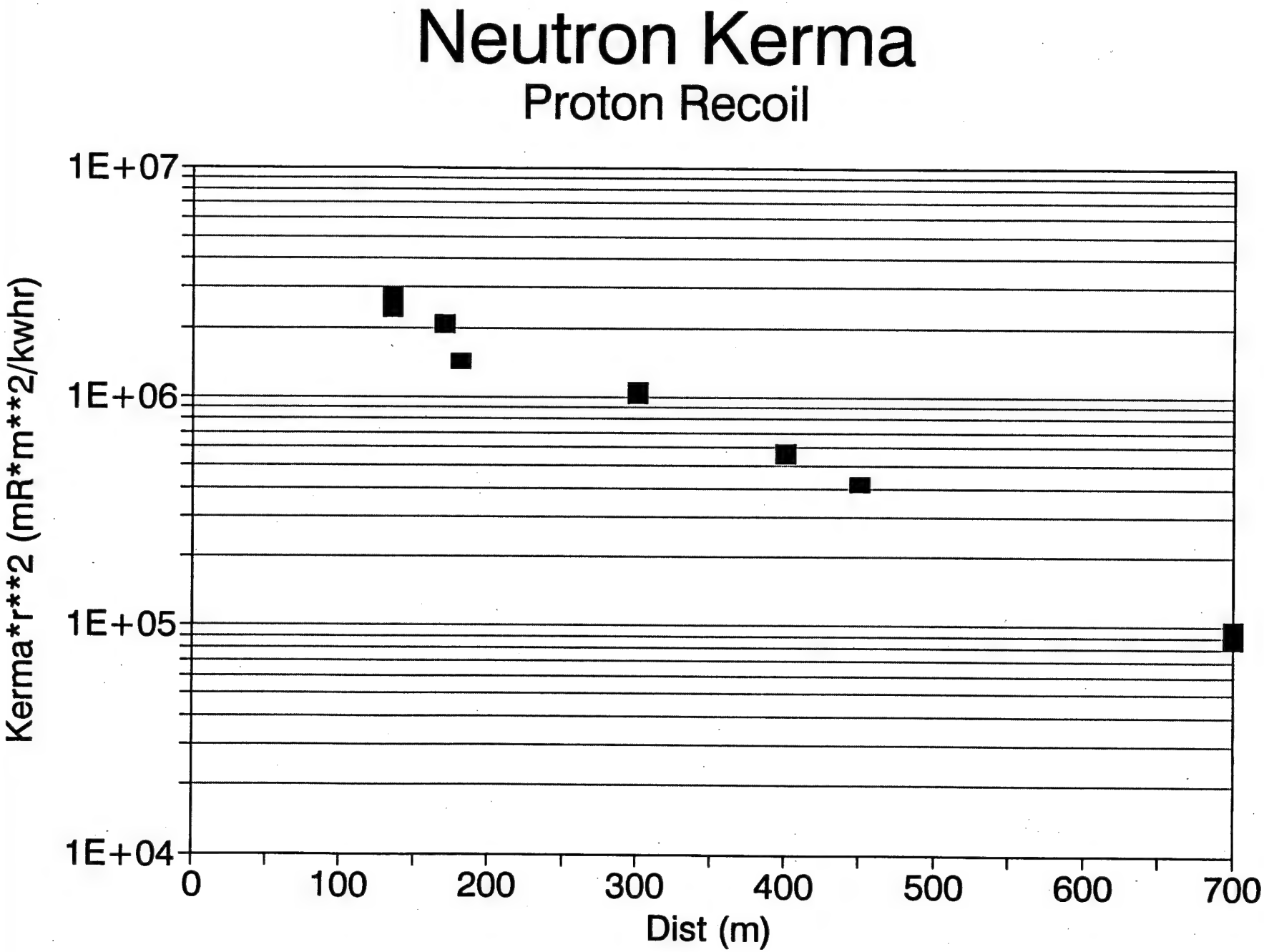
Neutron Kerma
Proton Recoil
Kerma*r**2 (mR*m**2/kwhr)
1E+07
1E+06
1E+05
1E+04
0
100
200
300
400
500
600
700
Dist (m)

Figure A-34.

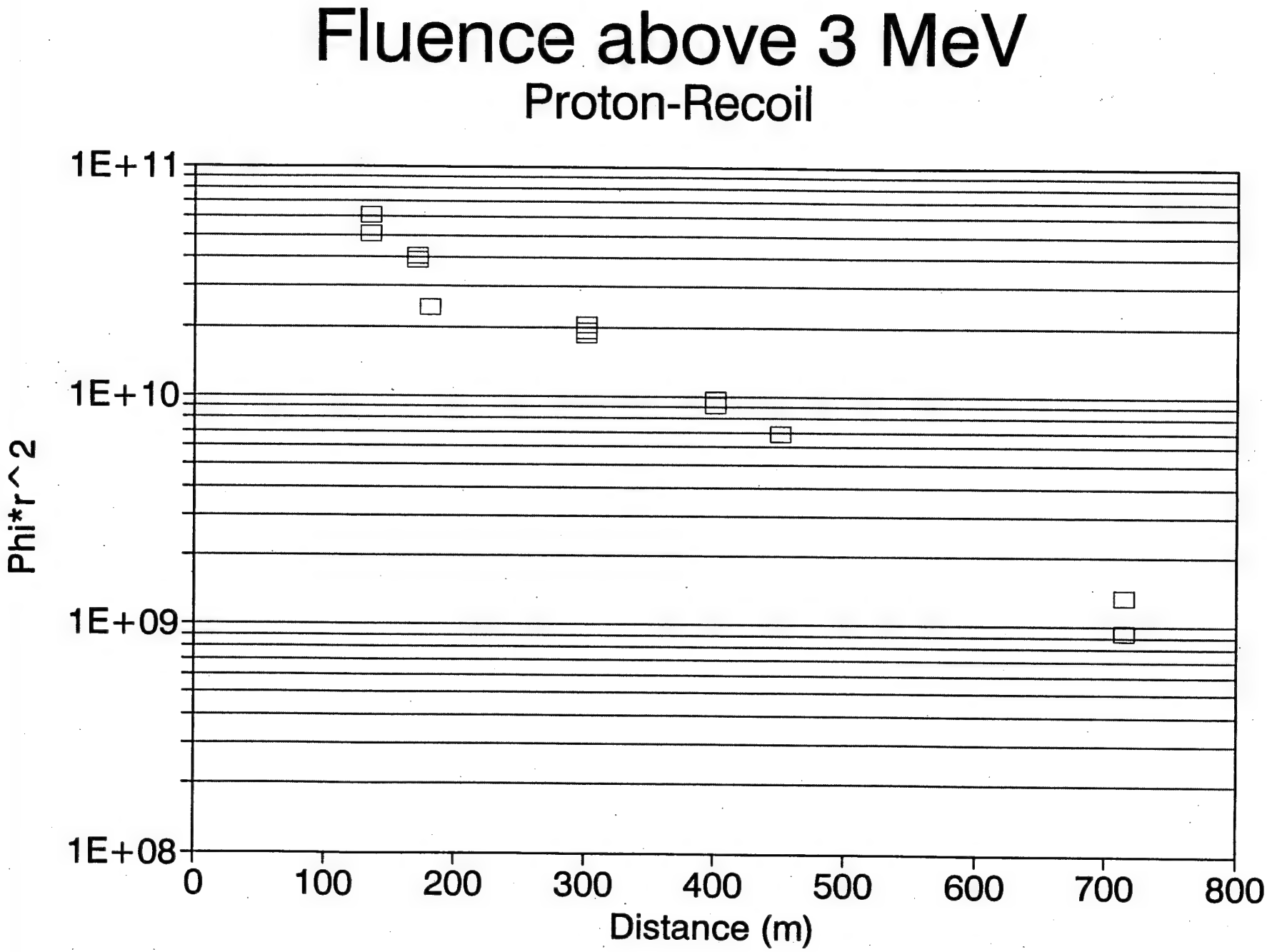
Fluence above 3 MeV
Proton-Recoil
1E+11
1E+10
1E+09
1E+08
Phi*r^2
0
100
200
300
400
500
600
700
800
Distance (m)

Figure A-35.

7. DATA SUMMARY/TLD DATA FOR DNA OUTDOOR EXPOSURES

As part of the experimental program, thermoluminescent detectors (TLDs) were exposed from about 60 to 700 meters from the reactor. TLDs are sensitive to gamma rays. There is a slight sensitivity to thermal and fast neutrons, but no corrections were made for this.

Various types of TLDs were used in an attempt to avoid unknown sensitivity to neutrons or X-rays which might have occurred if only one type were used. The various material/cover combinations are listed in Table A-18.

All calibrations were performed with the same Cs-137 source. This source was calibrated traceable to NIST to 3 percent. Data are reported in terms of mrad(TLD material) and mrad(tissue). The dose in mrad(material) is measured directly and is not dependent on the gamma-ray spectrum. The dose in mrad(tissue) depends on the gamma-ray spectrum. The conversion constants used to convert from material to tissue dose (rad(material)/rad(tissue)) were 0.84, 1.06, and 0.93 for LiF, CaF_2, and Al_2O_3, respectively, based on a calculated gamma-ray spectrum.

The TLDs were batch calibrated, not individually calibrated. Variations of TLDs within each batch were generally about 5 to 10 percent. To obtain better precision, several TLDs were used in each package exposed, and package averages were used. The consistency of each package provided a check on the internal consistency of the data. The uncertainties quoted in the tables are batch consistencies. One set of results was discarded due to too wide a spread in the package results.

TABLE A-18. TLD MATERIALS, SIZES AND COVERS

TLD Packages.				
Type	Size (mm)	Mass (g)	Cover	
			Material	g/cm^2
CaF_2(Mn)	6.4×6.4×1.8	0.235	Al	0.31
CaF_2(Mn)	3.2×3.2×0.9	0.029	Al	0.36
CaF_2(Mn)	3.2×3.2×0.9	0.029	Al/Sn	0.36/0.46
Al_2O_3	5(diam)×1(thick)	0.070	Al	0.36
LiF	3.2×3.2×0.9	0.024	Al	0.43
LiF	3.2×3.2×0.9	0.024	Li	0.1

The useable range of TLDs is from a few mRad to thousands of Rads. The lower range limited the use of the TLDs to about 700 meters, where about 5 mRad was measured for a 50-kWhr reactor run.

The readout procedures for the TLDs are shown in Table A-19:

TABLE A-19. READOUT PROCEDURES FOR TLDs

TLD readout procedure.					
Type	Pre-Exposure Anneal (min@°C)	Preheat (sec@°C)	Ramp (°C/sec)	Max. Temp. (°C)	Time (sec)
CaF_2(Mn) small	2min@400°C	-	30°C/sec	300	20
Al_2O_3	2min@300°C	-	10°C/sec	270	40
LiF	2min@300°C	5sec@150°C	25°C/sec	240	10
CaF_2(Mn) large	2min@400°C	1sec@200°C	30°C/sec	320	30

TLD measurements were made on two outdoor runs, SS92-66 and SS92-186. The results are listed in Tables A-20 through A-22. One of the sets of data, for the small CaF_2(Mn), had a wide dispersion in data. This was traced to improper annealing. These results will not be further discussed here.

Figure A-36 shows the variation of TLD dose with height above ground. Within the 10-percent intrinsic variability, there is no consistent trend.

At 715 meters, the doses at the 30-meter height are consistently higher than the doses at the 1-meter height. This is undoubtedly because the 30-meter doses had LOS to the reactor.

Figure A-37 compares dose as measured by the various materials. What is plotted are the ratios of doses as measured by the TLDs. LiF and Al_2O_3 average close to one, showing consistence of results. The LiF/CaF ratio averages about 1.2, indicating that the CaF is reporting about 20-percent less dose than the other dosimeters.

Gamma-ray dose versus distance is plotted in Figure A-38. The data seem to have an intrinsic variability of 10 to 15 percent at all distances, even though each point represents an average of several TLDs. Part of this variation may be due to height above ground, or local ground conditions. The data at 135 meters show a dependence on the angle from the reactor, or, equivalently, proximity to trees.

In SS92-186, some TLD covers were varied to look for X-ray and thermal neutron effects. The tin added to the CaF_2 TLD shields against X-rays. Tin-covered CaF_2 showed only a few percent lower dose than the aluminum-only covered TLDs, indicating negligible X-ray sensitivity. The Li-6 covers over the LiF TLDs and shields them against low-energy neutrons. The lower response on the TLDs with the Li-6 (10 to 15 percent) indicates the possibility of a thermal neutron response.

TABLE A-20. TLD DATA FROM SS92-66; DOSE IN MRAD(TLD MATERIAL)

mRad(TLD)/kwhr from SS92-66 (50kwhr)									
Distance (m)	Height (cm)	CaF(Big)	Error	CaF(Sm)	Error	AlO	Error	LiF	Error
135/0	300			15.67	0.11	28.11	0.04	21.22	0.06
	100			12.61	0.22	27.62	0.05	26.07	0.02
	10			10.11	0.54	29.85	0.06	25.72	0.04
135/90	300			25.86	0.13	32.46	0.06	27.57	0.02
	100			20.44	0.20	34.19	0.05	29.13	0.06
	10			18.00	0.24	35.04	0.09	29.57	0.03
135/180	300	32.63	0.03	28.74	0.05	35.84	0.07	32.70	0.05
	100			16.98	0.26	34.81	0.06	30.02	0.05
	10			20.85	0.04	35.22	0.07	32.53	0.09
170	300	14.82	0.09			17.37	0.06	16.11	0.03
	100	13.63	0.09			16.52	0.02	15.94	0.08
	10	15.26	0.04			17.22	0.08	15.68	0.04
300	300	2.75	0.09			3.55	0.03	3.23	0.03
	100	3.63	0.05			4.07	0.08	3.51	0.06
	10	3.63	0.04			3.84	0.04	3.59	0.02
400	300	1.24	0.04			1.33	0.05	1.15	0.06
	100	1.15	0.09			1.21	0.07	1.13	0.03
	10	1.15	0.03			1.28	0.05	1.10	0.05
450	300	0.69	0.11			0.88	0.04	0.99	0.06
	100	0.66	0.02			1.13	0.17	0.95	0.01
	10	0.69	0.06			0.92	0.04	0.81	0.09
715	3048	0.10	0.09			0.13	0.07	0.11	0.03
	3048	0.11	0.05			0.14	0.14	0.11	0.06
	100	0.10	0.07			0.09	0.05	0.09	0.10
Only last two points									

TABLE A-21. TLD DATA FROM SS92-186; DOSE IN MRAD(TLD MATERIAL)

mRad(TLD)/kwhr from SS92-186 (12 kwhr)									
Dist (m)	Height (cm)	LiF(Al)	Error	LiF(Li6)	Error	CaF(Al)	Error	CaF(Sn)	Error
62.6/90	100	130.21	0.039	121.53	0.060	136.83	0.062	134.86	0.028
63.4/180	100	124.12	0.055			130.39	0.050		
66.6/270	100	117.04	0.028			132.49	0.035		
135/0	100	27.44	0.056			29.71	0.034		
135/90	100	34.73	0.063	28.66	0.054	34.73	0.063	35.74	0.055
135/180	100	34.43	0.066			37.68	0.069		
181/silo	100	10.89	0.071			12.78	0.017		

TABLE A-22. TLD RESULT CONVERTED TO RAD(TISSUE)

Tissue dose for TLD's.					
SS92-66			mRad(Tissue)/kwhr		
	Dist	Height	CaF	AlO	LiF
	135/0	300		30.23	25.26
		100		29.70	31.04
		10		32.09	30.62
	135/90	300		34.90	32.82
		100		36.77	34.68
		10		37.67	35.20
	135/180	300		38.54	38.93
		100		37.43	35.74
		10		37.87	38.73
	170/0	300		18.68	19.18
		100		17.77	18.98
		10		18.51	18.67
	300/0	300		3.82	3.85
		100		4.38	4.18
		10		4.12	4.27
	400/0	300		1.43	1.37
		100		1.30	1.34
		10		1.38	1.30
	450/0	300		0.95	1.18
		100		1.21	1.13
		10		0.99	0.97
	700/0	3048		0.14	0.13
		3048	0.10	0.15	0.13
		100	0.09	0.10	0.11
SS92-186					
	62.6/90	100	129.09		155.02
	63.4/180	100	123.01		147.77
	66.2/270	100	124.99		139.34
	135/0	100	28.03		32.66
	135/90	100	32.77		41.35
	135/180	100	35.54		40.99
	181/silo	100	12.06		12.96

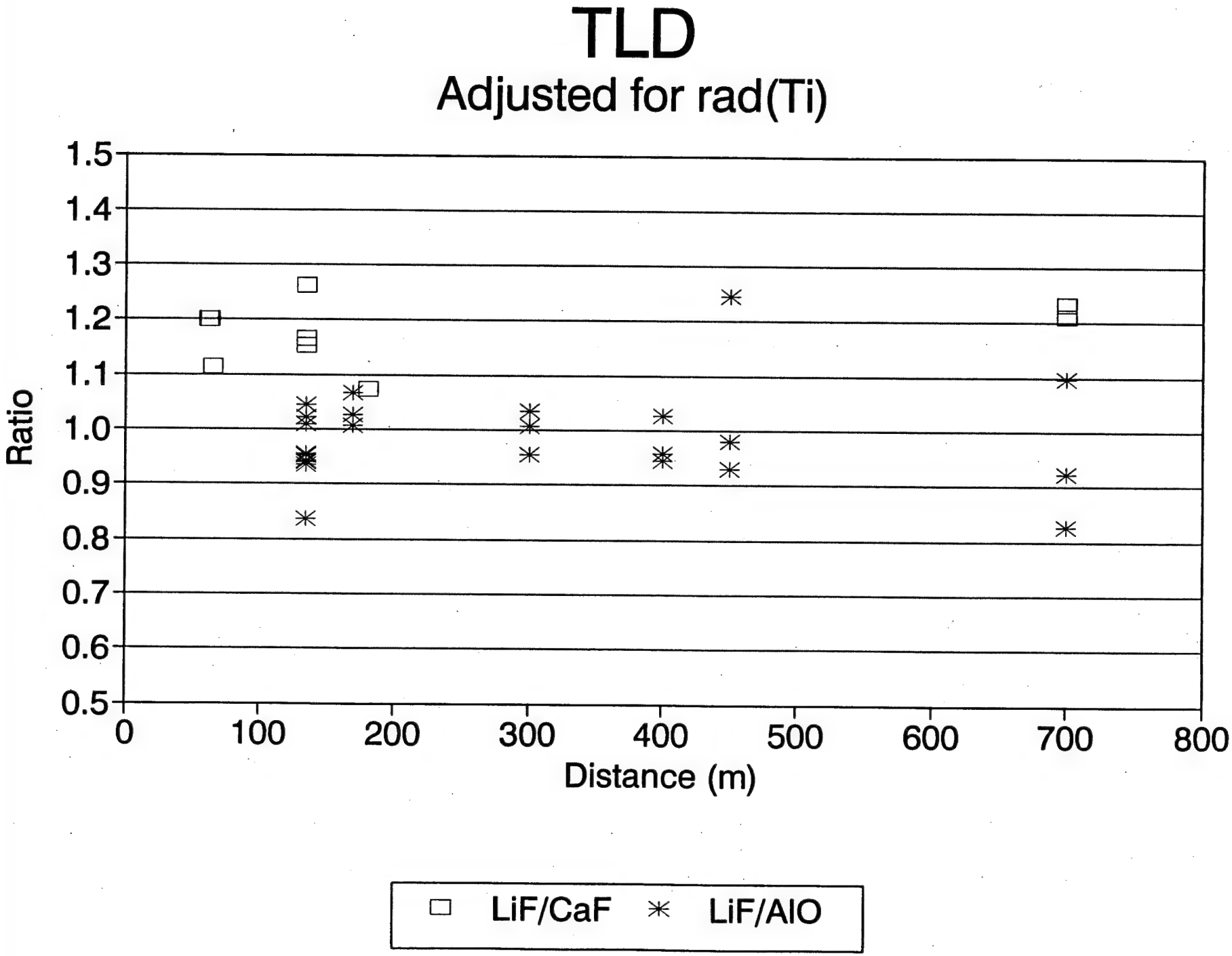
TLD
Adjusted for rad(Ti)
Ratio
1.5
1.4
1.3
1.2
1.1
1.0
0.9
0.8
0.7
0.6
0.5
0
100
200
300
400
500
600
700
800
Distance (m)
LiF/CaF
LiF/AlO

Figure A-37.

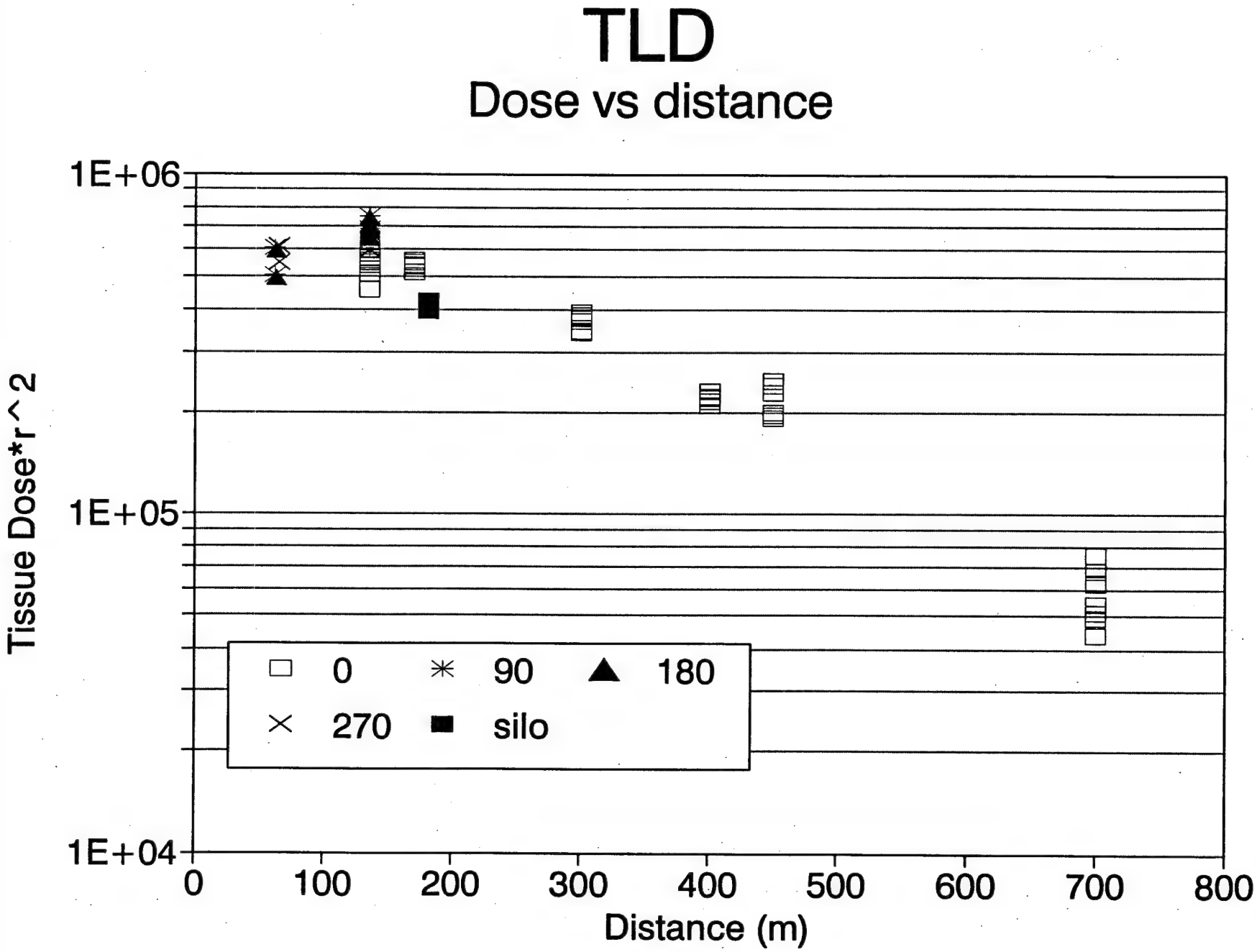
TLD
Dose vs distance
1E+06
1E+05
1E+04
Tissue Dose*r^2
0
100
200
300
400
500
600
700
800
Distance (m)
0
90
180
270
silo

Figure A-38.

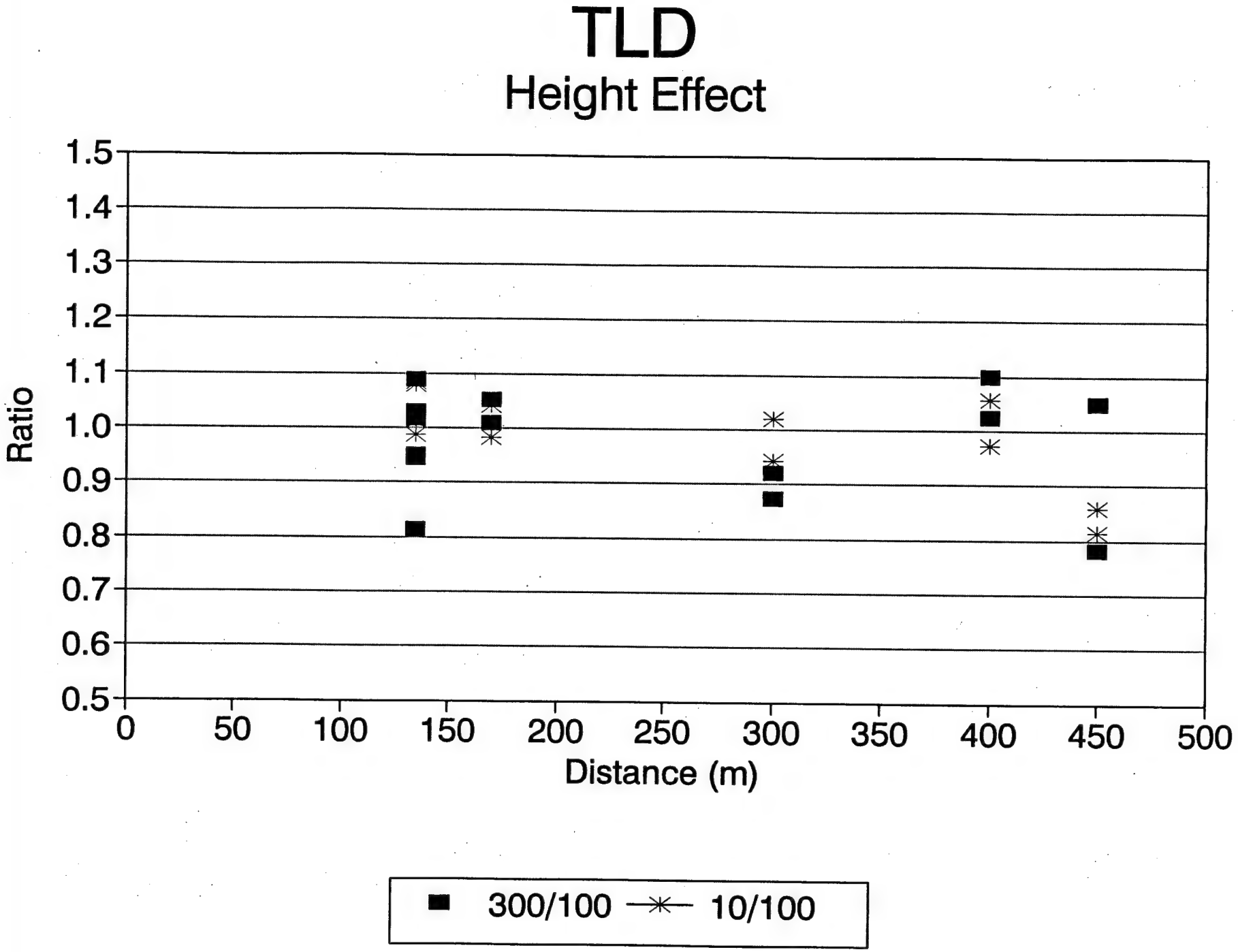
TLD
Height Effect
Ratio
1.5
1.4
1.3
1.2
1.1
1.0
0.9
0.8
0.7
0.6
0.5
0
50
100
150
200
250
300
350
400
450
500
Distance (m)
300/100
10/100

Figure A-36.

8. GEIGER COUNTER RESULTS

Eberline HP-270 Geiger counters were used to monitor the gamma-ray dose during many of the measurements. These were sensitive enough to take data even out to 2000 meters, although at that distance background was substantial. These measurements were not considered high priority, but the instruments were portable and easy to use. The detector height was 70 cm for measurements in 1992, 30 cm in following years.

The Geiger counters were calibrated with a Cs-137 source traceable to NIST. For determination of the dose in the APRF outdoor environment, a substantial correction was made for sensitivity to the gamma-ray spectrum. A computed outdoor gamma-ray spectrum was combined with a Geiger-counter sensitivity function[1] to find the correction factor of 1.46. All measured results were divided by this number to produce the numbers listed in this report. The counter dead time of 120 μsec was accounted for in the close-in runs.

Geiger counters are typically not sensitive to neutrons. It was feared that this might not be the case for the HP-270 because of a plastic covering. Therefore, a set of comparison runs was performed comparing the HP-270 against a Far-West GM-1, which has a demonstrated neutron sensitivity of approximately 0.2 percent[2].

Table A-23 shows the results of the comparison runs. In each case, the neutron source was Cf-252. In the first set, it was centered inside a 12.7-cm (5-in.) diameter polyethylene sphere. Data were taken bare, and then with the source behind a lead brick (5.08-cm (2-in.) thick). A final set of measurements was made with the source inside the polyethylene sphere, but with a boron cover to suppress thermal neutrons. Neutron doses were determined with a Remmeter.

TABLE A-23. COMPARISON OF NEUTRON SENSITIVITIES OF TWO GEIGER COUNTERS

Source	cpm		N/G Ratio	Ratio (HP270/GM-1)
	HP-270	GM-1		
Cf/poly	2233.3	45.6	1.2	49.0
Bare Cf	2466.7	48.3	2.2	51.1
Cf/lead	398.3	7.5	6.4	53.3
Cf/poly/B	2166.7	43.0	1.1	50.4

The data in Table A-23 indicate a fast neutron sensitivity of the HP-270 of about 1.5 percent. Since the neutron/gamma dose ratio varies with distance, the correction would be a maximum of 11 percent (N/G=7.5) at 60 meters to a minimum of 1 percent (N/G=0.4) at 2000 meters. This correction was not made in the results presented here because of the uncertainty in the neutron sensitivity, because of the uncertainty in the neutron dose, and because of a desire to keep the data presented here close to the data as taken.

The Geiger counter results are given in Tables A-24 and plotted in Figure A-39. Not plotted are the negative results during SS93-76.

Run SS92-155 included an attempt to measure the gamma rays at 170 meters. This failed for two reasons, both due to the long, high-power previous run. First, the power level of 5 watts was not enough to bring the count rate sufficiently over background. Second, the background decayed substantially over the course of the run, so it was not clear what background to subtract.

For the last two runs listed, there were no ground moisture measurements. These runs were done as a supplement to another experiment.

The background count rate for the Geiger counter was approximately 16 counts/minute. The data in Table A-24 show that the net count rate at 1600 meters was approximately the same as background. At 2000 meters, the net count rate was only about 1 count per minute. While long count times were used to accumulate a large number of counts, and errors of counting were calculated, it should be noted that any shift in detector sensitivity between background and field measurements would cause a large error in the results. This type of effect is responsible for the 1600-meter measured dose varying by up to a factor of two, and for the 2000-meter dose going negative on one measurement. The cautious users would consider this factor in their use of the data.

TABLE A-24. GEIGER COUNTER DATA

Run	Date	power (w)	dist (m)	net cpm	mRad/kwhr	error
SS92-154	27May92	8000	1600	15.953	1.06e-03	0.074
SS92-154	27May92	7500	1600	13.637	9.65e-04	0.099
SS92-154	27May92	7500	1080	244.003	1.73e-02	0.009
SS92-155	27May92	5	170			
SS92-158	29May92	500	715	88.937	9.44e-02	0.014
SS93-71	14Jun93	10	300	68.794	3.65e+00	0.039
SS93-72	14Jun93	20	300	140.460	3.73e+00	0.019
SS93-73	15Jun93	8000	2000	0.254	1.68e-05	2.546
SS93-74	15Jun93	8000	2000	0.278	1.85e-05	2.562
SS93-74	15Jun93	7500	2000	0.853	6.04e-05	0.792
SS93-74	15Jun93	7500	2000	1.717	1.21e-04	0.388
SS93-74	15Jun93	7500	2000	1.992	1.41e-04	0.348
SS93-75	16Jun93	7500	2000	2.187	1.55e-04	0.417
SS93-75	16Jun93	7500	2000	2.201	1.56e-04	0.380
SS93-75	16Jun93	7500	2000	0.687	4.86e-05	0.981
SS93-76	17Jun93	7500	2000	1.644	1.16e-04	0.452
SS93-76	17Jun93	7500	2000	0.687	4.86e-05	0.936
SS93-76	17Jun93	7500	2000	-0.924	-6.54e-05	0.836
SS93-77	17Jun93	7500	1600	11.414	8.08e-04	0.078
SS93-77	17Jun93	7500	1600	10.853	7.68e-04	0.070
SS93-77	17Jun93	7500	1600	9.687	6.85e-04	0.076
SS93-77	17Jun93	7500	1600	9.510	6.73e-04	0.101
SS95-33	12Jul95	4000	300	29563.7	3.92e+00	0.002
SS95-34	12Jul95	6000	400	16067.0	1.42e+00	0.001

1. L. Schanzler, Private Communication.

2. "Neutron Sensitivity of a Geiger Counter", C. R. Heimbach, CSTA-7677 (1995).

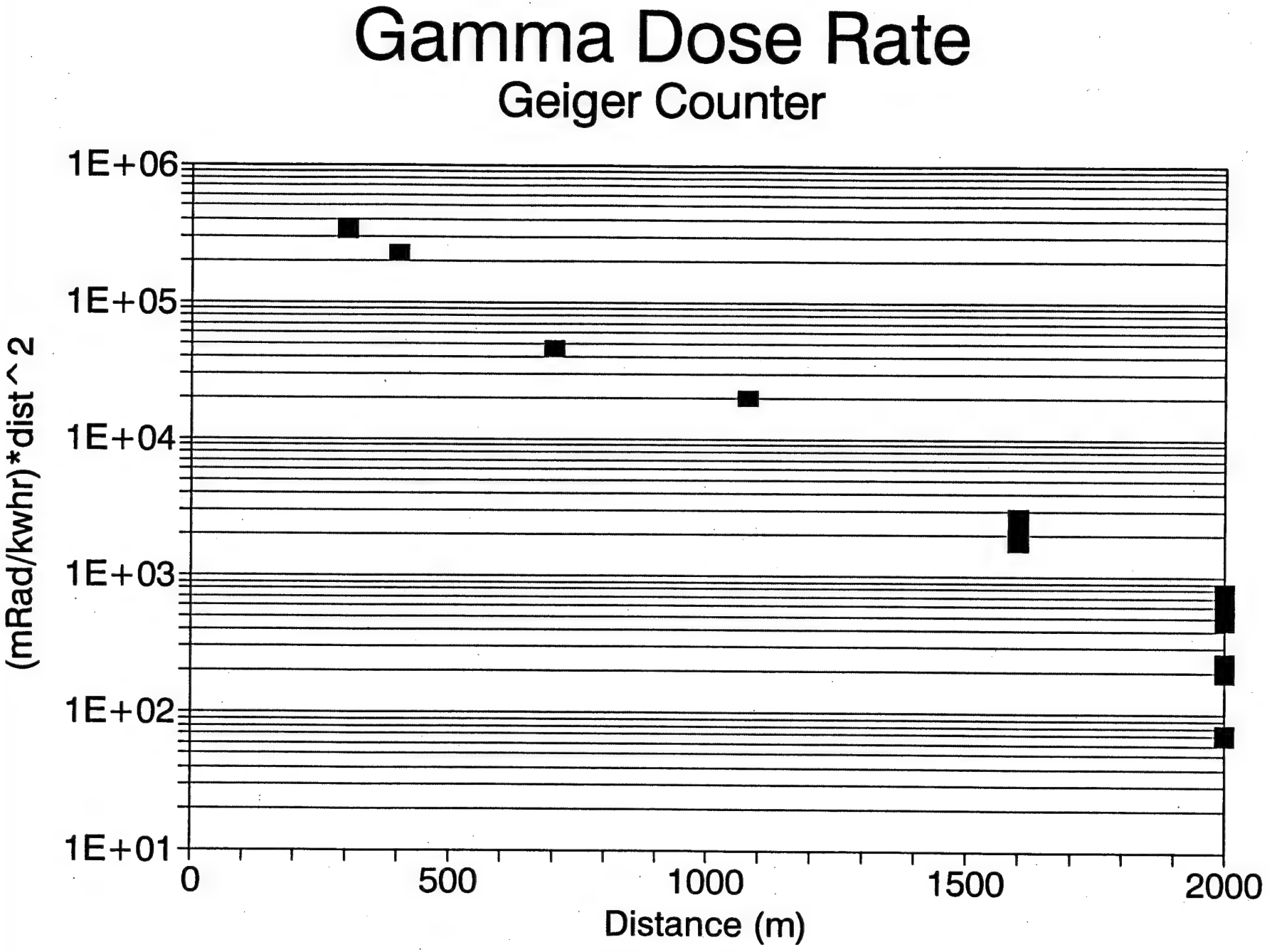
Gamma Dose Rate
Geiger Counter
1E+06
1E+05
1E+04
1E+03
1E+02
1E+01
(mRad/kwhr)*dist^2
0
500
1000
1500
2000
Distance (m)

Figure A-39.

9. THERMAL NEUTRON MEASUREMENTS IN A PHANTOM

For the Defence Nuclear Agency radiation transport program, APRF was asked to make thermal neutron measurements inside a phantom. It was hoped that this would verify calculational ability to make corrections for chlorine activation in concrete.

An acrylic phantom was borrowed from ETCA and an insert made to hold gold foils. Figure A-40 shows the insert. It was a 21-cm long by 5-cm diameter cylinder. Slots were used to hold gold and cadmium-covered gold foils. Figure A-41 shows the insert in place in the center phantom slab. During the actual runs, there was one top and one bottom covering slab. Figure A-42 shows the assembled phantom in place at 170 meters. The phantom was level. The bottom of the phantom was 78 cm above the ground. The reactor was slightly above horizontal.

Figures A-43 and A-44 are dimensional drawings of the insert and central phantom slab, respectively.

The phantom was exposed in two separate geometries. The first geometry (SS93-73 and SS93-74) included only bare gold foils, one per slot. The same foils were exposed for both runs. The gold foils were 0.005-inch thick by 7/16-inch diameter. The second geometry (SS93-75) included only cadmium-covered gold foils. These foils were identical to the first, but covered by 0.020-inch thick cadmium covers. In each case, the axis of the cylinder was pointed towards the reactor.

The results are listed in Table A-25 and plotted in Figure A-45. The distance represents the thickness of material from the front, and not the depth into the phantom. The difference is the size of the gaps. The bare-gold fluence increased substantially for the first 4 cm of phantom thickness as neutrons were thermalized. Then it declined as attenuation outweighed thermalization. The cadmium-covered-gold fluence declined at first, but showed a small increase as the rear of the phantom was approached.

TABLE A-25. GOLD FOILS RESULTS INSIDE ACRYLIC PHANTOM

Gold foil results inside phantom.				
Thickness (cm)	Bare Gold ($n/cm^2/kwhr$)	Cd-cov. Gold ($n/cm^2/kwhr$)	Φ(thermal) ($n/cm^2/kwhr$)	Cadmium Ratio
1.0	5.73E+07	6.64E+06	5.07E+07	8.63
2.6	8.69E+07	4.18E+06	8.27E+07	20.78
4.2	9.08E+07	3.11E+06	8.77E+07	29.24
5.8	8.41E+07	2.20E+06	8.19E+07	38.22
7.4	7.38E+07	1.67E+06	7.22E+07	44.23
10.2	6.56E+07	9.63E+05	6.46E+07	68.10
11.8	6.15E+07	1.00E+06	6.05E+07	61.41
13.3	5.95E+07	1.18E+06	5.83E+07	50.36
14.8	5.67E+07	1.73E+06	5.50E+07	32.71
16.3	4.47E+07	2.50E+06	4.22E+07	17.85

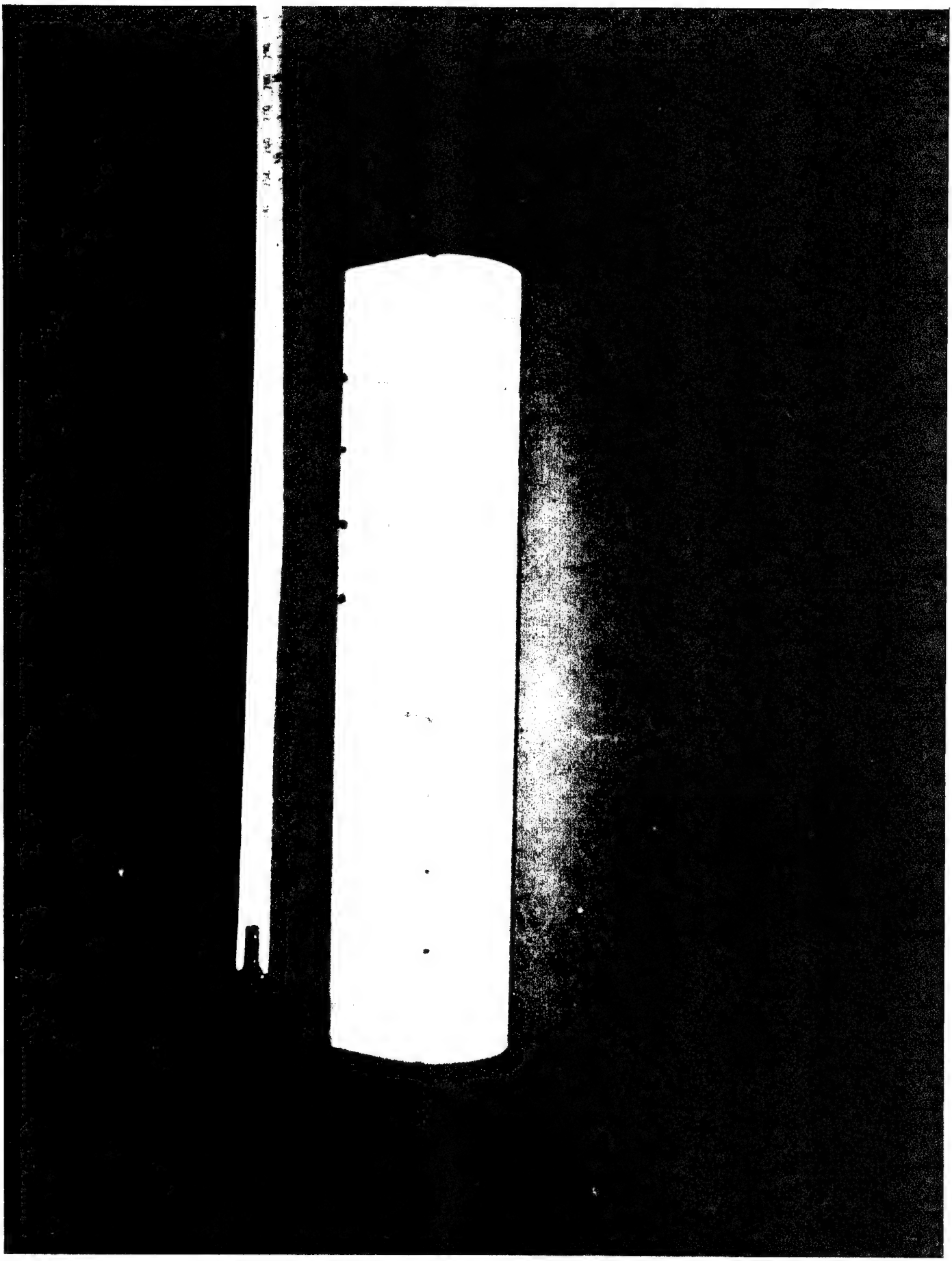

Figure A-40.

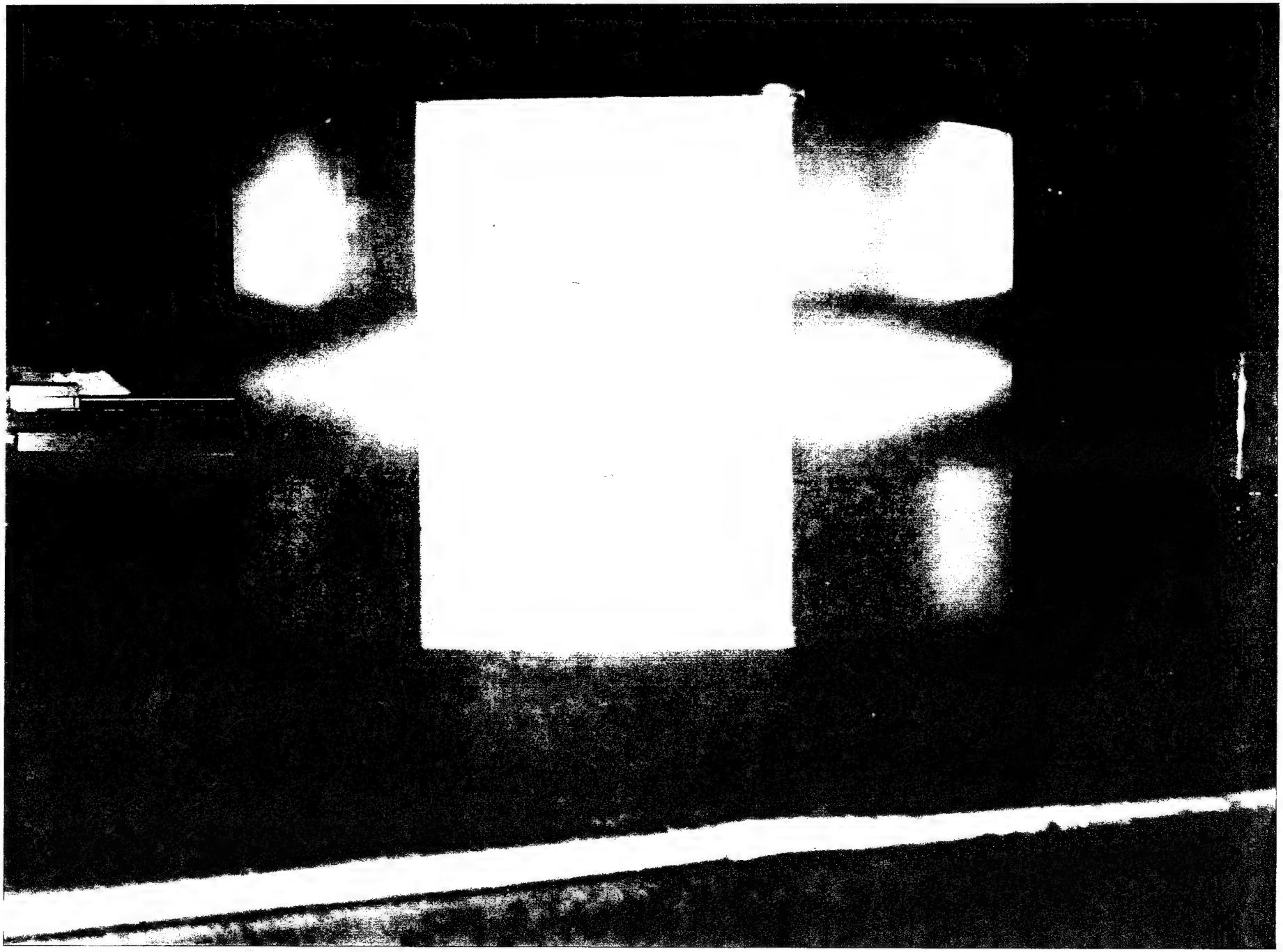

Figure A-41.

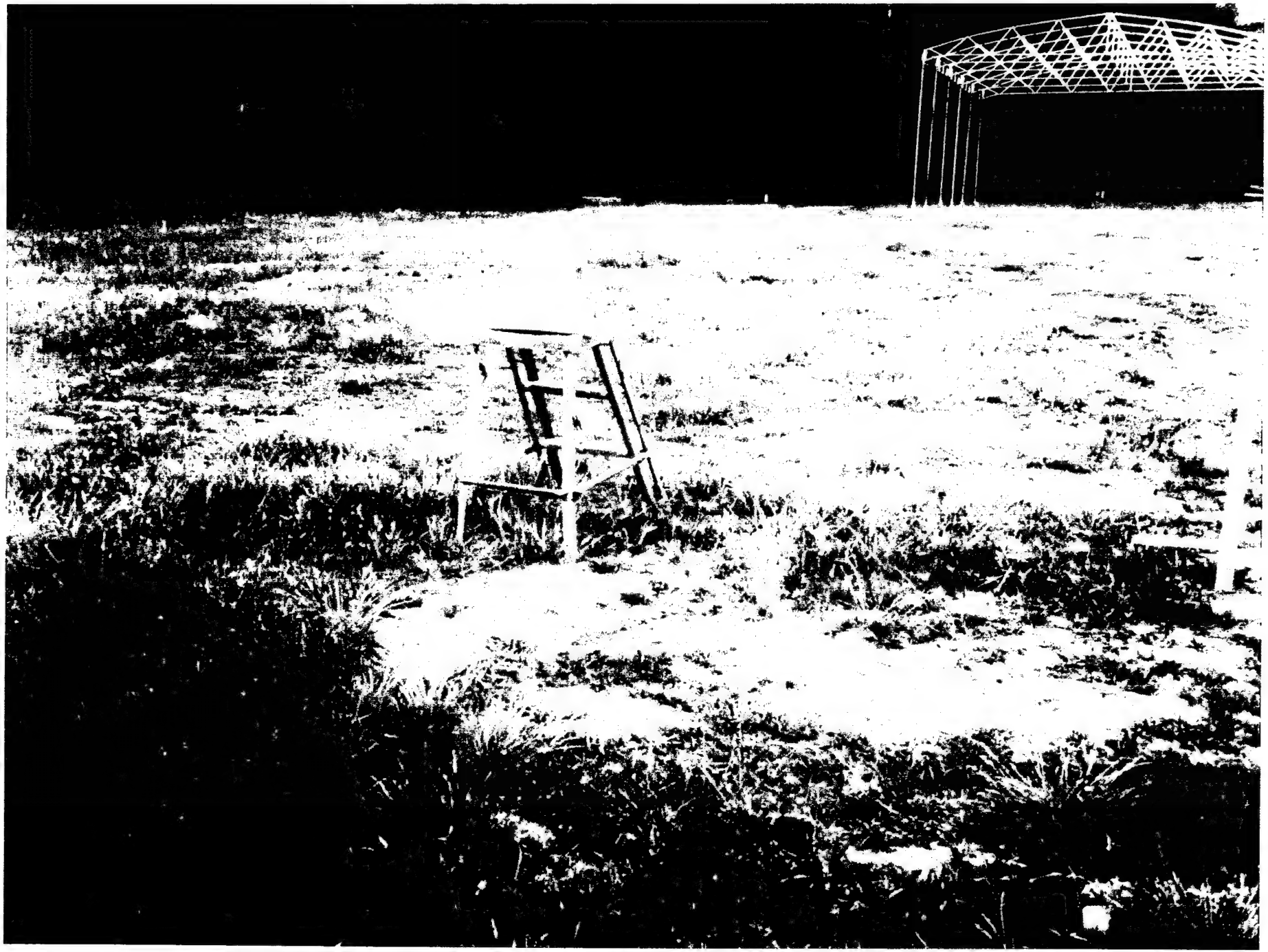

Figure A-42.

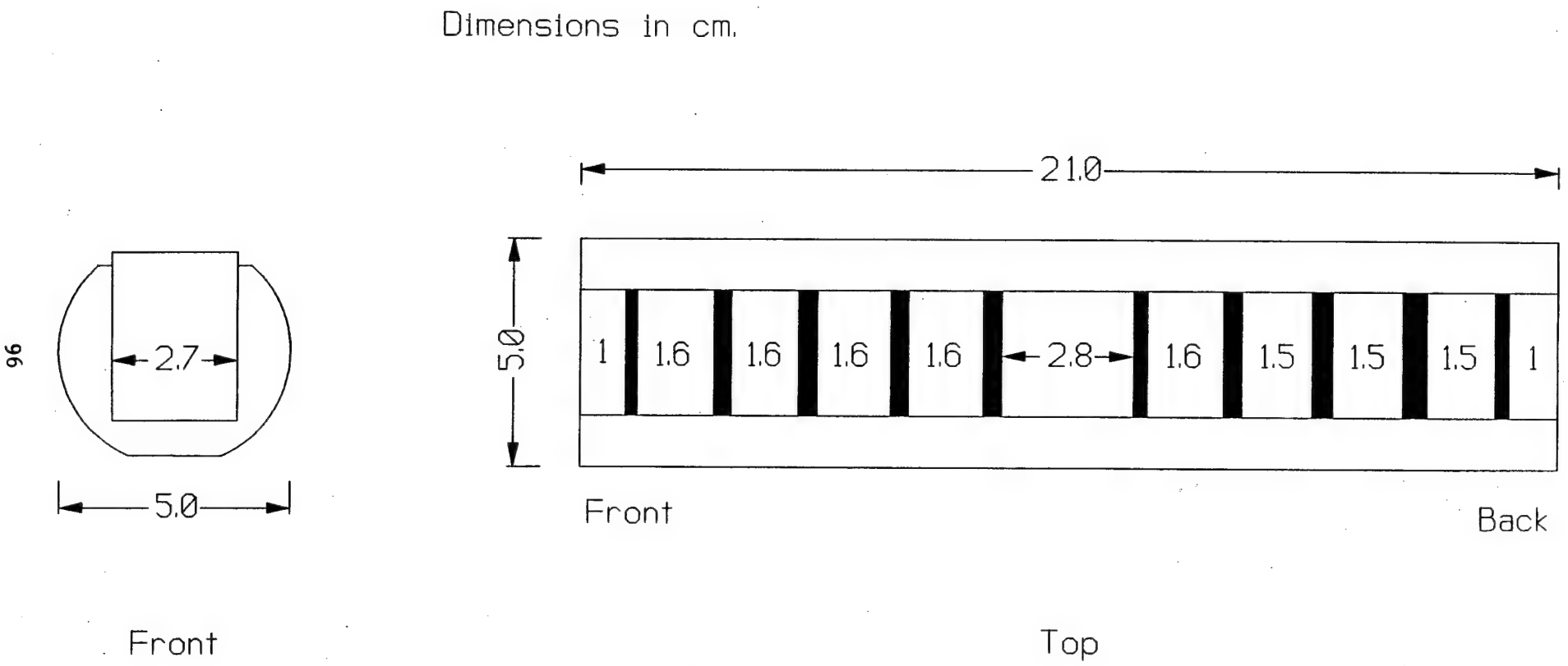
Dimensions in cm.
96
2.7
5.0
Front
21.0
5.0
1
1.6
1.6
1.6
1.6
2.8
1.6
1.5
1.5
1.5
1
Front
Back
Top

Figure A-43.

Dimensions in cm.

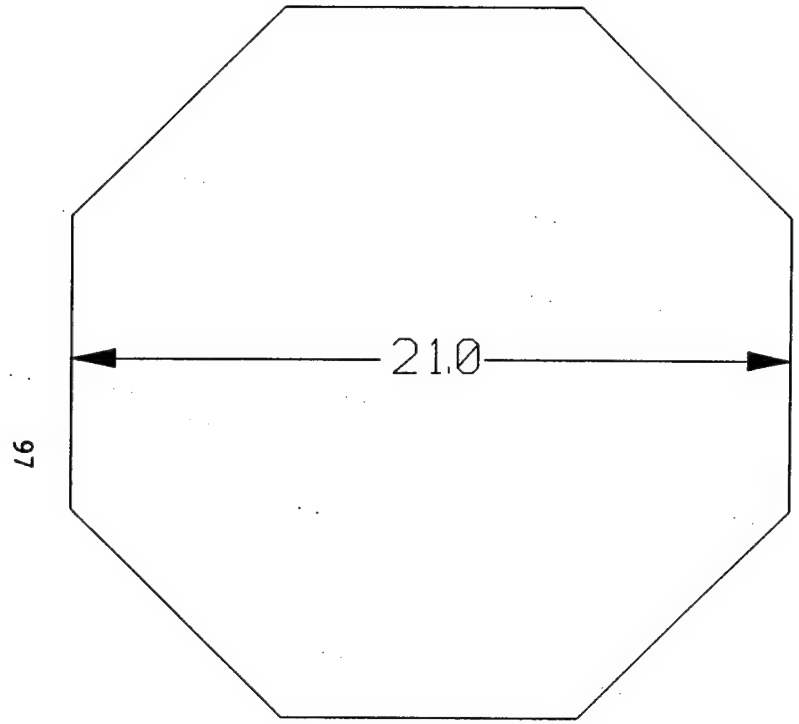

Top

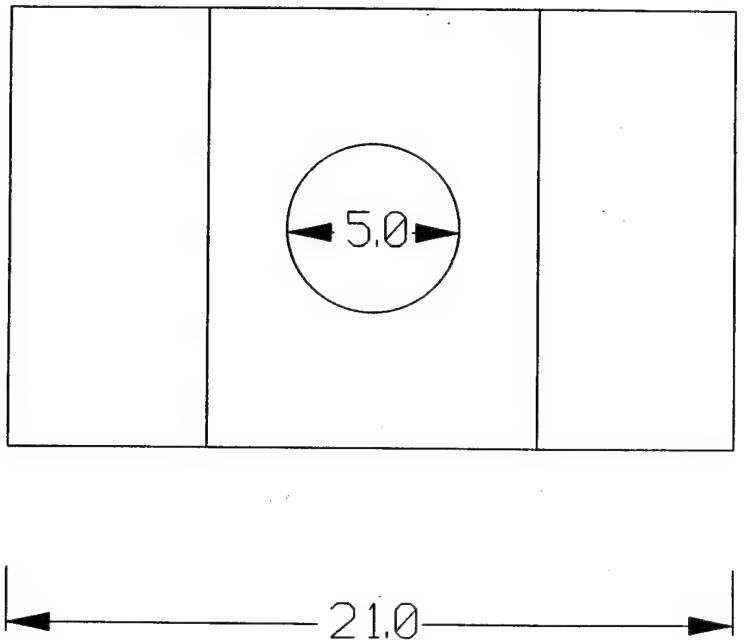

Front

Figure A-44.

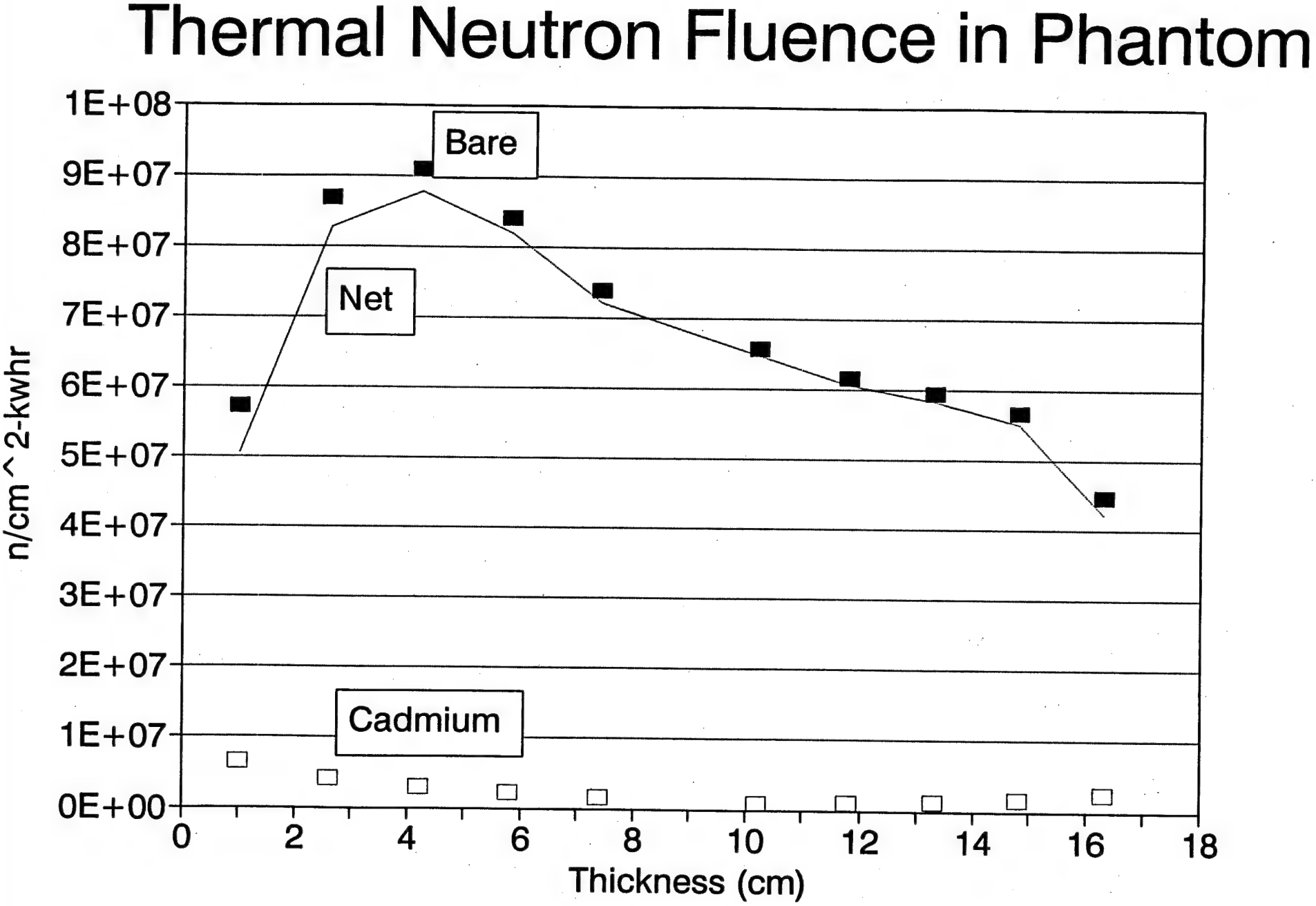
Thermal Neutron Fluence in Phantom
1E+08
9E+07
8E+07
7E+07
6E+07
5E+07
4E+07
3E+07
2E+07
1E+07
0E+00
n/cm ^ 2-kwhr
Bare
Net
Cadmium
0
2
4
6
8
10
12
14
16
18
Thickness (cm)

Figure A-45.

10. NON-CONSTANT GAMMA RAYS

As the reactor is operated, fission products accumulate. These fission products emit gamma rays in addition to the prompt gamma rays being emitted during fission. Also, neutrons interact with the environment and with the detectors, making them radioactive. All these effects contribute to reducing the measured neutron/gamma ratio as the reactor continues to operate.

An experiment was performed to study the size of this effect. A Geiger counter and a 5-inch Bonner sphere system were connected to scalars and located about 15 meters from the reactor. The distances were chosen to give a substantial count rate as the reactor was operated, but not to saturate the detectors. The scalars were programmed to record the count rate for a 2-second period every 5 seconds.

Figure A-46 shows the Geiger-counter results for two reactor pulses: P93-90 and P93-91. After the first pulse, the reactor was left in place for about an hour. After the second pulse, the reactor was moved into its storage pit. Figure A-46 shows that almost all of the Geiger-counter pulses resulted from the reactor.

Figure A-47 shows the net Geiger-counter pulses as a function of time after pulse. The solid line is a $t^{-1.2}$ fit normalized at 200 seconds after the pulse. As can be seen, the fit is quite good, but tends to underestimate the relative count rate at long times.

Figure A-48 shows the Bonner sphere results for the same two reactor pulses. The curves almost overlap, indicating that almost all the counts were due to induced radioactivity, either in the detector or in its environment. Figure A-49 shows the net Bonner sphere counts. These die away within 5 minutes of a pulse.

Figure A-50 shows a 1-hour steady-state reactor run (SS93-80) with the same detectors. Again, the Bonner sphere counts hardly change after the reactor is put in the pit at the end, indicating that the counts were due to environmental activation.

The Geiger counter showed a substantial residual gamma activity after shutdown. For the 1-hour run, the number of Geiger-counter counts in the hour after shutdown was 5.8 percent of the counts during the run. Thus, if a TLD was exposed for a 1-hour run and removed immediately after shutdown, it would show about 5 percent less dose than if it were left in place for an hour and the reactor was not moved. Typically, the reactor is stored in its pit about 20 minutes after shutdown. The Geiger-counter counts in the 20 minutes after shutdown were 3.3 percent of the counts during the run.

Of the detectors used in this test, the post-shutdown accumulation of dose would affect mainly the TLDs. Of the two runs with TLDs, one was of 6-hour duration (SS92-66) and the other (SS92-186) 1.5-hour duration. The 6-hour run should show negligible effect. The 1.5-hour run might show an additional 2 to 3 percent dose due to post-shutdown exposure. The exact effect would be complicated by the fact that the reactor was moving during its journey from the outdoor test pad to the pit. This would tend to decrease the exposures at 90 and 180°, and increase the exposures at 0 and 270°. The through-the-silo exposure would be increased the most. No correction was made for this effect in the data as given.

All the Geiger-counter measurements inside 450 meters were made with the system accumulating through the reactor run. This includes counts taken during the shutdown period before anyone could get to the site and stop the counting. The correction here would be similar to that for the TLDs. It would take approximately 30 minutes after shutdown before the Geiger-counter system could be stopped.

The data for the 1-hour steady-state test run are plotted again in Figure A-51. Here, the relative counts were normalized to their values 5 minutes into the run, and deviations plotted. It can be seen that the Bonner sphere count rate is almost constant, rising by about 1 percent during the run. Most of this is due to environmental activation, since the residual count rate was about 1 percent of the total.

The Geiger-counter rise was about 4 percent. This is due to an accumulation of fission products during the reactor run. Some of the reactor runs for this series of tests were as long as 7 hours. If the gamma decay follows a $t^{-1.2}$ behavior, a 7-hour run would show about double the gamma accumulation of the 1-hour run, for about an 8-percent total rise.

The increase of gamma fluence during the run would affect all gamma-ray measurements. For the TLDs, those exposed to the longer run would experience a slightly higher average dose per kWhr. Note that this would largely match the relatively higher post-run activation of the TLDs exposed to the shorter run. The net result should tend to cancel.

Geiger-counter measurement counts taken near the end of a 7-hour run should show 4 to 5-percent higher count rates than those taken near the beginning. Also, counts taken near the end of a long run should exceed those taken during a short run. This error is small compared to the uncertainties in the distant Geiger-counter measurements. No such effect was observed, probably because of statistics, and no corrections were made.

Figure A-52 shows the ratio of Bonner sphere to Geiger-counter counts as a function of time. The accumulation of gamma rays reduces the ratio from about 10, soon after the beginning of the run, to about 9 after 1 hour. This might be expected to decrease another 5 percent (to 8.5) after several hours of operation.

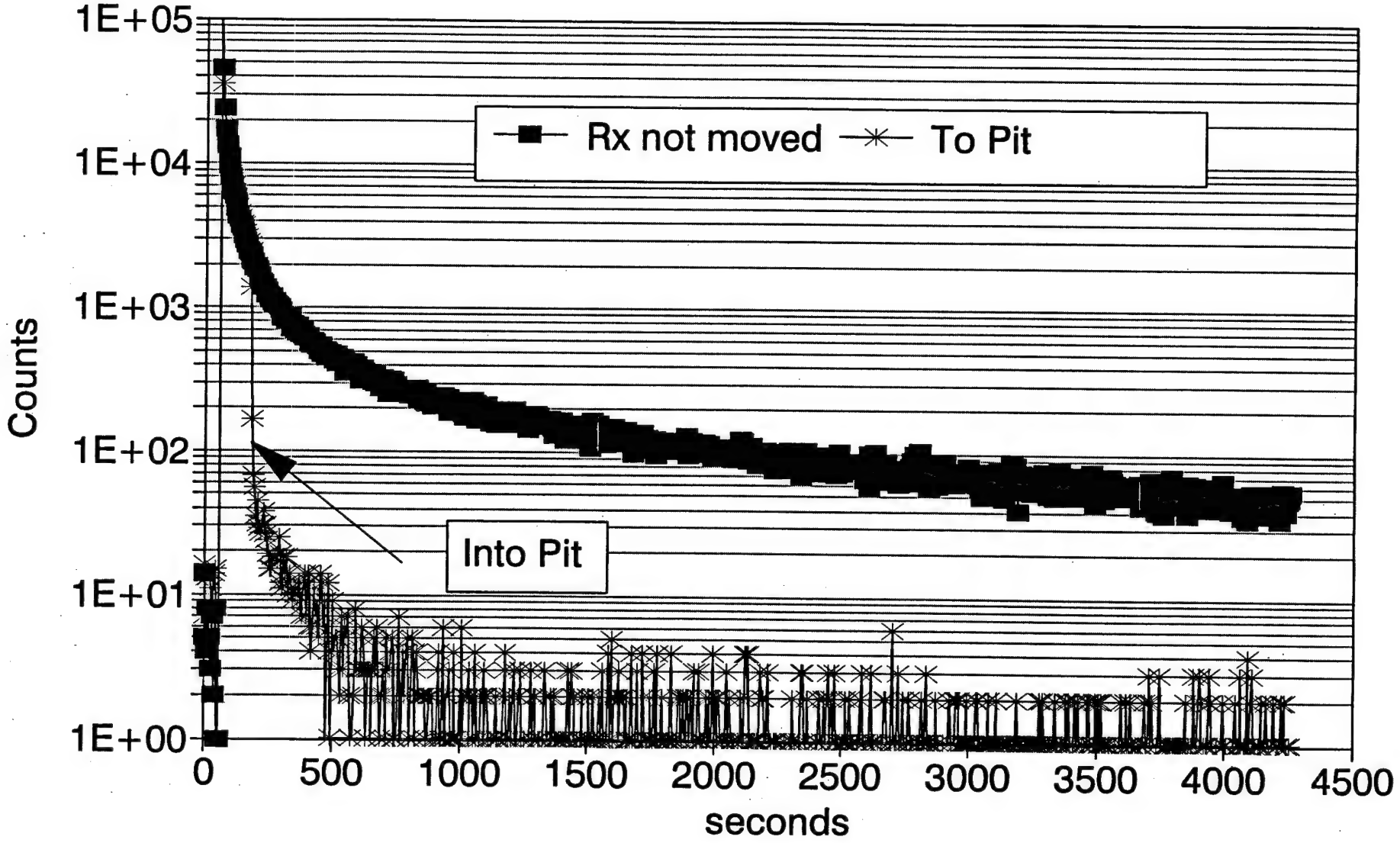
Pulse
Geiger Counter
1E+05
1E+04
1E+03
1E+02
1E+01
1E+00
Counts
Rx not moved
To Pit
Into Pit
0
500
1000
1500
2000
2500
3000
3500
4000
4500
seconds

Figure A-46.

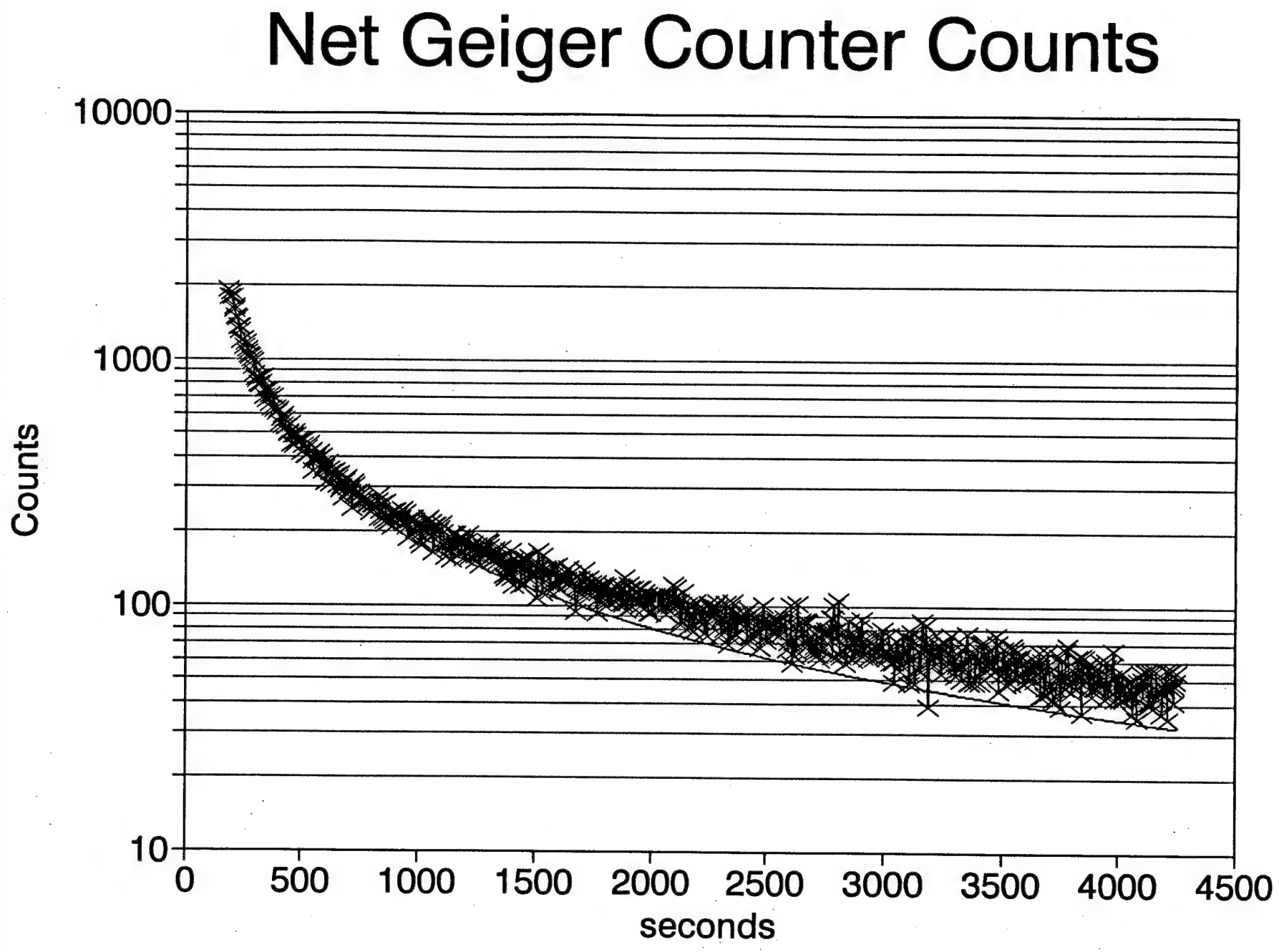
Net Geiger Counter Counts
10000
1000
100
10
Counts
0
500
1000
1500
2000
2500
3000
3500
4000
4500
seconds

Figure A-47.

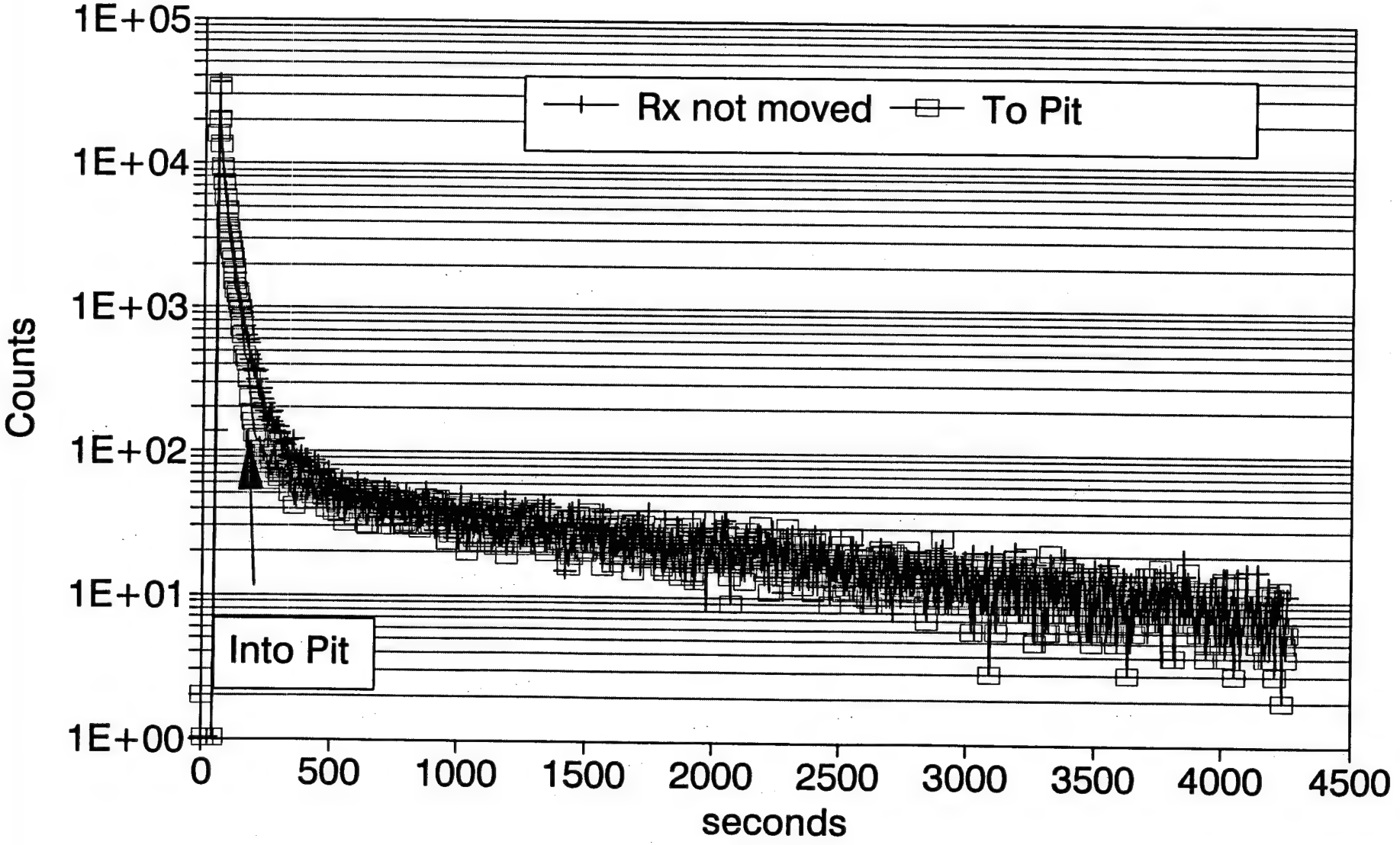
Pulse
Bonner Sphere
Rx not moved
To Pit
Into Pit
Counts
1E+05
1E+04
1E+03
1E+02
1E+01
1E+00
0
500
1000
1500
2000
2500
3000
3500
4000
4500
seconds

Figure A-48.

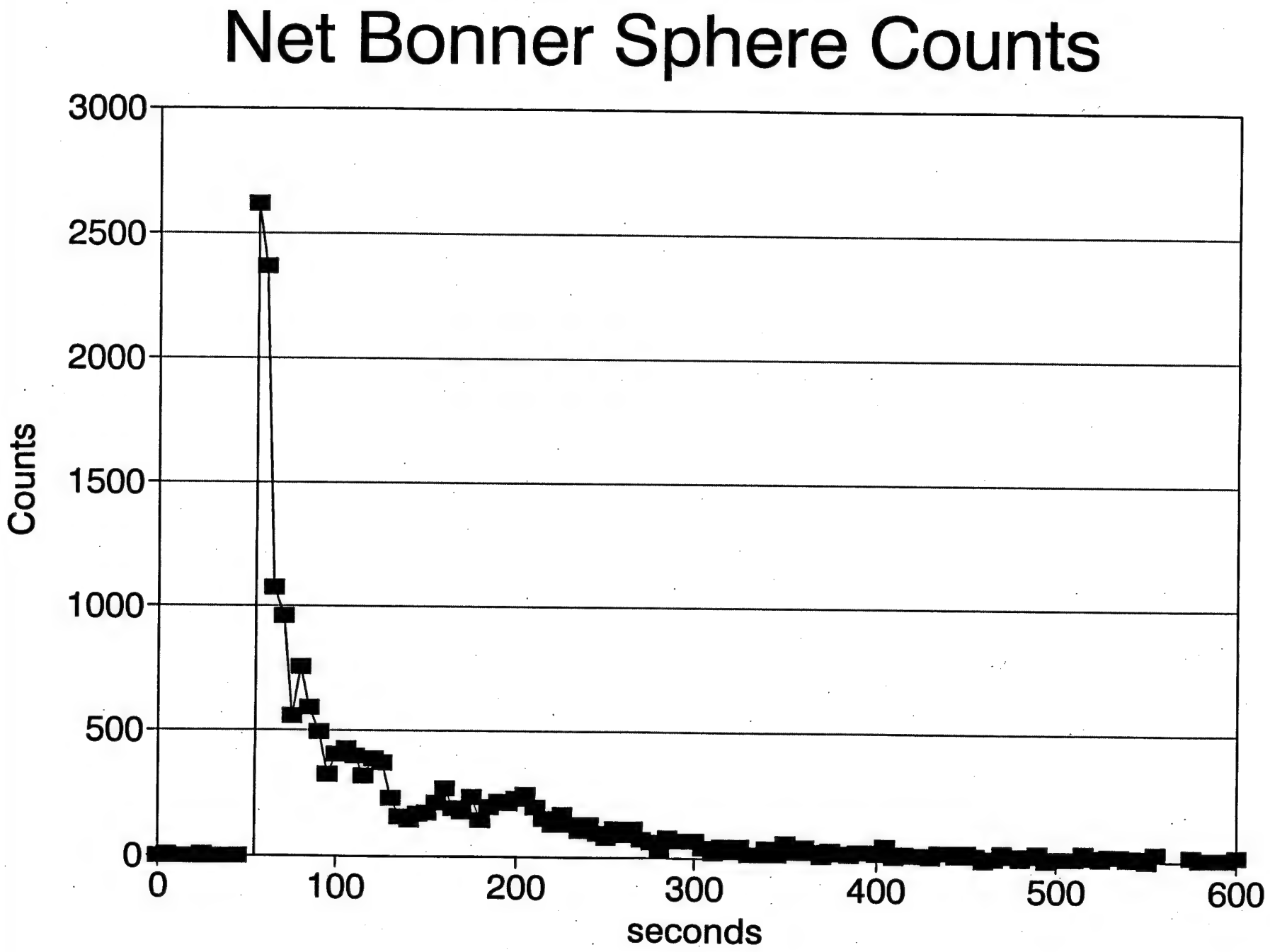
Net Bonner Sphere Counts
3000
2500
2000
1500
1000
500
0
Counts
10⁴
0
100
200
300
400
500
600
seconds

Figure A-49.

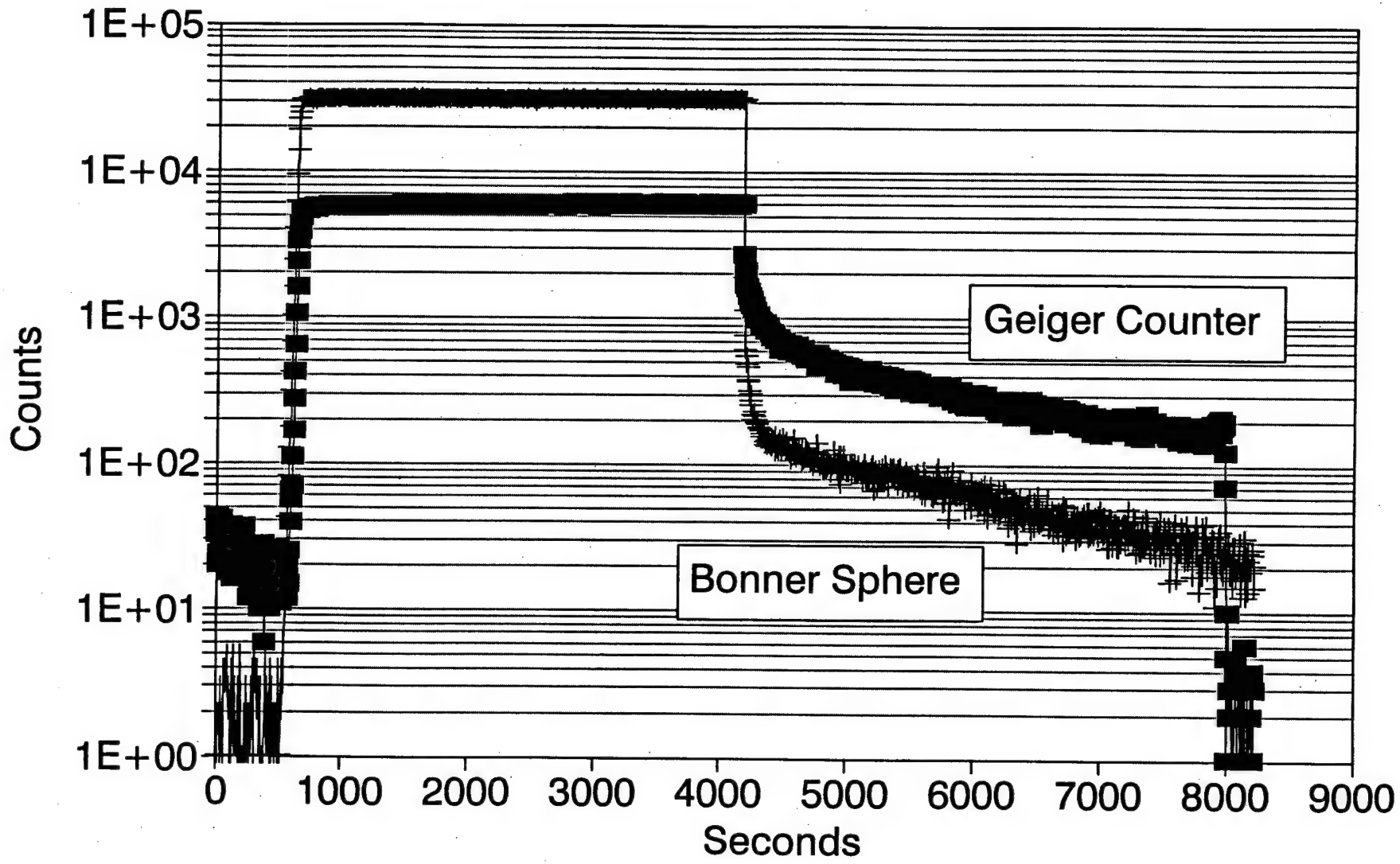
SS93-80
Count Rate Through Steady-State Run
1E+05
1E+04
1E+03
1E+02
1E+01
1E+00
Counts
Geiger Counter
Bonner Sphere
0
1000
2000
3000
4000
5000
6000
7000
8000
9000
Seconds

Figure A-50.

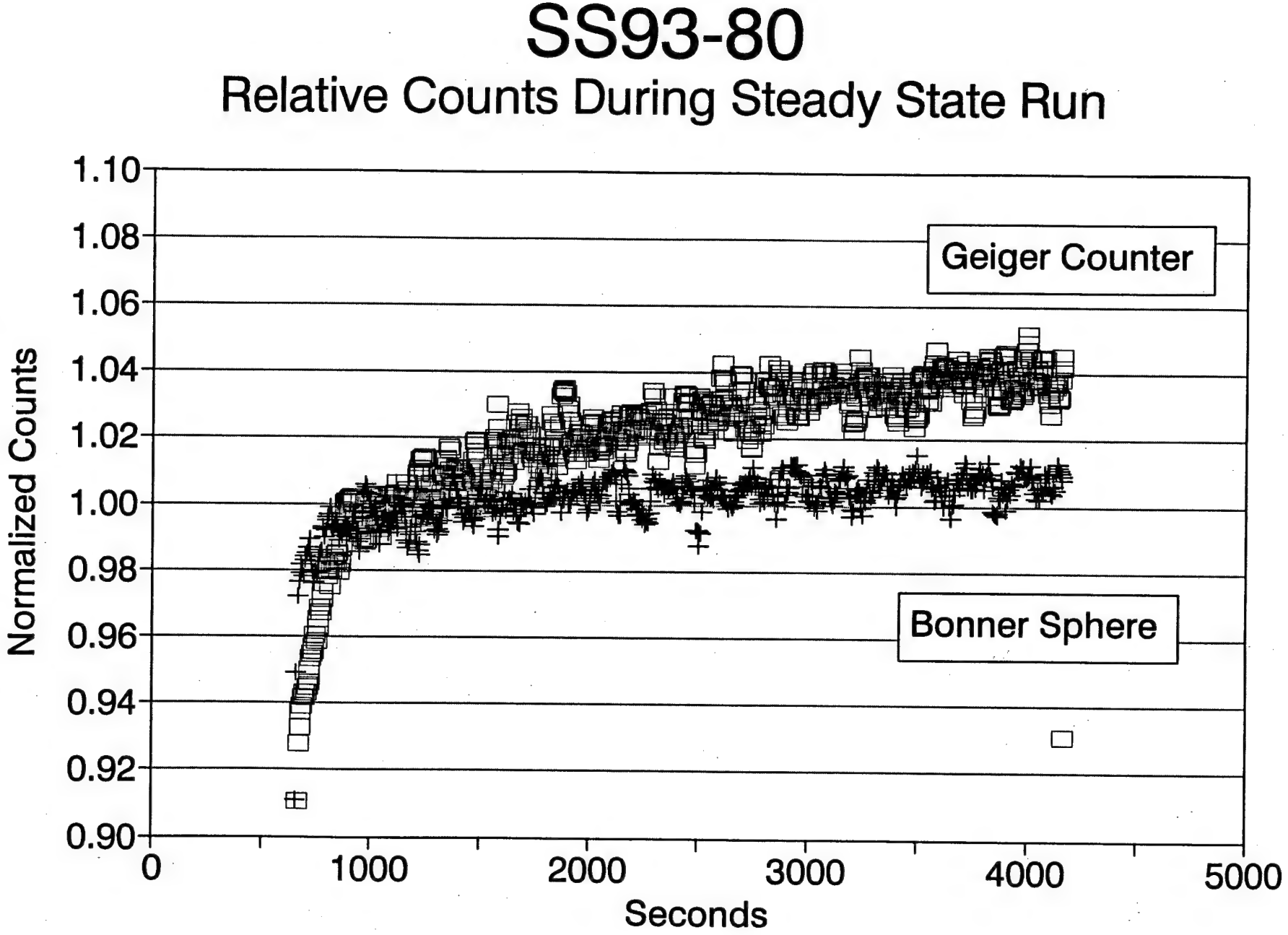
SS93-80
Relative Counts During Steady State Run
Normalized Counts
1.10
1.08
1.06
1.04
1.02
1.00
0.98
0.96
0.94
0.92
0.90
0
1000
2000
3000
4000
5000
Seconds
Geiger Counter
Bonner Sphere

Figure A-51.

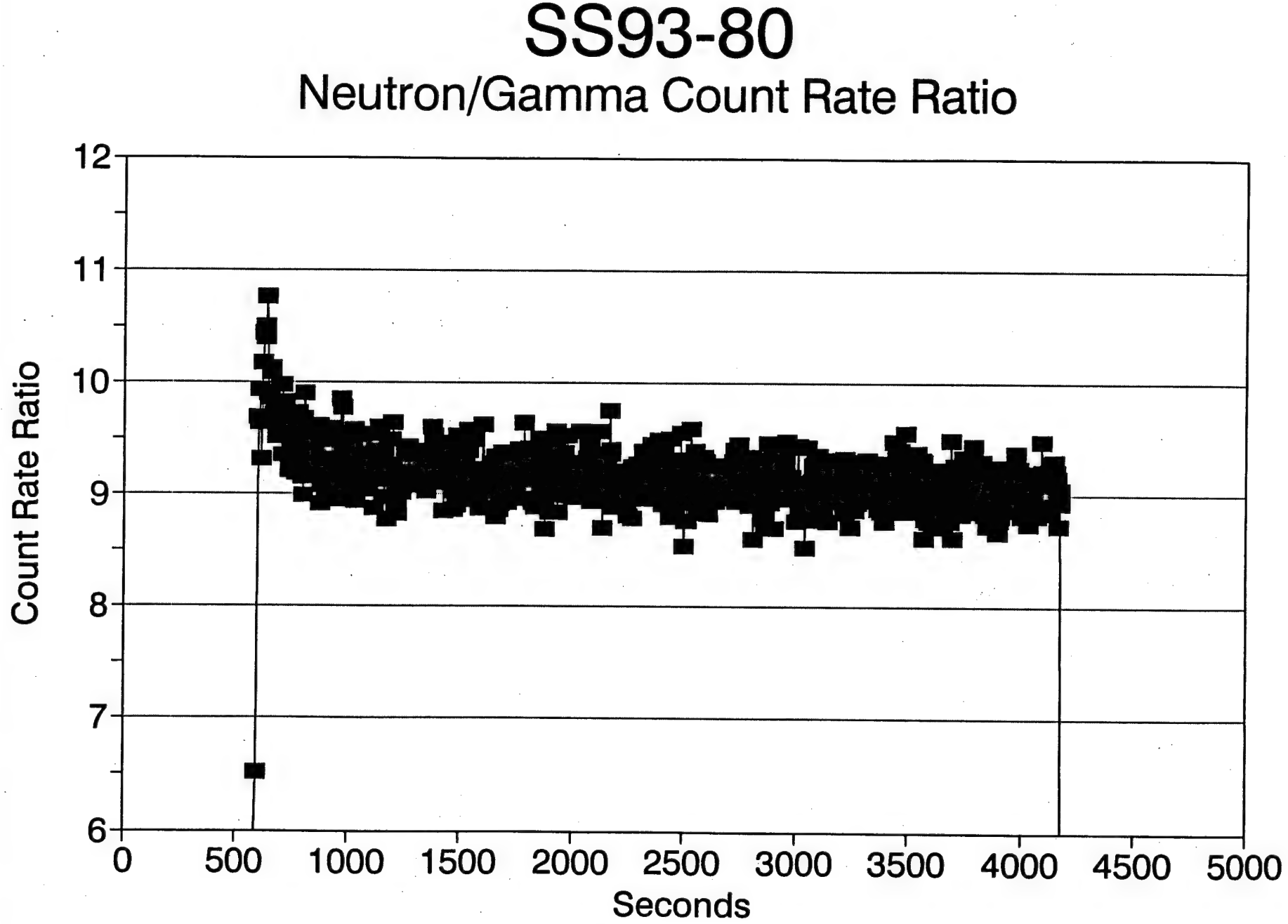

Figure A-52.

(Page 108 Blank)

11. RADIATION MAPPING INSIDE SILO

The reactor silo contains various materials which may act to scatter neutrons or to generate secondary gamma rays. Of particular concern was a flash X-ray machine, which has a large quantity of insulating oil. Concern about this was one reason radiation was measured at the different angles around the reactor.

To address scattering centers inside the silo, the neutron and gamma-ray distributions inside the silo were mapped. The reactor was in the center of the silo, 20 feet up. Gold and sulfur foils and TLDs were placed at various positions around the silo (see fig. A-53).

The reactor was run for 2 kWhr (SS93-81). The results are listed in Table A-26.

The data are plotted in Figure A-54, multiplied by r^2, and normalized to the averages. The dose is quite uniform. The thermal neutron fluence does not depend on distance from the reactor, and thus appears higher in the farther positions (1, 4, 5, and 7).

The position near the flash X-ray machine (No. 7) shows only a slight rise above the others. This effect appears localized. There is no significant increase in radiation as monitored by the detectors near to, but not on, the flash X-ray machine.

TABLE A-26. RADIATION MEASUREMENTS AT LOCATIONS AROUND SILO

Package	Distance (m)	Φ(Thermal) ($n/cm^2/kwhr$)	Cad Ratio	Φ(>3 MeV) ($n/cm^2/kwhr$)	Tissue Dose (R/kwhr)
1	15.2	2.52e+08	1.38	7.39e+08	2.5
2	11.4	2.52e+08	1.25	1.59e+09	4.6
3	11.4	2.76e+08	1.32	1.49e+09	4.7
4	15.2	2.82e+08	1.50	7.13e+08	2.3
5	15.2	1.94e+08	1.35	7.75e+08	2.3
6	11.4	1.96e+08	1.22	1.63e+09	4.2
7	17.9	3.19e+08	1.49	7.29e+08	2.8
8	11.4	2.39e+08	1.24	1.64e+09	4.5

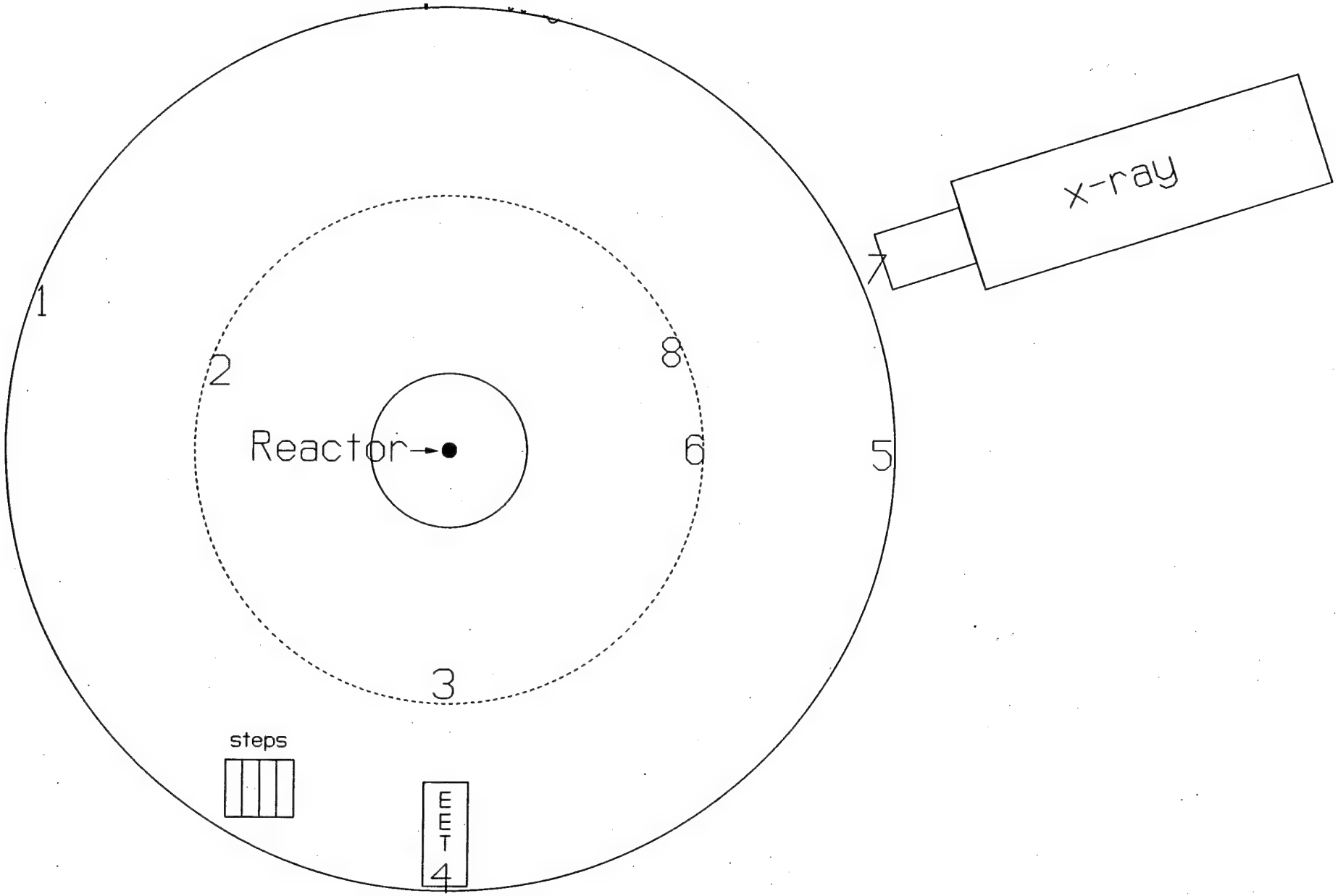

Figure A-53.

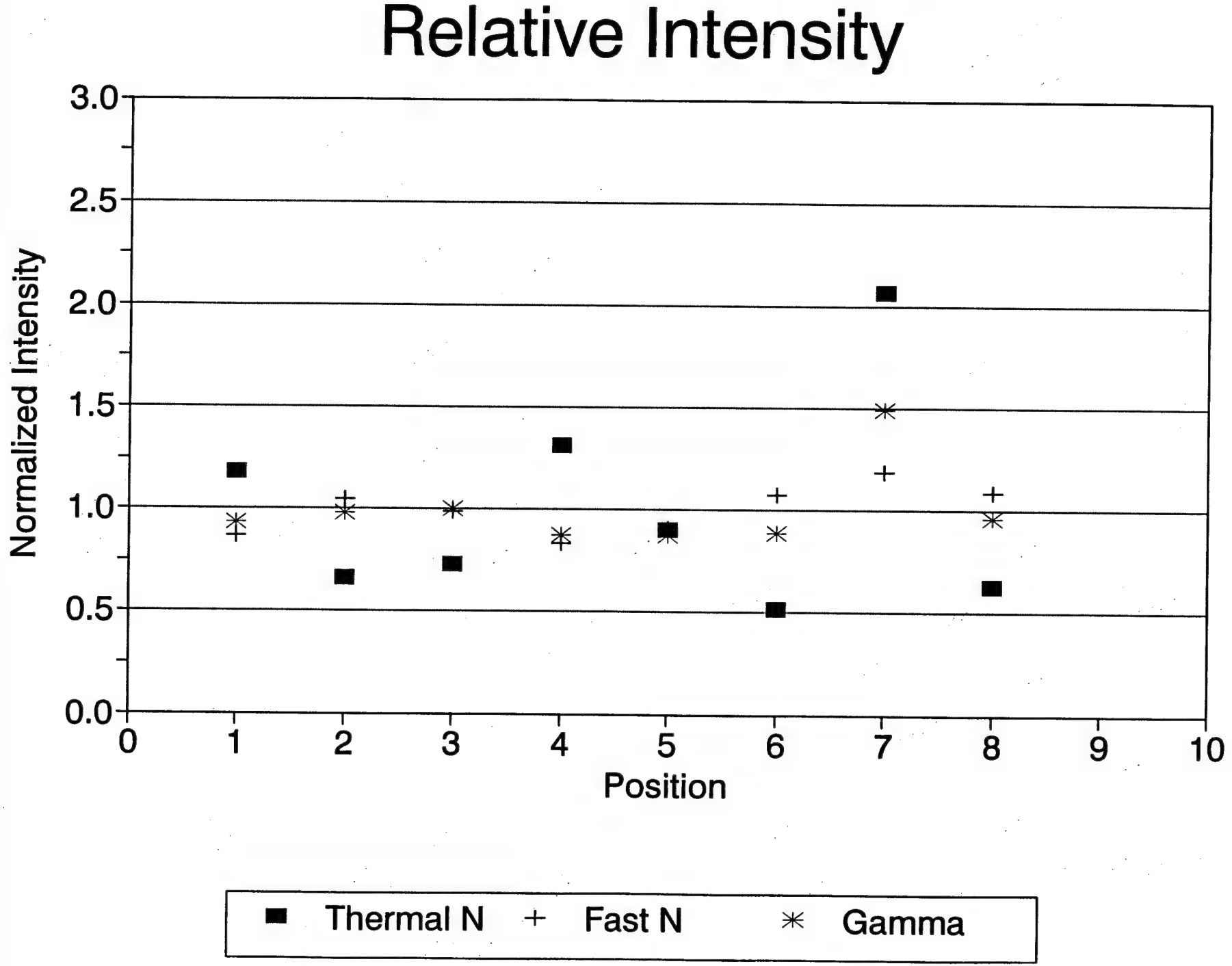

Figure A-54.

(Page 112 Blank)

DISTRIBUTION LIST

Addressee	No. of Copies
Commander U.S. Army Test and Evaluation Command ATTN: AMSTE-SI-F Aberdeen Proving Ground, MD 21005-5055	1
Commander U.S. Army National Ground Intelligence Center ATTN: IANG-RMT (Mr. Ward) IANG-RMT (Mr. Shuff) 220 Seventh Street Charlottesville, VA 22901-5396	1 1
Commander U.S. Army Tank-automotive and Armaments Command ATTN: AMSTA-SF Warren, MI 48397-5000	1
Commander U.S. Army Research Laboratory (Adelphi) ATTN: AMSRL-OP-IS-FI AMSRL-WT-NH (Mr. Kerris) 2800 Powder Mill Road Adelphi, MD 20783-1145	1 1
Commander U.S. Army Materiel Command ATTN: AMCDG-T AMCICP-M AMCICP-RDE 5001 Eisenhower Avenue Alexandria, VA 22333-0001	1 1 1
Commander U.S. Army Infantry Center ATTN: ATZB-IST Fort Benning, GA 31905	1
Commander U.S. Army Training and Doctrine Command ATTN: ATDO-I Fort Monroe, VA 23651-5000	1
Commander U.S. Army Chemical Center ATTN: AMSMI-CM-CU Redstone Arsenal, AL 35898-5140	1
Commander U.S. Army Ordnance Center and School ATTN: ATSL-OSI-I Aberdeen Proving Ground, MD 21005-5201	1
Commander U.S. Army Intelligence Center and School ATTN: ATSI-CD-TT ATSI-ETD-T Fort Huachuca, AZ 85613	1 1

Addressee	No. of Copies
Commander U.S. Army Foreign Materiel Intelligence Group ATTN: IAFE-OP-O Aberdeen Proving Ground, MD 21005-5301	1
Commander U.S. Air Force Aerospace Technology Center ATTN: DXM Wright-Patterson AFB, OH 45433-6508	1
Program Executive Officer Armored Systems Modernization ATTN: SFAE-ASM-SS-T (Mr. Ryzyi) Warren, MI 48397-5000	1
Director U.S. Army Tank-Automotive Research, Development and Engineering Center ATTN: AMSTA-RSS (Mr. Thompson) Warren, MI 48397-5000	1
Deputy Commander U.S. Army Combined Arms Combat Development Activity ATTN: ATZL-CST Fort Leavenworth, KS 66027	1
HQDA ATTN: ATZL-FIT Washington, DC 20310-1086	1
Director U.S. Army Nuclear and Chemical Agency ATTN: MONA-NU (Mr. Bash) MONA-NU (Mr. Ford) MONA-NU (Mr. Bliss) MONA-ZB (Technical Library) 7150 Heller Loop, Suite 101 Springfield, VA 22150-3198	1 1 1 1
Deputy Chief of Staff Operations and Plans Nuclear Division ATTN: DAMO-SSN (Mr. Luger) 400 Army Pentagon Washington, DC 20310-0400	1
Director for International Cooperation ATTN: SARD-IN (Mr. Riley) Assistant Secretary Research, Development and Acquisition 103 Army Pentagon Washington, DC 20310-0103	1
Research and Technology ATTN: SARD-TT (Mr. Yuhas) Assistant Secretary Research, Development and Acquisition 103 Army Pentagon Washington, DC 20310-0103	1

Addressee	No. of Copies
Director Assessment and Evaluation ATTN: SARD-DOV (Mr. Mlinarchik) Assistant Secretary Research, Development and Acquisition 103 Army Pentagon Washington, DC 20310-0103	1
Defense Nuclear Agency ATTN: RARP (Mr. Kehlet) TDTR (Mr. Kennedy) SPWE (Mr. Wittwer) 6801 Telegraph Road Alexandria, VA 22310	1 1 1
Oak Ridge National Laboratory Laboratory Records ATTN: Joe Pace Jeff Johnson PO Box 2008 Oak Ridge, TN 37831-6285	1 1
SAIC, Inc. 10260 Campus Point Drive ATTN: Dean Kaul, Mail Stop 33 Steve Egbert, Mail Stop 33 San Diego, CA 92121	1 1
U.S. Department of Commerce National Institute for Standards and Technology Bldg 235 ATTN: David Gilliam Dale McGrarry Gaithersburg, MD 20899	1
DOE/EML ATTN: Paul Goldhagen 376 Hudson Street New York, NY 10014	1
Los Alamos National Laboratory Dr. Roger Byrd, MS D 436 Los Alamos, NM 87545	1
Nuclear Effects Laboratory ATTN: STEW-S-NE-R (Michael Flanders) (Mary Sparks) White Sands Missile Range, NM 88002	1 1
CRC Research Institute 4677 Old Ironside Drive Suite 200 Santa Clara, CA 95054	1
Director Armed Forces Radiobiology Research Laboratory ATTN: MRAD (CDR Kearsley) Bethesda, MD 20814-5145	1

Addressee	No. of Copies
Naval Surface Warfare Center ATTN: Mr. Garden Riel, Code 1241 New Hampshire Avenue White Oak, MD 20903-5000	1
Pennsylvania State University 231 Sactett Bldg ATTN: Anthony Baratta University Park, PA 16802	1
Director U.S. Army Research Laboratory ATTN: AMSRL-OP-IS-FI AMSRL-WT-T AMSRL-OP-AP-L, Bldg 305 Aberdeen Proving Ground, MD 21005-5066	1 1 2
Commander U.S. Army Aberdeen Test Center ATTN: STEAC-RS (Mr. Heimbach) STEAC-AD-A Aberdeen Proving Ground, MD 21005-5059	15 1
Defense Technical Information Center 8725 John J. Kingman Rd., STE 0944 Fort Belvoir, VA 22060-6218	2

Distribution unlimited.